FFS | TOWARDS FOSSIL-FREE STEEL

FINAL REPORT 02/2024

2021-2023

TOWARDS FOSSIL-FREE STEEL

FFS | TOWARDS FOSSIL-FREE STEEL

FFS - Towards Fossil-free Steel: final report

ISBN
978-952-62-4014-5 (printed version)
978-952-62-4015-2 (PDF)

Publisher and contact information

Process Metallurgy Research Unit
Faculty of Technology
University of Oulu
PO Box 4300 I 90014 University of Oulu
FINLAND

Editors
Petri Sulasalmi | Seppo Tikkanen

Graphic design and layout Konsti&Taito
Language editor Acolade Oy
Printed by Oy Nord Print Ab

FFS TOWARDS FOSSIL-FREE STEEL

FFS FINAL REPORT

Jarmo Lilja
Chairman of FFS Steering Group
Process Development Manager,
Group Key Expert SSAB Europe Oy

INDUSTRY PREFACE

Since 1984, member companies of the Association of Finnish Steel and Metal Producers have collaborated with universities and research units and formed national technology programmes and projects to improve the competitiveness of the Finnish metal industry. This has been possible with generous funding from Tekes, and Business Finland since 2017. The programmes have traditionally focused on the utilisation of new technologies, material and energy efficiency, product quality, and the development of new processes and products. A well-known issue with greenhouse gases and global warming has revolutionised metal producing companies' strategies. This is especially true in the steel industry, which creates a major share of global CO_2 emissions. The restrictions and pressure of the European and national emissions reduction targets have completely changed the steelmaking community's focus on the emissions trading system. R&D funding systems in both Finland and Europe now strongly support the green transition. The focus of R&D is on new reduction technologies, new green energy solutions, and other technologies supporting the reduction of CO_2 emissions and sustainable production.

The SSAB Raahe Steel Works emits around 4 Mt/a of CO_2, corresponding to 7% of total CO_2 emissions in Finland. SSAB's strategy supports the national target of carbon neutrality in 2035 and aims to bring fossil-free steel to the market as early as 2026 and to be completely fossil-free by 2035. This target was brought forward by fifteen years in January 2022 when SSAB also introduced a plan to build new greenfield mini-mill-type steelworks in both Raahe and Luleå, Sweden. The planning of the FFS – Towards Fossil-free Steel project was started in 2020 to assist SSAB in achieving these fossil-free production targets. FFS is a continuation of the previous Metal Producers' programme SYMMET – Symbiosis of metals production and nature (2018–2020) and is part of the current Metal Producers' strategic research agenda. SSAB also conducted the Energy4HYBRIT (2019–2020) pre-study, co-financed with Business Finland's energy aid, which studied the green energy demand and supply of the Raahe mill. SSAB's main topics in FFS included studies of EAF- and DRI-based metallurgy, fossil-free energy solutions, and recycling strategies.

Fossil-free steel production calls for new production technologies and green energy sources. At Raahe, over 90% of the energy currently used is based on fossil fuels, including coal and natural gas. In addition to the replacement of fossil coal used for the reduction of iron ore with hydrogen, another type of non-fossil fuel is needed for the various processes involved in steelmaking. There is therefore a need to expand the FFS consortium with companies from other industries that have not previously participated in the Metal Producers' R&D Network. SSAB was delighted to see new entrants to the FFS consortium: the large energy companies Fortum and Valmet, and the limestone-based products producer Nordkalk. The participation of Ovako Imatra, as a steel producer with electric steelmaking and ambitious carbon neutrality targets, was highly appreciated. The other two industrial partners included Tapojärvi and Luxmet, making a valuable contribution to the project. The three public research partners, University of Oulu, Åbo Akademi, and VTT, have a long history of cooperation with Finnish metal producers.

The first phase of FFS ends in December 2023. We are already looking forward to the second phase, where successful work will continue with refined targets and exploiting the results of FFS. The consortium greatly appreciates the support of Business Finland in making the FFS project possible.

Timo Fabritius
Professor, Head of Unit
Process Metallurgy Research Unit
University of Oulu

ACADEMY PREFACE

The FFS project launched a transition in which a concept for producing fossil-free steel is being realised for the first time in the world. In addition to metallurgical research, the transition requires systemic research related to hydrogen production, fossil-free energy, and energy storage, not forgetting the sidestreams of future fossil-free steel plants. An important impact of the FFS project has been its support for fundamental and academic research in the many fields of steelmaking driving the green transition forward in the steel industry. Not only has this been crucial in several niche topics such as reduction metallurgy, phase equilibria, thermodynamic simulations, and the use of hydrogen as a fuel in metallurgy, but equally in the use of advanced characterisation techniques that deepen understanding of nanoscale phenomena. The close linkage provided by FFS has enabled multidisciplinary research groups in Finnish universities to profile their activities and avoid overlaps, thus maximising their skills coverage at the national level in all the fields relevant to sustainable steelmaking.

An excellent example of pioneering research has been studies of using biochar as a foaming agent in an electric arc furnace (EAF), consisting of unique laboratory device development and piloting biochar in the industrial environment, with encouraging results. The pioneering research openings, results, and expertise generated by the FFS consortium have been observed in the EU, and research partners have been desired cooperation partners in several EU consortiums related to sustainable steelmaking. Furthermore, international collaboration has been realised as a form of research exchange and the joint use of unique laboratory devices in Europe.

As a result of the excellent collaboration, seven master's theses and 48 journal and conference publications have been produced during FFS. However, much remains to be written and published, as new results will be produced until the very end of the project. All the theses and publications are based on profound interdisciplinary joint research. This collaboration not only supports the industry in the green transition but also emphasises the importance of metallurgy as a research field among the other less applied research areas in academia.

FFS | TOWARDS FOSSIL-FREE STEEL

TOWARDS FOSSIL-FREE STEEL IN A NUTSHELL

FFS – The Towards Fossil-free Steel project – is an important step on a path from coal-based to fossil-free steelmaking in Finland. FFS builds competence and new information for future investments and process selection and optimisation. The introduction of fossil-free steel products to the market is a big opportunity for the Finnish metal-using industry, enabling the development of their own fossil-free steel product portfolio.

THE MAIN TARGETS IN THE FFS PROJECT ARE

1. To enable the production of fossil-free steel by establishing the most economically viable new technologies and solutions for the different parts of iron and steelmaking processes and integrating them into existing processes.
2. To enable the replacement of fossil fuels (coal, natural gas) used for the reduction of iron ore and process energy (lime kilns, steelmaking, hot rolling) through new green energy solutions (electrification, use of hydrogen, biofuels, and biocarbon).
3. To determine the volumes, compositions, and properties of secondary materials evolving in new processes and to develop solutions for utilising these materials as a raw material or newly developed products to minimise the landfilling of waste materials

FACTS

Duration	3/2021 – 12/2023
Budget about	€10.7m
Funding	Business Finland, participating companies, and research partners

PARTNERS

The FFS project consortium consists of ten industrial partners and three research organisations: SSAB Europe Oy; Ovako Imatra Oy; Fortum Power and Heat Oy; Nordkalk Oy; Valmet Technologies Oy; Tapojärvi Oy; Luxmet Oy; University of Oulu; Åbo Akademi; and VTT. Andritz, ABB, and Finnsementti Oy were supporting partners.

SSAB · OVAKO · fortum

TAPOJÄRVI · Nordkalk · Valmet

LUXMET · OULUN YLIOPISTO · Åbo Akademi

VTT · ANDRITZ · ABB · FINNSEMENTTI

CARBON-NEUTRAL PROCESSES

FFS TOWARDS FOSSIL-FREE STEEL

CONTRIBUTORS

Seppo Ollila | SSAB Europe, corresponding person
Jarmo Lilja | SSAB Europe
Eetu-Pekka Heikkinen, Petri Sulasalmi, Manuel Mehtälä
University of Oulu

3.1 EAF metallurgy

The steel industry is moving towards fossil-free steel production, which requires the conversion of the traditional blast furnace-based steel production route to electric. The production of fossil-free steel with the HYBRIT and electric arc furnace processes is a significant change in the steel industry and a big step forward in terms of the environment. The steelmaking process changes significantly when moving from the present blast furnace-based iron production to a fossil-free sponge iron (DRI)-based steelmaking process.

BACKGROUND

Hydrogen-reduced DRI is a new raw material for the EAF process, whose melting behavior is not exactly known. As the raw material and material base changes, so does the analysis of the steel in terms of impurity levels. It must be possible to precisely control impurity contents in special steel production in order to produce high-quality products.

SOLUTION, METHOD

Energy and material balance model developed at the university of Oulu has been used to calculate effect of different raw materials like hydrogen reduced DRI and different scrap grades. The aim of this study was to model, how higher levels of metallic impurities affect to analysis and properties of steel and strip steel products. Based on results of simulation in HSC Sim model, steel mechanical properties were modelled with Remaster coil simulation tool. The energy and material balance model has been used together with the capacity calculations to find the optimal process.

RESULTS, FINDINGS, OUTPUT AND IMPACT

For SSAB, the basic dimensions and parameters of the coming new EAF process had to be designed using different calculation models and know-how from steelmaking to ensure effective use of different raw materials e.g. big amount of scrap and hydrogen reduced DRI. Different production scenarios have been compared to the target capacity, e.g. in terms of heat size and an understanding of the optimal production method has been formed. The productivity of the process and the time from tap to tap have been assessed and optimal parameters have been obtained using models and calculations.

The higher share of scrap in EAF charge causes higher metallic impurity levels in steel analysis. The main goal of HSC Sim simulations was to determine how much steel contains metallic impurities with different ratios of raw materials and various metallic impurity levels. With some practices metallic impurities can be removed from liquid steel in laboratory scale, but impurities cannot be removed along EAF route cost-effectively. However, management of impurities is possible with dilution by DRI and using cleaner scrap as a raw material.

According to study metallic impurities affect to yield and tensile strengths which increase when levels of impurities increase. Elongation and toughness decrease at the same time. Thickness of steel affect to changes of properties and differences between thicknesses increase during levels of impurities increase. However, the differences between changes were small for the steel grade under consideration.

Copper is the most critical impurity when significant amount of scrap is used as the raw materials. State of the art EAF process today is using a big hot heel, even more than 60 %. Hot heel hinders the transition to the production of cleaner steel grade. Developed energy and material balance model can be used to calculate this transition. According to the figure, it takes several heats to reach lower impurity levels with high hot heel.

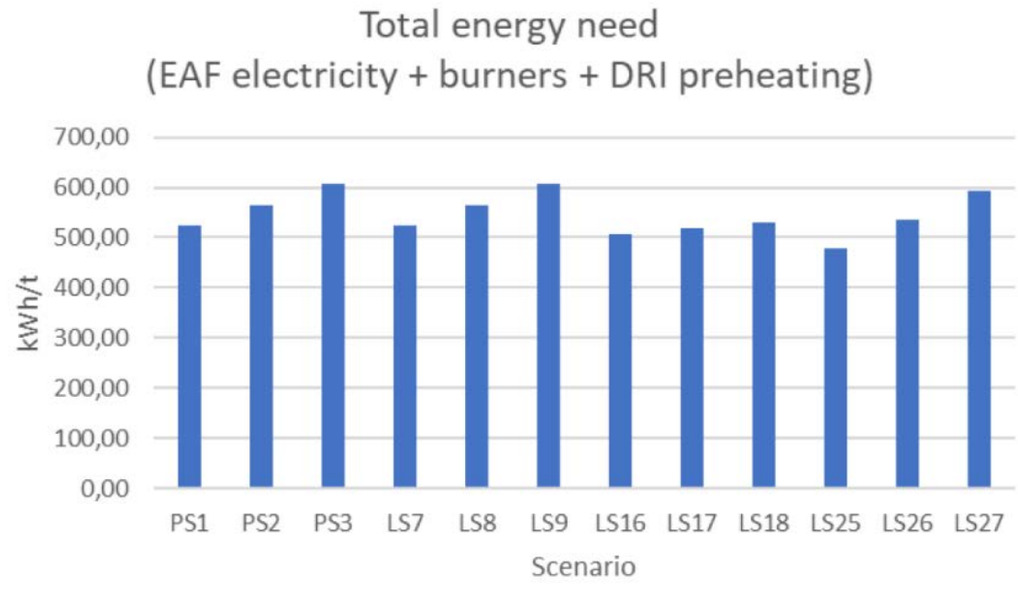

FIG 1 The total need of energy calculated by mass and energy balance model in the different scenarios including electricity for EAF, energy from gas burners and energy for DRI preheating. Rights owned by University of Oulu.

REFERENCES

Manuel Mehtälä, Management of metallic impurities in production of strip steels in EAF process, Master thesis, University of Oulu, 2023.

FFS | TOWARDS FOSSIL-FREE STEEL

CONTRIBUTORS

Ville Fomkin | Ovako Imatra, corresponding person
Anna Yrjönen | Carbofex
Jarmo Lilja, Seppo Ollila, Timo Paananen | SSAB Europe

3.2 EAF slag foaming

Hydrogen-reduced DRI is a new raw material, and its exact behaviour in steelmaking processes is unclear. This requires a lot of new research to control and optimise the process. Fossil-free steel production requires many new bio-based materials to replace the use of fossil coal, for example.

BACKGROUND

Effective slag foaming is essential in today's ultra-high-power EAF. The thermal load caused by the arc on the walls is high. Slag foaming is utilised to prevent the overheating of the walls. Fossil coal has typically been used to foam slag through the formation of CO. In the future, it must be replaced by fossil-free material like charcoal.

The feasibility of biochar has been investigated in several RFCS projects for EAF carbon injection material. In these projects, a good candidate material has not been found. A literature review and laboratory tests therefore had to be carried out to find suitable test material for industrial-scale trials.

SOLUTION, METHOD

The results of the laboratory experiments have been tested on an industrial scale at the Ovako, Imatra steelworks in the EAF process. The aim of this experiment was to validate the results of laboratory tests on an industrial scale and to find a fossil-free material that could foam the slag in the EAF. Based on laboratory tests, the biochar with the best slag foaming properties was selected for the production-scale slag foaming tests.

RESULTS, FINDINGS, OUTPUT, AND IMPACT

Selected biochar was used in four heats at EAF in Ovako, and the results of the slag foaming were promising. The trials proved that with the correct type of biochar it was possible to foam the slag. Biochar itself is in many ways a very different material from the fossil coke dust that is normally used. Although the analyses are very similar, the biochar density is lighter, and grain size is very small. This light and fine dust is difficult to transport and inject into the furnace. As a result of the experiments, it was found that certain modifications were needed to the existing injection equipment. The next step is to produce a larger amount of suitable material and run longer tests while trying to modify the feeders to work better with different types of coal powders. The research has increased knowledge about what kind of bio-based carbon material is suitable for slag foaming. In cooperation with biochar manufacturers, increased knowledge has also been gained about how suitable biochar can be produced and transported. Several producers are now investing in bio-coal production, and the next step is to find the most cost-effective material from these potential suppliers.

FIG 2 Foaming slag in EAF. Rights owned by Ovako.

REFERENCES

Eetu Hoikkaniemi, Use of biochar as a slag foaming agent in EAF steelmaking, Master's thesis, University of Oulu, 2022

FFS | TOWARDS FOSSIL-FREE STEEL

CONTRIBUTORS

Mikko Jokinen I LUXMET, corresponding person
Dr Matti Aula, Dr Dimitar Valev I LUXMET
Ville Fomkin I Ovako Imatra
Seppo Ollila I SSAB Europe
Henri Pauna I University of Oulu

3.3 OES online measurements

New steelmaking raw materials and materials also require advanced measurements to study and control the process. The rough environment in the electric arc furnace is challenging for online measurements. LUXMET is developing a measurement method which utilises the light emitting from the arc to analyse the slag composition and steel temperature.

BACKGROUND

The Luxmet research activities focused on developing online slag composition analysis for the ladle furnace process. The project was conducted in collaboration with the University of Oulu, Ovako Imatra, and SSAB Raahe.

The main objective of the work was related to reducing the use of lime and other slag additions in the ladle furnace, as well as paving the way for the transition from the blast furnace to electric arc furnace steelmaking.

SOLUTION, METHOD

Based on experience in the field of real-time optical emission measurements in high temperature metallurgical processes, the Luxmet optical emission measurement and analysis platform was chosen as the starting point for the implementation. Extensive development work was needed to adapt the system hardware for ladle furnace arc optical emission measurements.

RESULTS, FINDINGS, OUTPUT, AND IMPACT

A system was developed for measuring the arc emissions and, based on this data, determine the presence of selected elements in the slag. The development work was initially done during three measurement campaigns at Ovako Imatra, and the results were verified during two longer campaigns at SSAB Raahe.

The benefits of the solution are that the developed system enables real-time slag analysis to be done so that the process can be controlled dynamically. This reduces the use of additives and increases energy efficiency and the quality of the process's end results.

FIG 3 Sensor installed at ladle furnace at SSAB Raahe. Photographer Mikko Jokinen, rights owned by Luxmet Oy.

FFS TOWARDS FOSSIL-FREE STEEL

CONTRIBUTORS

Petri Sulasalmi, Eetu-Pekka Heikkinen, Ville-Valtteri Visuri
Process Metallurgy Research Unit I University of Oulu

3.4 Development of mass and energy balance models of new process routes for carbon-neutral steelmaking

BACKGROUND

The new way of making of steel requires planning and research on future production scenarios. The use of scrap, direct reduced iron (DRI), and their mixes will form the main raw material mix in the electric arc furnace (EAF) in the future. The limited availability of good-quality scrap in the future will increase the need for DRI. DRI enables genuinely fossil-free steel production. In addition, when using scrap with moderate or high impurity levels, DRI can also be used to dilute the impurity content of steel when added to the raw material mix. The raw material mix can consist of many scrap types, as well as different DRIs. Furthermore, when DRI is used in high proportions, the hot-heel practice is used to aid the melting of DRI. There will also be other changes in the traditional EAF process: the need for slag formers differs due to gangue in DRI. Injected and charged carbon, as well as burner gases, must be replaced with non-fossil alternatives, etc. All this yields a large number of possible steelmaking scenarios for the EAF process in the future. In this work, a mass and energy balance model for the electric arc furnace (EAF) process was developed to study the mass and energy balance of the EAF process in various production scenarios.

MATERIALS AND METHODS

The mass and energy balance model of the EAF process was implemented using HSC Sim software. The model consists of a total of 11 modules. The EAF process module forms the core of the model. The flow sheet of the model is presented in Figure 4.

The model allows several raw materials to be fed: four types of scrap, two types of DRI, slag formers, injected carbon, charge carbon, briquettes, and lanced oxygen. The model contains modules for preheating scrap and DRI. A gas burner module is included to introduce the possibility of chemical in addition to electrical heating. There is a module for the post-combustion of EAF off-gas which contains CO and H_2. In the model, the thermal energy of post-combusted off-gas is utilised in scrap preheating, a practice that is used in EAF steelmaking. The off-gas and dusts exit the EAF as a mixture. After scrap preheating, the off-gas and dust mixture is directed to the cooling module, where excess heat is released and not further employed in the model. However, the amount of excess heat is obtained as a result which allows an assessment of a possible utilisation for a chosen purpose. Finally, the dusts are separated from the off-gas in a separator module. The model's material outputs are molten steel, molten slag, splashes, cooled off-gas, and cooled dust. The model takes a hot heel practice into account which allows a share of molten steel from the previous melting to be used as an input in the next melting. The model is equipped with a user interface which allows the main inputs such as raw material compositions, temperatures of raw materials and output materials, and the share of DRI and scrap, etc. to be fed.

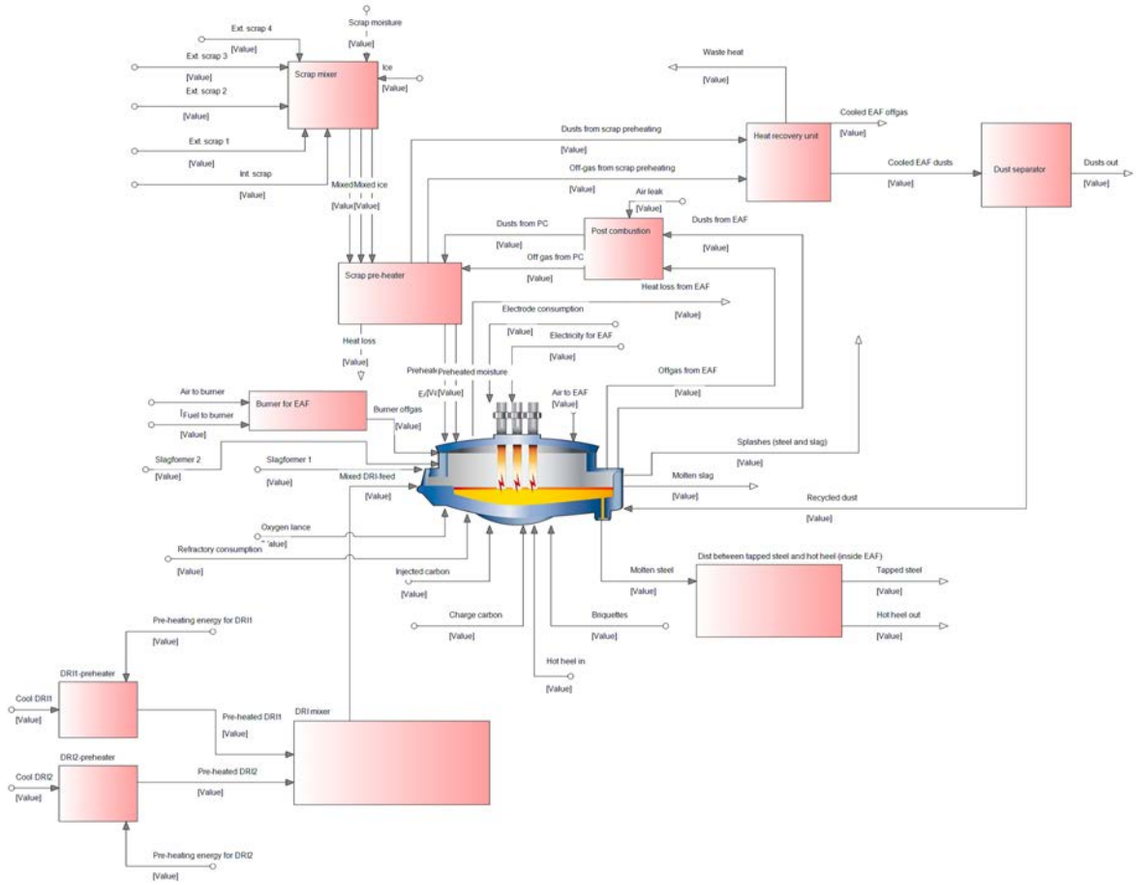

FIG 4 Flow sheet of the HSC Sim based mass and energy balance model.

RESULTS AND DISCUSSION

The model outputs have various results. The compositions are of molten steel and molten slag, as well as off-gas, dust, and splashes. The total energy consumption and CO_2 emissions are calculated. The main focus in the scenario studies, which were undertaken for SSAB as a commissioned project, was on total energy consumption in several production alternatives. Dozens of production scenarios were modelled by varying the basic scenarios. Figure 5 presents the scrap-DRI ratios in basic scenarios. Figure 6 presents an example of the results (total energy need and direct CO_2 obtained in various scenarios.

	Basic scenario 1	Basic scenario 2	Basic scenario 3
Scrap/DRI, %	80/20	50/50	20/80

FIG 5 Scrap-DRI ratios in studied scenarios.

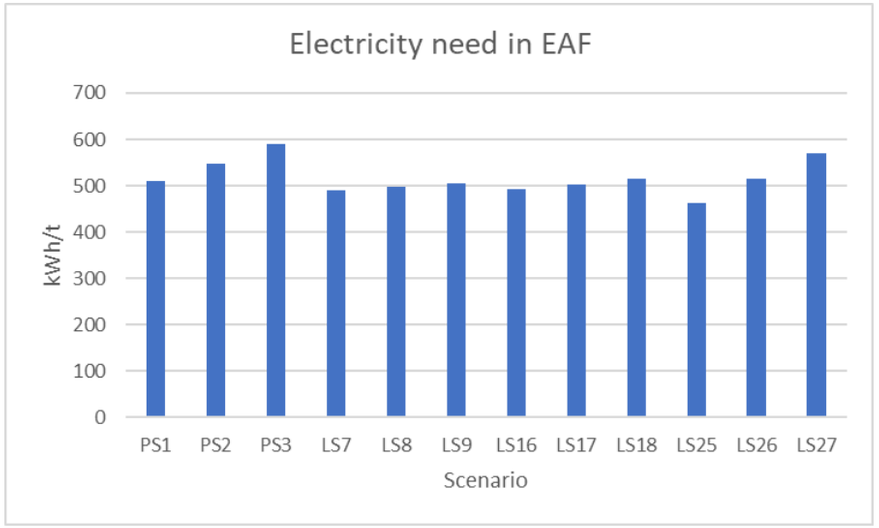

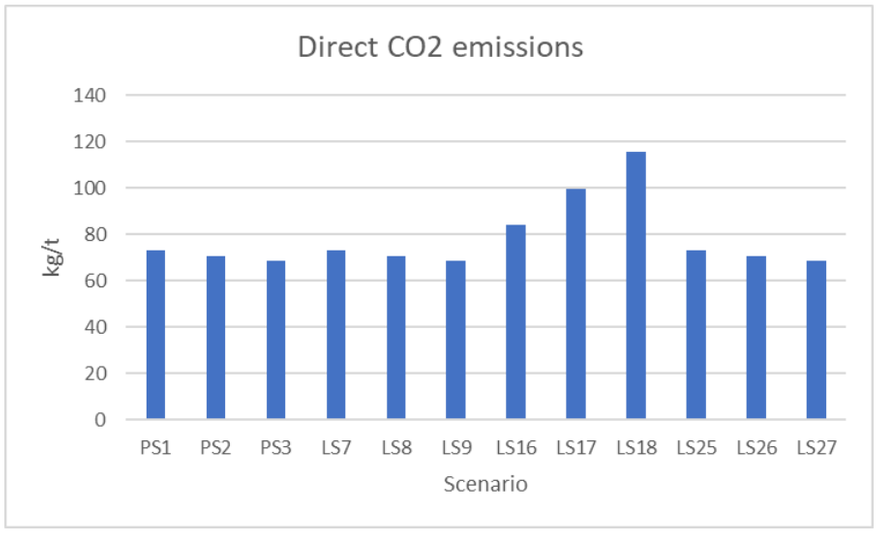

FIG 6 Example results from scenario studies: electricity consumption of EAF (upper figure) and direct CO_2 emissions (lower figure).

PUBLICATIONS AND THESES

Mitas B., Visuri V.-V., Schenk J., (2022) Mathematical Modeling of the Ejected Droplet Size Distribution in the Vicinity of a Gas-Liquid Impingement Zone, Metallurgical and Materials Transactions B, 53, pp. 3083–3094

M. Pylvänäinen, Nissilä J., Visuri V.-V., Laurila J., Niemi A. H., Tuomikoski S., Paananen T, Liedes T. Effect of Gas Forming Compounds on the Vibration of a Submerged Lance in Hot Metal Desulfurization, Steel Research International, 94, 2300072

Vuolio T., Visuri V.-V., Tähtilä H., Pekuri P., Fabritius T. (2024) The Synergistic Effect of Na2O on Hot Metal Desulfurization Kinetics in CaO-Na2O-SiO2-Al2O3-MgO Slag System, Chemical Engineering Science, 284:119525

Vuolio T., Visuri V.-V., Sorsa A., Paananen T., Tuomikoski S, Fabritius S. (2023) Machine Learning Assisted Identification of a Grey–Box Hot Metal Desulfurization Model, Materials and Manufacturing Processes, 38, 15, pp. 1983–1996

FFS TOWARDS FOSSIL-FREE STEEL

CONTRIBUTORS

Milja Raitanen, Henri Pauna, Tommi Kokkonen
Process Metallurgy Research Unit I University of Oulu

3.5 Alternative electrical melting process designs and melting behaviour of DRI

BACKGROUND

The use of direct reduced iron (DRI) will increase in steelmaking in the future. This is because the use of electrical melting processes is becoming increasingly common. Scrap has been a typical raw material in electric arc furnace (EAF) steelmaking, but the availability of good-quality scrap will be more difficult in the future as the demand increases. Scrap and DRI have different characteristics, especially if DRI is produced using H_2 as a reductant, and product does not contain any carbon. It is therefore important to study the behaviour of DRI when it is melted. DRI will play a special role in the future because it allows the production of genuinely fossil-free steels. On the other hand, the use of DRI with scrap will be important because it can be utilised to dilute the impurities originating in scrap. In this task, a literature review on the use of DRI as a raw material in the EAF process was conducted. In the second part, special equipment, an EAF simulator, has been developed and constructed to experimentally study the melting of scrap and DRI.

MATERIALS AND METHODS

The literature review starts by briefly introducing the various direct reducing processes (shaft furnaces, rotary hearth furnaces, rotary kilns, and fluidised beds) of iron. The form of iron ore in which the ore is fed to the process and the reducing agents for each process are also introduced. The EAF process is then introduced: the process design, process stages, and alternative process designs. A major emphasis is then placed on DRI as a raw material. The review goes through the charging practices of DRI and scrap. The effect on the energy consumption of the EAF when using DRI is assessed. The effect of DRI on the refractories and EAF slag composition and amount is also assessed. Finally, the review focuses on DRI's effect on dust formation, emissions and other parameters.

The unique EAF simulator was constructed during the FFS project in the Process Metallurgy Research Unit at the University of Oulu. Figure 7 shows the graphite electrodes and interior of the EAF simulator.

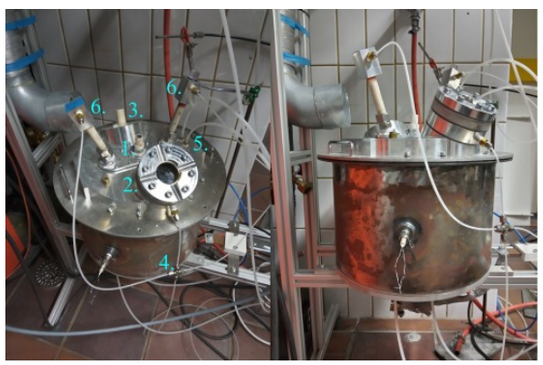

1. Inlet for the electrode
2. Window for camera
3. Port for OES equipment or off-gas/exhaust-gas removal
4. Argon gas inlet
5. Water cooling of the roof
6. Ports for material addition and/or OES equipment

FIG 7 The EAF Simulator.

The simulator enables the melting of burden material using electrical energy. The simulator consists of a steel frame which is insulated from inside. The innermost part contains a frame for a crucible in which sample is melted. A crucible roughly the size of a coffee cup can be used. Furthermore, the EAF simulator contains a roof equipped with holes for graphite electrodes. There are also two windows in the roof: one for observing experiments visually and for recording purposes, and one for the optical emission spectrometer (OES). The simulator underwent several improvements and changes after it was tested multiple times. The equipment is unique, and it establishes the possibility of studying the future fossil-free EAF process with various raw material mixes and enables the optimisation of the EAF process and the development of advanced monitoring and measurement technologies.

RESULTS AND DISCUSSION

According to the literature review, the most significant changes in the EAF process when using a larger share of DRI instead of scrap are increased slag masses and electrical energy consumption, as well as the longer process duration. The changes increase costs and/or decrease the efficiency of the process. In addition, the use of DRI results in several other changes: refractory wear becomes more complicated to control, demand for additive carbon and slag-forming agents increase, electrodes wear out faster, and the consumption of by-products changes. The use of DRI also has positive effects, including enhanced slag foaming (carbon-containing DRI) and decreased demand for natural gas burners. With respect to emissions, the direct and indirect CO_2 emissions of DRI melting were scarcely available. Furthermore, there is demand for more experimental data from pilot plants and industrial EAFs melting 100% DRI. To enable a massive growth of the technology, more research and industrial tests will be needed.

Preliminary melting tests were carried out with an EAF simulator for different materials. The first test was done with a steel plate, which was placed in the crucible and melted with an electric arc. The arc was successfully ignited, and some melt was produced, but the seal of the electrode melted. This led to a change of design regarding the electrode sealing. After the modifications, several other melting tests were conducted. The tested materials included blast furnace pellets, DRI pellets, and slag samples. Figure 8 presents images from the EAF simulator experiments.

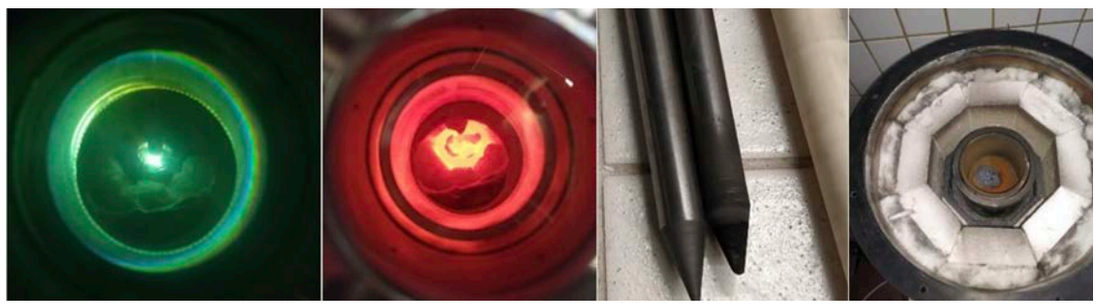

FIG 8 Images from EAF Simulator experiments.

PUBLICATIONS AND THESES

Raitanen, M. (2023) DRI as the Raw Material of EAF, Bachelor's thesis, University of Oulu

FFS TOWARDS FOSSIL-FREE STEEL

CONTRIBUTORS

Eetu Hoikkaniemi, Petri Sulasalmi, Aki Koskela, Riku Mattila
Process Metallurgy Research Unit I University of Oulu

3.6 Replacing fossil-carbon with alternative carbon sources as a slag foaming agent

BACKGROUND

Slag foaming is employed in an electric arc furnace (EAF) to improve the energy efficiency of the process, protect steel from reoxidation, and reduce noise pollution. Slag foaming is promoted by injecting suitable carbonaceous material into the slag–steel interface. Typically, the employed carbonaceous material (i.e. foaming agent) is fossil-based, e.g. coke dust, anthracite, or petrol coke. To produce fossil-free steel in the EAF (or to reduce the carbon footprint of the process in general), a non-fossil based alternative to traditional foaming agents must be found. For this, the use of biochar as a replacement for fossil-based carbon in slag-foaming practice has been studied. The results of previous studies related to the use of biochar as a foaming agent have been somewhat ambiguous: in some laboratory-scale experiments, foaming was successfully produced with biochar, although the measurement techniques of the foaming strength were quite unsophisticated; in the industrial-scale test, the results were unsatisfactory. In this study, the suitability of biochar for foaming purposes was studied in laboratory-scale experiments using several biochars and coke dust as a reference material. A unique experimental setup was developed for the studies. The work was started with a diploma thesis in which the experimental setup was built, and experiments with one biochar and coke dust were undertaken. Subsequently, the work continued with a series of experiments with a wider scope.

MATERIALS AND METHODS

In the diploma thesis, a literature review on the theory of slag foaming and previously undertaken studies related to the use of biochar as a foaming agent in an EAF was conducted before the experiments. Based on the previous studies, it was uncertain that biochar would be suitable for the application. However, guidelines related e.g. to slag basicity, effective viscosity, and FeO content were obtained from the theory for planning the experimental part. Figure 9 presents the experimental setup.

High-temperature experiments were conducted in a chamber furnace where slag was first melted in a MgO-C crucible before starting the injection. The injection of carbonaceous material into molten slag was conducted via a quartz lance. During the injection, nitrogen was used as a carrier gas. The experiments were monitored using a laser-aided visualisation system and recorded for post-processing, allowing the accurate measuring of the foaming. Several biochars of different quality in terms of fixed-C content were studied. The biochar was pre-treated (drying, grinding) sufficiently before the tests. Several slags of different basicity and FeO content were used. Regarding the effect of basicity, industrial slag was used. Basicity was modified by CaO addition to study the effect of FeO content on the synthetic slags used.

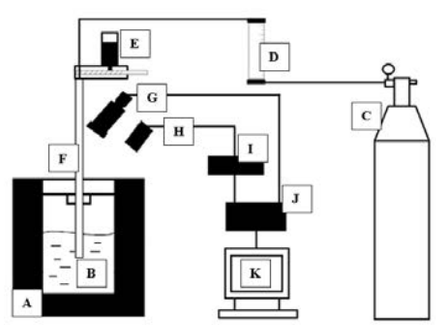

A-Crucible (MgO-C)
B-Slag or steel+slag
C-Carrier gas inlet
D-Rotameter
E-Screw feeder for carbonaceous powder
F-Lance (quartz pipe)
G-CCD camera
H-Laser illumination optics
I-Laser unit
J-Control unit
K-Computer

	MOISTURE (wt-%)	FIXED-C (db) (wt-%)	V.M. (db) (wt-%)	ASH (db) (wt-%)
Coke dust	0.23	82.95	1.47	15.58
BC1	9.46	87.19	0.83	11.98
TORRE_L	4.58	30.48	63.58	5.94
TORRE_H	4.05	51.66	40.89	7.45
BC2_F	1.49	45.88	26.76	27.36
BC2_C	4.97	60.51	24.55	14.94
HYCA	0	100	0	0

FIG 9 Experimental setup for slag foaming studies and proximate analysis of tested biochars.

RESULTS AND DISCUSSION

The experimental setup proved to work very well. In the diploma thesis, coke dust and BC1 were tested. The tests were started with coke dust to ensure that foaming was achieved with a material that was known to work in an industrial environment. Biochar A was very similar to coke dust in terms of fixed-C content. The slag was modified industrial slag from DRI melting with a basicity (SiO_2/CaO) of 1, 2, and 3. With both materials, the foaming was produced successfully when the basicity was 2 and 3. With a basicity of 1, the foaming was not produced with either material, suggesting that the basicity was too low, which is in accordance with the theory of foaming. In terms of foaming strength (i.e. the volume expansion of the slag), coke dust and BC1 performed equally well. In the subsequent experiments, multiple biochars of lower quality than BC1 were tested. A very high-grade char (HYCA) obtained as a by-product of methane pyrolysis was also tested. The test matrix was divided into two parts to study 1) the effect of basicity and 2) the effect of FeO content. In part 1, slag basicities of 1, 2, and 3 performed similarly to the first tests. In part 2, synthetic slags were used, and FeO content varied between them. In terms of the fixed-C content of the tested chars, the results in parts 1) and 2) were very coherent. It was clearly revealed that provided slag basicity was sufficiently high (at least 2), the higher the fixed-C content, the stronger the foaming was. With a slag basicity of 1, no foaming was produced with any of the carbonaceous materials. With higher basicity slags, foaming was produced. Again, coke dust and BC1 worked well, but HYCA also showed good performance (even better than the other two). In test series 2, it was noted that the overall foaming performance with synthetic slags was weaker than with industrial slags. However, the results were very coherent regarding fixed-C: better foaming was produced when fixed-C was high. The results were also in accordance with the theory of foaming in that the FeO content should be of a sufficient range to obtain good foaming. With a FeO content below 20 w-%, only weak foaming or no foam at all was produced. When FeO content was increased to 20 and 30 w-%, stronger foaming was observed. A further increase to 45 w-% decreased foam generation. This is in accordance with foaming theory, as high FeO decreases slag viscosity, which in turn does not favour foaming. Overall, the experiments were successful, and the results strongly suggested that biochar was indeed a suitable alternative to fossil-based carbon in foaming practice, as long as the quality of the biochar was sufficiently high and slag basicity was high enough.

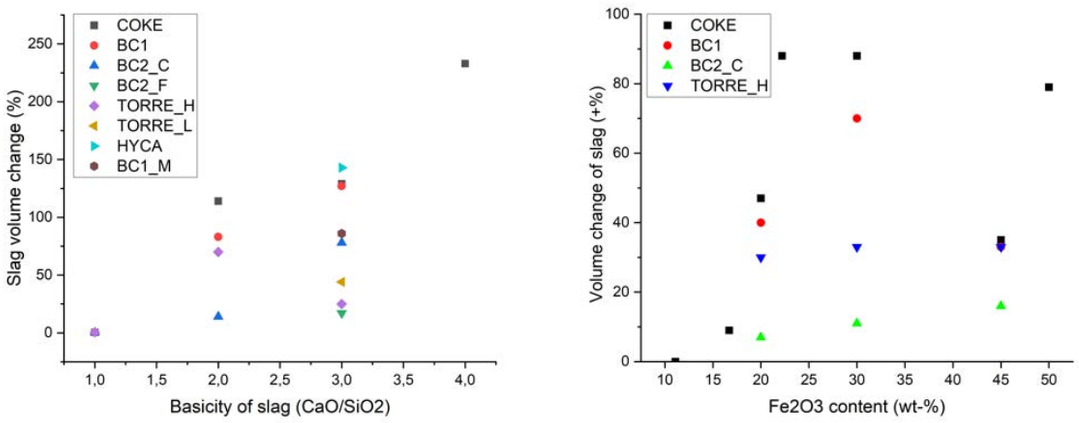

FIG 10 Results from foaming experiments in series 1) (left) and 2) (right)

PUBLICATIONS AND THESES

Hoikkaniemi, E., (2022) Use of Biochar as a Slag Foaming Agent in EAF Steelmaking, Master's thesis

E. Hoikkaniemi et al. (2023) Biochar as a slag foaming agent in EAF: A novel experimental setup, 5th European academic EAF Symposium, Oulu, Finland

FFS TOWARDS FOSSIL-FREE STEEL

CONTRIBUTORS

Manuel Mehtälä, Eetu-Pekka Heikkinen, Petri Sulasalmi
Process Metallurgy Research Unit I University of Oulu

3.7 Control of impurities in DRI/Scrap-based EAF steelmaking

BACKGROUND

Scrap used as a raw material in an electric arc furnace (EAF) includes more metallic impurities (Cu, Cr, Ni, Mo, Sn) than iron ore. Increasing the amount of impurities therefore causes unpredictable variation in steel analysis. Scrap-based production may cause an accumulation of impurities. The accumulation of impurities, also called tramp elements, causes a negative impact on the quality of recycled steel. Impurities increase strength and decrease toughness and the elongation of strips. The possibility of removing impurities in the EAF process is very limited. However, they can be managed by using cleaner scrap and diluting with DRI. In this task (OU WP1/Task 4), the aim was to study how higher levels of metallic impurities affected the analysis of steel and strip steel products in different scenarios.

MATERIALS AND METHODS

The work started with a short description of the EAF process, which was followed by a literature survey of steel scrap classification and standards, the trends of metallic impurities, practices for removing impurities, and the effect of metallic impurities on steel. Finally, the limit values of the metallic impurities of steel products were surveyed. The work was continued by means of mass and energy balance modelling using the model developed in OU WP1/Task 1 employing HSC Sim software. Based on the results of the mass and energy balance modelling, the mechanical properties of the strip steel products were modelled using Remaster software. The HSC simulations consisted of three production scenarios. Table 1 presents the scrap-DRI ratios in the studied scenarios. The impurity levels of scrap are presented in Table 2. The main idea of the HSC Sim simulations was to study the impurity level within produced steel when using a scrap of varying impurity content and direct reduced iron (DRI) as raw materials in different ratios.

	Basic scenario 1	Basic scenario 2	Basic scenario 3
Scrap/DRI, %	100/0	80/20	50/50

TABLE 1 Scrap-DRI ratios in HSC Sim simulations.

Percentile of data	Ni	Cr	Mo	Cu	Sn
10th percentile	0.06	0.05	0.008	0.163	0.009
25th percentile	0.079	0.083	0.011	0.242	0.012
50th percentile	0.097	0.117	0.014	0.294	0.014
75th percentile	0.123	0.154	0.021	0.341	0.021
90th percentile	0.148	0.2	0.03	0.388	0.035

TABLE 2 Impurity levels of scrap.

RESULTS AND DISCUSSION

According to the literature review, the removal of impurities from liquid steel is impossible via the EAF route. The management of impurities is possible with dilution by DRI and using cleaner scrap as a raw material. To study the dilution with DRI, HSC Sim and Remaster modelling were employed together to obtain the properties of the final strip products. Table 3 shows the results of HSC Sim modelling related to impurity content within liquid steel.

Percentile and		**Chromium**			
content in scrap	10. perc. 0.05	25. perc. 0.083	50. perc. 0.117	75. perc. 0.154	90. perc. 0.200
Scenario 1	0.05	0.083	0.116	0.153	0.199
Scenario 2	0.043	0.072	0.102	0.134	0.174
Scenario 3	0.034	0.056	0.079	0.104	0.135
Percentile and		**Copper**			
content in scrap	10. perc. 0.163	25. perc. 0.242	50. perc. 0.294	75. perc. 0.341	90. perc. 0.388
Scenario 1	0.165	0.244	0.297	0.344	0.392
Scenario 2	0.144	0.214	0.26	0.302	0.344
Scenario 3	0.114	0.169	0.205	0.238	0.27
Percentile and		**Nickel**			
content in scrap	10. perc. 0.06	25. perc. 0.079	50. perc. 0.097	75. perc. 0.123	90. perc. 0.148
Scenario 1	0.061	0.08	0.098	0.124	0.149
Scenario 2	0.053	0.07	0.086	0.109	0.131
Scenario 3	0.042	0.055	0.068	0.086	0.103
Percentile and		**Molybdenum**			
content in scrap	10. perc. 0.008	25. perc. 0.011	50. perc. 0.014	75. perc. 0.021	90. perc. 0.03
Scenario 1	0.008	0.011	0.014	0.021	0.03
Scenario 2	0.007	0.01	0.012	0.019	0.027
Scenario 3	0.006	0.008	0.01	0.015	0.021
Percentile and		**Tin**			
content in scrap	10. perc. 0.009	25. perc. 0.012	50. perc. 0.014	75. perc. 0.021	90. perc. 0.035
Scenario 1	0.009	0.012	0.014	0.021	0.035
Scenario 2	0.008	0.011	0.012	0.019	0.031
Scenario 3	0.006	0.008	0.01	0.015	0.024

TABLE 3 Content of metallic impurities of steel with different percentiles in scenarios 1–3.

The mechanical properties of strip steels were modelled with the Remaster coil simulation tool. As for impurities, the model only considers copper, nickel, chromium, and molybdenum. The Remaster coil simulation tool models six mechanical properties of steel by utilising historical data: yield strength values (RP02, REH, REL); breaking strength (RM); elongation (A5); and toughness (CV). The mechanical properties of ten steel grades were studied. According to the modelling results, the effects of metallic impurities on the mechanical properties of steel in modelling were similar to those in the literature in general. Yield and breaking strengths increased with levels of impurities. Elongation and toughness decreased at the same time. There were also some deviant behaviours with some steel grades, but differences in composition explain them. The thickness of steel affects the changes of properties, and differences between thicknesses increase as levels of impurities increase. However, the differences between changes were small for the steel grade under consideration. This study explored the effects of thicknesses with only one steel grade, and the generalisability of this conclusion requires further investigation.

PUBLICATIONS AND THESES

Mehtälä, M., (2023) Management of metallic impurities in production of strip steels in EAF process, Master's thesis, University of Oulu

FFS TOWARDS FOSSIL-FREE STEEL

CONTRIBUTORS

Julius Norrena, Tuomas Alatarvas, Jari Ruokamo
Process Metallurgy Research Unit, University of Oulu

3.8 Low-fossil alloying and production of high-alloyed steels and their effect on continuous castin

BACKGROUND

The planned transition of SSAB to fossil-free steelmaking will deploy thin slab casting to allow direct rolling after casting, decreasing specific energy consumption. Thin slab casting utilises higher casting speeds than conventional slab casting, and mould powder requirements differ accordingly. The rule-based selection of mould powders was reassessed in a completed master's thesis. An ongoing master's thesis focuses on the sustainable use of mould powders in continuous casting operations during steelmaking. In the thesis, industrial mould powders are characterised to assess their melting and solidification behaviour during steelmaking.

Defect formation is an issue which significantly reduces the material and energy efficiency of continuous casting. Its primary causes are related to steel composition, machine configuration, and the operation of the casting process. For example, residual elements in steel are known to contribute to defect formation by increasing microsegregation tendencies (sulphur, phosphorus) and contributing to the formation of chainlike manganese sulphide (MnS) precipitates (sulphur), which both decrease ductility during continuous casting. The eventual consequence of these detrimental metallurgical phenomena during continuous casting may be either a transverse or longitudinal crack in the as-cast product. Another detrimental phenomenon is the decrease in ductility caused by the formation of nitride precipitates due to the microalloying of elements such as niobium (Nb) and boron (B). Among others, these phenomena exemplify how the composition of steel and its adjustments essentially affect the formation and therefore the prevention of defects.

The importance of composition-related metallurgical phenomena in defect formation implies that a phenomenological approach to quality prediction is necessary to produce both existing and novel steel grades without defects. While many quality prediction approaches have been developed, they are not phenomenological, as they concentrate on the extensive utilisation of features (predictors) extracted from sensor measurements. Thus far, the lack of applicable tools at a global scale has probably contributed to the use of purely data-based models instead of models combining fundamental modelling and machine learning (ML) algorithms into phenomenological quality prediction models for the continuous casting of steel.

When considering the production of novel steel grades such as high-manganese steels or changes to existing alloying practices, it is essential to assess the availability of metallurgically reasonable and scientifically validated models for quality prediction. Although the individual quality prediction models themselves are usually specific to the steel grades or groups of similar steel grades to reliably assess the causes of defects, the stepwise development and validation of phenomenological models also provides a basis for a similar analysis for novel steel grades. In other words, by indicating that the proposed phenomenological approach to quality prediction succeeds with different steel grades, the procedure can also be utilised outside its original domain. This approach is best described as a phenomenological quality prediction framework, which is developed in this work based on the available fundamental tools for the modelling of solidification, heat transfer, and microstructure evolution during the continuous casting of steel.

MATERIALS AND METHODS

To investigate the melting and solidification behaviour of mould powders, equipment available at the Process Metallurgy Research Unit is utilised, including high-temperature furnaces and DSC–TGA (differential scanning calorimetry – thermogravimetric analysis). Characterisation before and after the experiments is carried out with devices available at the Centre for Material Analysis, such as FESEM (field emission scanning electron microscope) and XRD (X-Ray Diffraction). Furthermore, the high-temperature viscosity of the molten powders is estimated with Thermo-Calc software. InterDendritic Solidification (IDS) is a thermodynamic-kinetic-empirical model for simulating microstructural phenomena during the non-equilibrium solidification of steel in continuous casting. It considers phase transformations, the formation of different precipitates and inclusions, the microsegregation of solutes, grain growth, and the decomposition of austenite. Steel composition and cooling information are required as inputs in IDS. In this work, strand temperature profiles for IDS simulations are provided by Tempsimu, which is a fundamental tool for the three-dimensional simulation of steady-state heat transfer during continuous casting. Phenomenological quality criteria are extracted from the results of IDS simulations as features to predict the studied defects with ML models. By studying numerous different steel grades and defects, the phenomenological quality prediction framework is also developed and validated in a stepwise manner towards novel steel grades.

RESULTS AND DISCUSSION

As a result of the completed master thesis, ferrite potential was recommended for the classification of steel grades as peritectic and non-peritectic grades. According to the revised criteria, industrial tests with replaced mould powders were conducted, with promising results. Theesults concerning the prediction of transverse cracking with decision tree classifiers for two steel types are presented here. For peritectic C–Mn steel, 88% of defective and 96% of defect-free products are predicted correctly, as depicted in Figure 11. For the low-carbon B–Ti microalloyed steel, 98% of defective and 91% of defect-free products are predicted correctly, as depicted in Figure 12. These case studies exemplify the great potential of the phenomenological quality prediction framework.

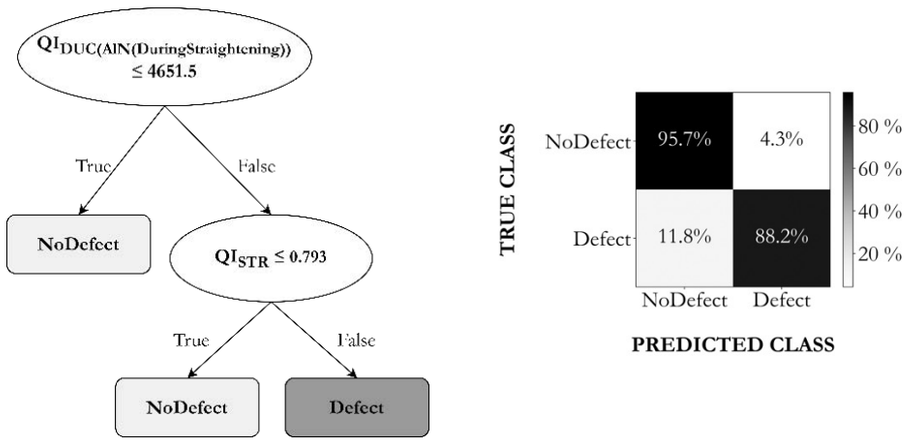

FIG 11 The decision tree predicting transverse cracking in peritectic C-Mn steel and the confusion matrix of predictions.

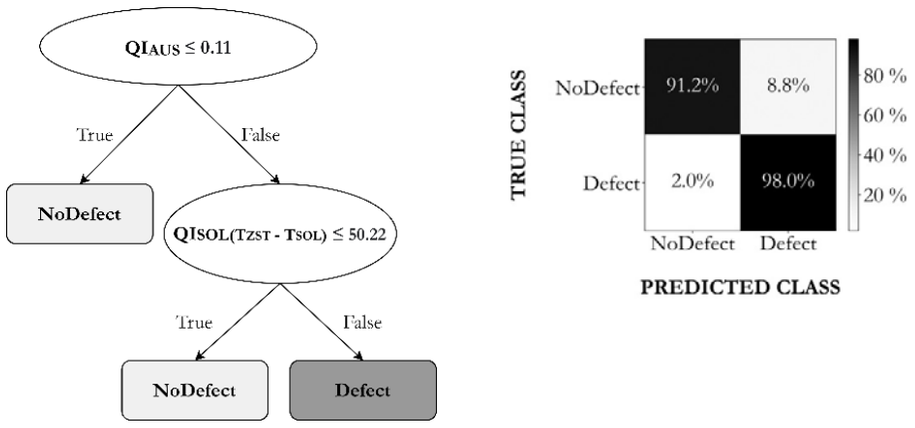

FIG 12 The decision tree predicting transverse cracking in low-carbon, B–Ti microalloyed steel, and the confusion matrix of predictions.

PUBLICATIONS AND THESES

Pyhtilä. T. (2022) Review of selection rules for casting powders. Master's thesis, University of Oulu.
Norrena, J., Louhenkilpi, S., Visuri, V.-V., Alatarvas, T., Bogdanoff, A., and Fabritius, T. (2023) Assessing the Effects of Steel Composition on Surface Cracks in Continuous Casting with Solidification Simulations and Phenomenological Quality Criteria for Quality Prediction Applications. Steel Research International, Vol. 94, No. 5. 2200746.

Norrena, J., Louhenkilpi, S., Visuri, V.-V., Alatarvas, T., Tähtilä, H., and Fabritius, T. (2023) Development of Machine Learning Models for Predicting Defect Formation in Continuous Casting of Steel with Phenomenological Quality Criteria from Solidification and Heat Transfer Simulations. 10th International Conference on Modelling and Simulation of Metallurgical Processes in Steelmaking (SteelSIM2023).

Norrena, J., Louhenkilpi, S., Visuri, V.-V., Alatarvas, T., Bogdanoff, A., and Fabritius, T. (2023) Development of Interpretable Machine Learning Models for Predicting Transverse Cracks in Continuous Casting of Steel with Phenomenological Quality Criteria from Solidification and Heat Transfer Simulations. Steel Research International (Submitted)

FFS TOWARDS FOSSIL-FREE STEEL

CONTRIBUTORS

Aidin Heidari, Mikko Iljana
Process Metallurgy Research Unit, University of Oulu

3.9 Fundamentals of iron ore reduction with H_2

BACKGROUND

The iron and steel industry is one of the most important industries, playing an undeniable role in the world's economy and having a huge effect on many other industries. Iron production needs a large amount of energy and reducing agents, which are coal and natural gas in the blast furnace and direct reduction respectively. In both routes, CO_2 is the main by-product, which makes ironmaking a significant element of global CO_2 emissions. Approximately 7% of total CO_2 in the world comes from the iron and steel industry. Researchers and industries are therefore seeking alternative technologies to decrease CO_2 emissions and make the process more environmentally friendly. Using hydrogen as a reducing agent has been considered the main alternative for the transition to fossil-free ironmaking. Hydrogen can be utilised in three different ways. First, a hydrogen injection into the blast furnace is used. In this method, some of the coke is replaced by hydrogen, which mitigates CO_2 emissions. Yet because the blast furnace has been designed to operate with coke, it is impossible to replace all the coke with hydrogen. The second method is direct reduction (DR), using hydrogen as a reducing gas, which can be conducted in shaft furnaces or fluidised bed reactors. The process can be done with 100% hydrogen, and if the hydrogen is produced with fossil-free methods like water electrolysis, the whole process is fossil-free. The third method is plasma hydrogen reduction, in which iron ore can be melted and reduced simultaneously in a plasma arc zone. Of the mentioned routes, hydrogen direct reduction is closer to scaling-up and industrialisation, and even some companies have started to design their plants. Thermodynamics and kinetics have been widely studied by researchers. Studies show that the reduction of iron ore with hydrogen is considerably faster than reduction with carbon monoxide. Hydrogen can diffuse faster because of its small molecules and higher mobility, and it also has a higher reaction rate. The kinetics of reduction is complex, and the reduction rate depends on many factors like temperature, gas flow, particle size, and mineralogy. Many elements of this field require more study and research.

Elements	Fe_{tot}	FeO	SiO_2	CaO	MgO	Al_2O_3	TiO_2	V_2O_5
Mass%	66.7	0.6	1.85	0.43	1.3	0.32	0.35	0.26

TABLE 4 The chemical composition of the blast furnace pellet.

Elements	Fe_{tot}	FeO	SiO_2	CaO	MgO	Al_2O_3	TiO_2	MnO
Mass%	65.79	2.2	3.78	0.73	0.45	0.64	0.23	0.028

TABLE 5 The chemical composition of the DRI pellet.

MATERIALS AND METHODS

Direct Reduced Iron (DRI) and blast furnace (BF) pellets were used as samples in this study. DRI pellets were obtained from a commercial supplier, and the blast furnace pellets were obtained from a steel-making plant.

To study the reduction of pellets, experiments were undertaken with the Linseis STA PT1600. This is simultaneous thermobalance (TG + DSC) with mass spectrometer gas analysis in reducing atmosphere up to 1,600 °C that can work with 100% hydrogen. Isothermal tests were conducted for 8-gram coarse single pellets at five different temperatures (700, 800, 900, 1,000, and 1,100 °C) with 100% H_2 and 100% CO with a flowrate of 2,000 ml/min.

To study the reduction behaviour of pellets on the surface, DRI and BF pellets were cut into thin slices using a diamond saw to obtain disc-shaped samples. The thickness of the discs was approximately 1–2 mm. All the samples were mounted on the APXPS system standard catalysis cell. The reduction experiments were carried out at the APXPS end station of the SPECIES beamline at the MAX IV Laboratory in Lund, Sweden. The samples were exposed to different gas mixtures at various temperatures and gas flowrates. Pure hydrogen, pure carbon monoxide, and various mixtures of both gases were used as reducing agents. The gas flowrates varied from 0.5 to 10 sccm. The temperature varied between 650 and 685 degrees Celsius.

RESULTS AND DISCUSSION

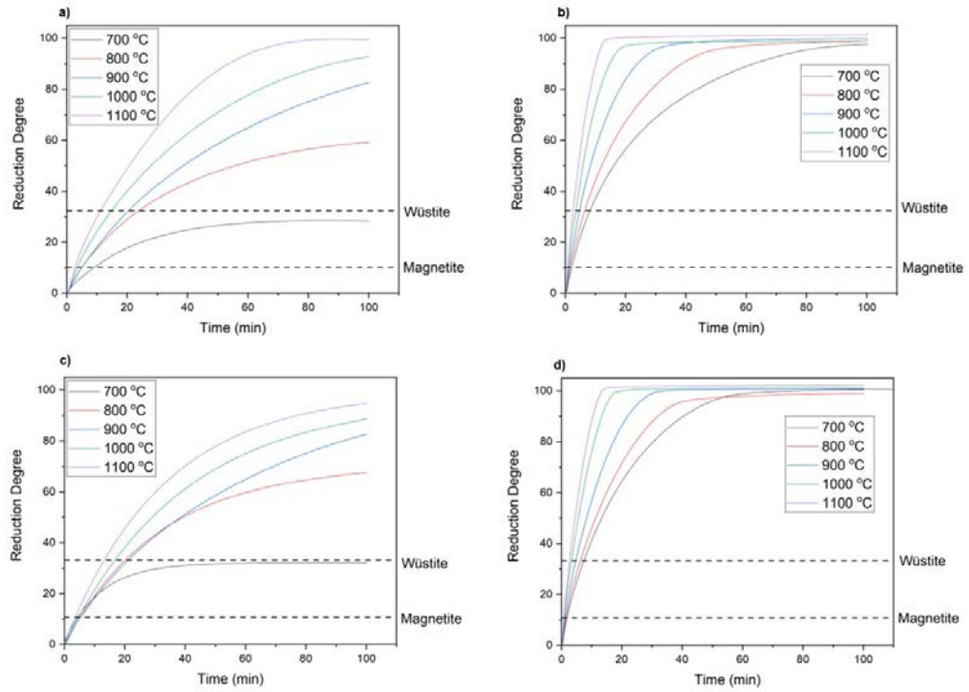

FIG 13 Reduction of single pellets at different temperatures a) DRI with 100% CO, b) DRI with 100% H_2, c) BF with 100% CO, and d) BF with 100% H_2.

It can be inferred from Figure 13 that in the reduction of both pellets, it was observed that hydrogen was significantly more efficient than carbon monoxide. However, when the reduction process was conducted at 700 and 800 °C, the BF pellet exhibited faster reduction rates and achieved higher levels of reduction, particularly when using carbon monoxide. This phenomenon was attributed to the greater presence of magnetite in the chemical composition of the DRI pellet. Conversely, at higher temperatures of 1,000 and 1,100 °C, the reduction of the DRI pellet outpaced that of the BF pellets, resulting in a greater reduction percentage, especially when carbon monoxide was the reducing agent. This divergence was mainly due to the higher porosity evident in the structure of the DRI pellets. The future plan includes a comprehensive investigation of various aspects related to pellet reduction. This will involve a detailed study of the morphology of reduced pellets, enabling a better understanding of their structural changes during the reduction process. Additionally, the plan encompasses an examination of the porosity in both initial and reduced pellets using microtomography, offering insights into how the internal structure evolves. Furthermore, the research aims to establish a compatible kinetics model to enhance the predictive accuracy of the reduction process. Finally, the strength of the reduced pellets will be explored, providing valuable data on their mechanical properties and durability. This multifaceted approach will contribute to a more thorough and informed analysis of pellet reduction processes.

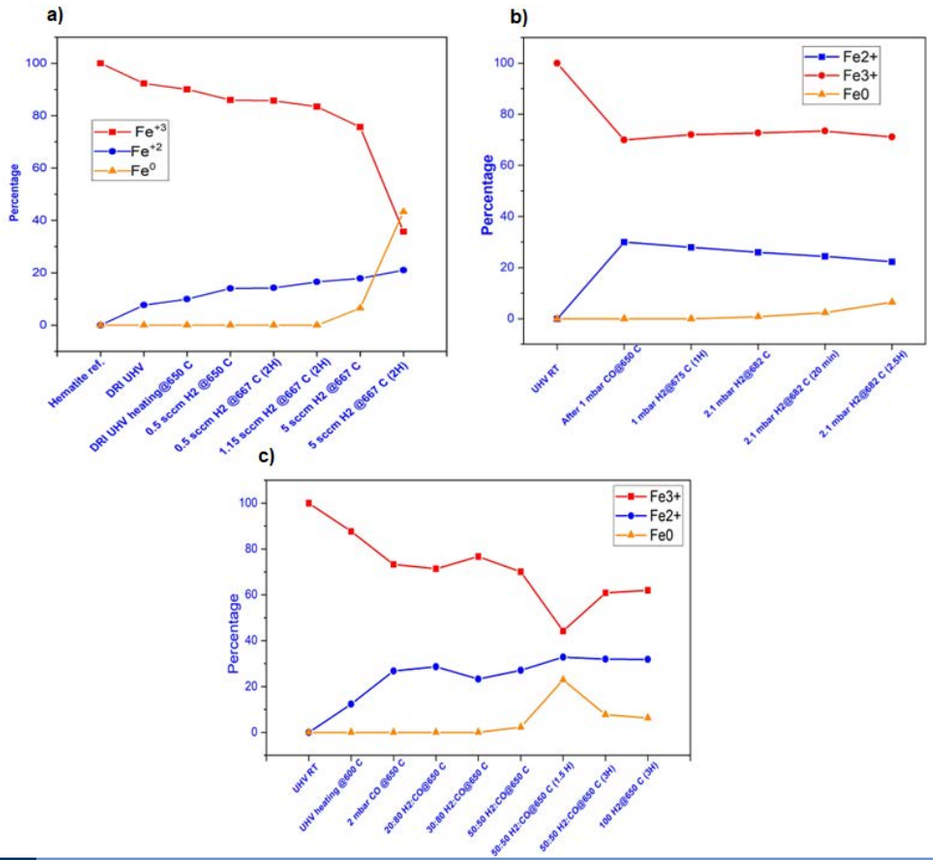

FIG 14 The percentage of Fe3+, Fe2+, and Fe0 during the reduction of a) a DRI pellet with H_2, b) a BF pellet with H_2, and c) a BF pellet with H_2-CO in different conditions.

Figure 14 reveals several key findings regarding the surface reduction process. First, increasing the gas flow, particularly with hydrogen, significantly enhanced the rate of reduction by promoting gas interaction at the reaction interface and facilitating surface diffusion. Moreover, raising the pressure resulted in an extended gas residence time and a notable increase in the reduction rate, with a more pronounced effect observed during the final stage of wüstite to metallic iron reduction. Notably, BF pellets achieved a reduction of approximately 20% when CO was added to the reducing gas mixture, while the presence of CO hindered the reduction of metallic iron in DRI pellets due to the higher magnetite content, which is less responsive to CO reduction at lower temperatures. Finally, reoxidation was detected during the reduction of BF pellets using a 50:50 H_2/CO gas mixture, with further investigation revealing that the water vapour and carbon dioxide generated during the reduction process became trapped in tiny surface porosities due to low flowrates and temperatures, leading to a significant increase in partial pressure and subsequent reoxidation, transforming reduced iron back into wüstite and magnetite.

PUBLICATIONS AND THESES

Heidari A., Iljana M., and Fabritius T. (2023) A comparison of reduction behavior of DRI and blast furnace pellets in CO-H_2 atmosphere, METEC & 6th ESTAD, Düsseldorf, Germany

Heidari A., Ghosalya M., Heikkilä A., Iljana M., Urpelainen S., and Fabritius T. (2023) Surface reduction behavior of iron oxides, oFEMS EUROMAT 2023, Frankfurt, Germany

Iljana M., Heikkinen E.-P., and Fabritius T. (2021) Estimation of Iron Ore Pellet Softening in a Blast Furnace with Computational Thermodynamics, Metals 2021, 11(10), 1515

Iljana M., Paananen T., Mattila O., Kodrakov M., and Fabritius T. (2022) Effect of Iron Ore Pellet Size on its Metallurgical Properties, Metals 2022, 12(2), 302

Heidari A., Niknadah N., Iljana M., and Fabritius T. (2021) A Review on Kinetics of Iron Ore Reduction by Hydrogen, Materials, 14(24), 7540

Iljana M., Abdelrahim A., Bartusch H., and Fabritius T. (2022) Reduction of Acid Iron Ore Pellets under Simulated Wall and Center Conditions in a Blast Furnace Shaft, Minerals 2022, 12(6), 741

FFS TOWARDS FOSSIL-FREE STEEL

CONTRIBUTORS

Emiliano Salucci, Antonio D'Angelo, Snigdha Ghosh, Lei Shao, Meng Li, Guanwei Zhou, Henrik Saxén | Åbo Akademi

Timo Paananen, Jarmo Lilja | SSAB

3.10 Iron ore reduction with H_2

To substantially reduce the carbon dioxide emissions in steelmaking, the iron ore reduction step must be undertaken by a reductant other than carbon (monoxide). The present task studied the use of hydrogen by carrying out reduction experiments on iron ore fines at a laboratory scale, followed by the mathematical modelling of the reduction of single particles. Many reduction experiments were undertaken to provide information used in the estimation of parameters in a single-pellet model based on a three-interface shrinking core approach. A one-dimensional static model of a direct reduction shaft was developed and applied to analyse efficient ways of operating the industrial process, and how its performance changed with variations in the boundary conditions.

BACKGROUND

The main reason for the large emissions of carbon dioxide in traditional steelmaking is the use of coal and coke in the reduction of iron ores. As the processes have evolved over time and been subject to optimisation, it is no longer possible to substantially reduce the emissions, particularly since the blast furnace process cannot operate without coke. The option of modifying the other main production route of primary steelmaking, i.e. the direct reduction (DR) process, operating on hydrogen instead of natural gas has been suggested as a potential solution. For sustainable operation, the hydrogen must originate from non-fossil resources (e.g. water electrolysis based on green electricity), and the technological challenges of operating a DR furnace on pure hydrogen must be resolved. The present task of the FFS project addressed several important issues in the development and operation of future hydrogen-based DR processes, with the main focus on experimental work on the hydrogen reduction of iron ore fines, the modelling of the reduction of single iron oxide particles, and the simulation and optimisation of the industrial hydrogen-based DR process.

MATERIALS AND METHODS

Iron oxide fines were reduced by hydrogen-containing gas in small beds or monolayers in AutoChem 2920 and Belcat II analysers respectively (Figure 15, top row). The progress of the reduction was followed by off-gas thermal conductivity (TCD) or composition measurements (Figure 15, bottom row). Experiments undertaken at many different temperatures and with H_2-Ar gas mixtures clearly demonstrated the effect of hydrogen concentration and temperature on the reduction rate. The initial and reduced fines were analysed by XRD and SEM to study the changes and progress of the reactions. The total iron content and specific surface were also measured.

A single-particle model based on a three-interface shrinking core approach was developed (Figure 16, left) with special attention paid to the numerical robustness of the model executed in different conditions. This is imperative for a successful estimation of kinetic parameters. As the reduction in the small bed of fines (AutoChem 2920) is affected by changes in the gas composition along with the gas flow, a dynamic model of the small bed was also developed.

To analyse the behaviour of industrial DR shaft furnaces operating on hydrogen, a one-dimensional static simulation model was developed and applied to study the effect of operation conditions on reduction performance. The model estimates the gas and solid temperatures and composition along the vertical coordinate of the shaft and can be used for a fast prediction of the effects of different parameters and boundary conditions on the internal state and for techno-economic analysis.

RESULTS AND IMPACT OF THE WORK

Extensive reduction experiments in gas mixtures with different hydrogen ratios and temperatures (400–1,000 °C) were undertaken in the project (Salucci et al. 2023). The results of the experiments revealed the role of hydrogen concentration, gas flowrate, and temperature on the rate of the reduction steps. This formed the basic information needed for the estimation of parameters in the kinetic models. Using the single-particle reduction model developed based on the shrinking-core concept combined with a dynamic model of the bed, it was demonstrated that the gas composition changes observed in the reduction experiments could be qualitatively reproduced without a parameter estimation. The right panel of Figure 16 shows the simulated thermal conductivity of the outgoing gas for "reduction experiments" carried out at different temperatures, exhibiting regions where the progress of the reactions is limited by equilibrium constraints, exactly as in the experimental setup (Figure 15). This demonstrated the feasibility of the model, which is a prerequisite for a future successful kinetic parameter estimation phase.

In the simulations of the industrial DR shaft furnace, primary attention was focused on addressing the limitations of the process and finding remedies to relax key constraints (Yu et al. 2021). A notable limitation is that the water-hydrogen ratio of the gas in the upper shaft approaches equilibrium, which makes the iron oxide reduction reactions very slow. This leads to the formation of a "chemical reserve zone", where the temperature is also constant (Figure 17, red lines in the left subpanels). Although the existence of corresponding reserve zones in the blast furnace is advantageous, it is detrimental for the operation of the DR furnace, as it reduces the utilised furnace volume and limits hydrogen utilisation. As a remedy, the injection of reducing gas at dual levels was proposed and studied, showing encouraging results (Figure 17, blue lines in the left subpanels).

The DR shaft model was also used to study means of enhancing the thermal and chemical efficiency of the process (Shao et al. 2023). The sensitivity to different design variables and boundary conditions was analysed in an extensive simulation study that clarified the primary means for achieving an efficient state of the operation of the process (Figure 17, right). This is particularly important, as the operating costs of the DR furnace using green hydrogen are considerably higher than for a blast furnace. The model developed provides a means to finding optimal operations conditions considering the prevailing external conditions (e.g. the price of green electricity, penalty for CO_2 emissions, etc.) and makes it possible to analyse how innovative modifications of the system could improve its performance. Furthermore, the simulation model will be an important tool for process analysis and troubleshooting when hydrogen-based DR furnaces are built on an industrial scale.

Another important result is that the research activities in FFS on hydrogen reduction and its implication for the steelmaking processes initiated several research proposals under Horizon Europe with the international partners of FFS. Three of these have now been granted and will support the research at the laboratory, promoting further international collaboration in the field.

REFERENCES

Salucci E, Ghosh S, Russo V, Grénman H, and Saxén H. (2023) Modelling of iron oxide reduction with hydrogen. Proceedings of the 33rd European Symposium on Computer Aided Process Engineering (ESCAPE33), Athens, Greece, June 2023.

Salucci E, D'Angelo A, Ghosh S, Russo V, Grénman H, and Saxén H. (2023) Modelling of iron oxide reduction with hydrogen – from intrinsic kinetics to dynamic bed operation. Paper presented at the 14th European Congress of Chemical Engineering (ECCE2023), Berlin, Germany, September 2023.

Salucci E, Ghosh S, Russo V, Grénman H, and Saxén H. (2023) Modelling of iron oxide reduction with hydrogen. Paper presented at the SteelSim 2023 conference, University of Warwick, UK, September 2023.

Shao L, Xu J, Saxén H, and Zou Z-S. (2023) A numerical study on process intensification of hydrogen reduction of iron oxide pellets in a shaft furnace. Fuel, Vol. 348 (2023) 128375.

Yu S, Shao L, Zou Z-S, and Saxén H. (2021) A Numerical Study on the Performance of the H_2 Shaft Furnace with Dual-row Top Gas Recycling. Processes, Vol. 9 (2021) 2134.

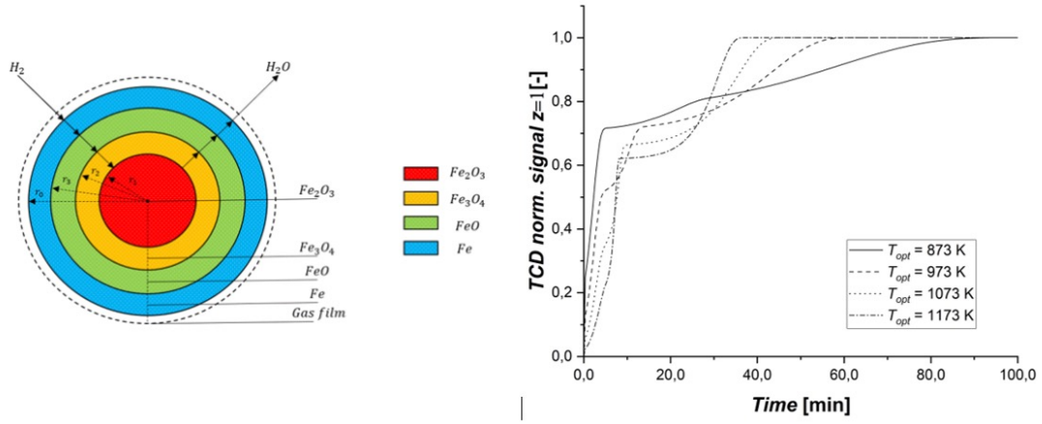

FIG 16 Three-interface shrinking core model (left) and simulated thermal conductivity of gas flowing out from the bed at different operating temperatures (right).

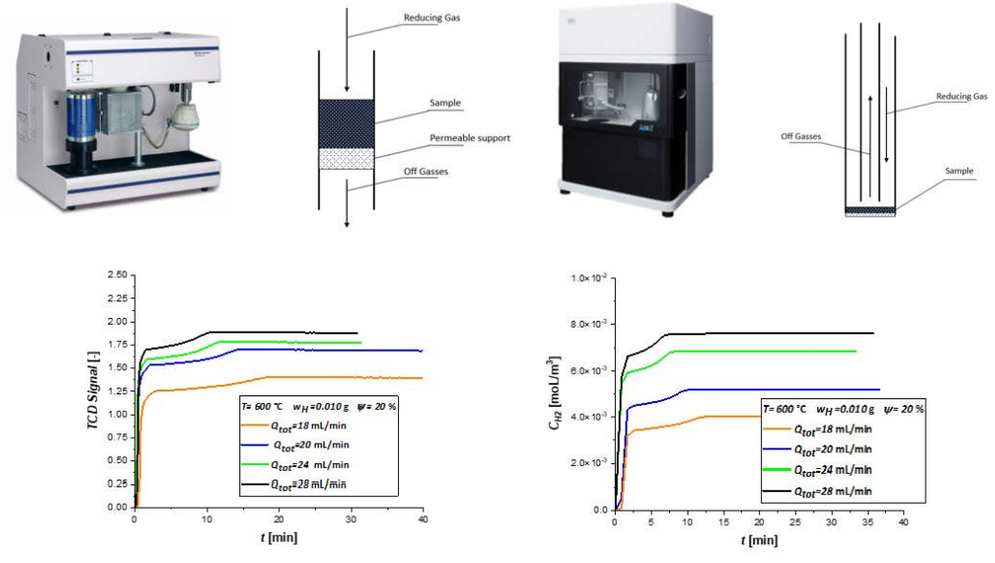

FIG 15 Top:AutoChem 2920 analyser with bed configuration (left) and Belcat II analyser with mono-layer configuration (right) for small-scale hydrogen reduction experiments. Bottom: Composition of outgoing gas by thermal conductivity measurements (left) and micro-gas chromatograph measurements (right).

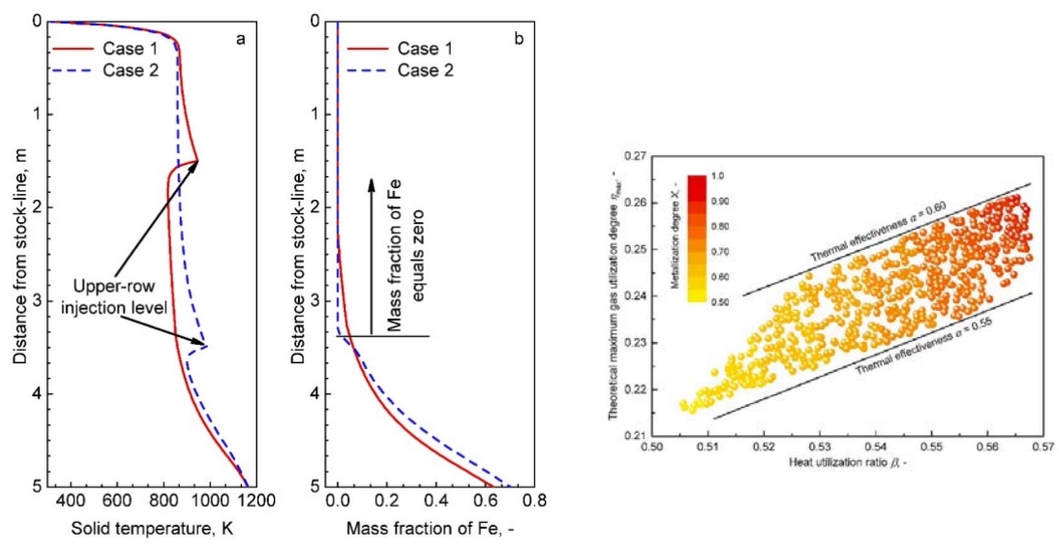

FIG 17 Left: Vertical simulated solid and gas temperatures and mass fraction of iron in the burden for hydrogen-based DR shaft operation with single (red lines) and dual (blue lines) gas injection levels. Right: Gas utilisation degree versus heat utilisation ratio for different operation points of the DR shaft furnace. The achieved metallisation degree is indicated by the colours of the points.

FFS TOWARDS FOSSIL-FREE STEEL

CONTRIBUTORS

Henri Pauna I Process Metallurgy Research Unit, University of Oulu
Mikko Jokinen I Luxmet Ltd.

3.11 Online slag composition analysis and evaporation studies at ladle furnaces

BACKGROUND

To speed up the slag composition analysis of electric steelmaking, which traditionally requires e.g. sample preparation, online solutions are required. One such analysis method is optical emission spectroscopy (OES), which can withstand the harsh measurement environment and measure light directly from the electric arc plasma and surfaces without the need of external interference (such as laser-based plasma). In this project, the purpose of the OES analysis by UOULU was 1. to identify slag species from the spectra, 2. to evaluate the molten bath temperature, and 3. to study the evaporation behaviour of slag species in the plasma. The monitoring of lime was especially of interest due to the relatively high CO_2 emissions, which were related to the production and use of lime.

MATERIALS AND METHODS

Optical emission spectroscopic applications in the steel industry are based on measuring the light from high-temperature objects such as electric arc plasma and molten or solid surfaces. In the case of electric arc plasma, the emitted light consists of unique optical emission lines that originate in atoms and molecules radiating within the plasma, allowing the identification of radiating species. In the case of surfaces, the radiation consists of thermal radiation, allowing temperature estimation. In this project, OES spectrometers were installed by Luxmet Ltd. in the ladle furnaces of Ovako and SSAB to measure the light from the electric arc and the molten surface. In addition, new applications of OES were studied with the hydrogen plasma smelting reduction (HPSR) and steelmaking burners.

RESULTS AND DISCUSSION

Figure 18 shows a five-minute example from the SSAB ladle furnace with the time evolution of the estimated temperature in Kelvin, and optical emission line intensities for Na I, CaO, and Ca II, where I and II refer to neutral and ionised atoms respectively. Eight spectra from the instances of the vertical dashed lines are illustrated in e) – l). The temperatures were determined with an equation derived from Wien's law, as in previous research on the industrial electric arc furnace [1]. The increases in Na I and temperature are well correlated, indicating the use of burners at these instances to maintain the temperature of the melt. Spectra in e) and f) show optical emissions from the arc plasma, and g) – l) from the molten surface. Figure 19 showcases the identification of radiating species from the spectra. The optical emissions from Ca I, Ca II, and CaO especially show promise for online analysis related to lime. One of the most notable achievements of the measurements was that ultraviolet (UV) light could also be detected from some heats at the ladle furnace. The visibility of UV light has been problematic in the past due to the absorption of light by dust, but these results show promise in analysing the spectra above 340 nm. Several important species such as Al I, Ca II, and Mn I reside in UV light. In addition, new fields of OES analysis, namely HPSR and the oxyfuel cutting burner, were investigated during this project.

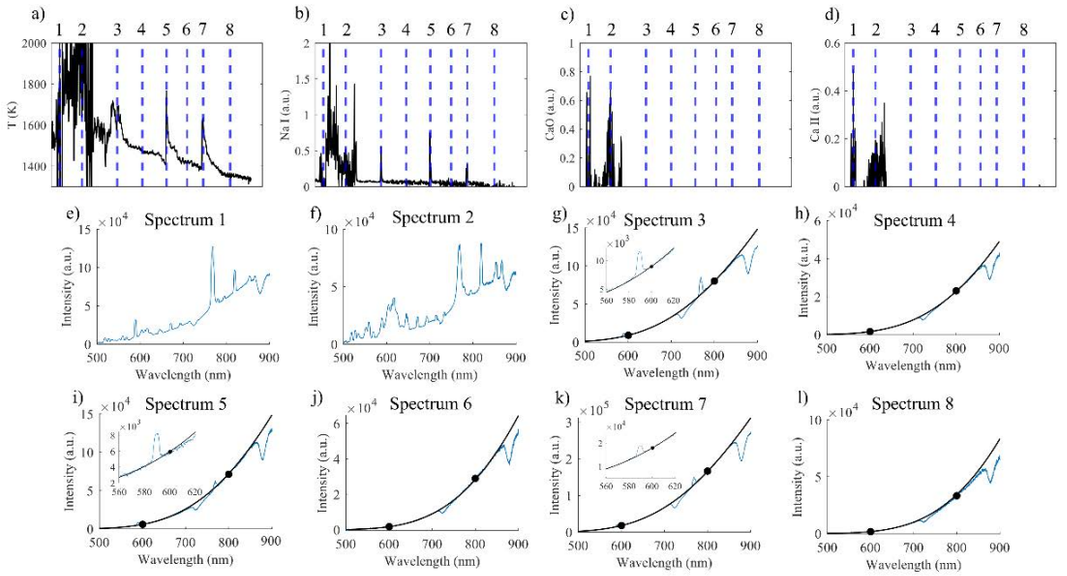

FIG 18 Five-minute time evolution graphs from the SSAB LF for a) temperature, b) Na I, c) CaO, and Ca II derived from the spectra. The vertical dashed lines depict the example spectra that are shown in e) – l), where the spectrum is in blue, the fitted temperature curve is the black line, and the two dots mark the wavelengths used for the temperature fit. A magnification of around Na I is shown in g), i), and k).

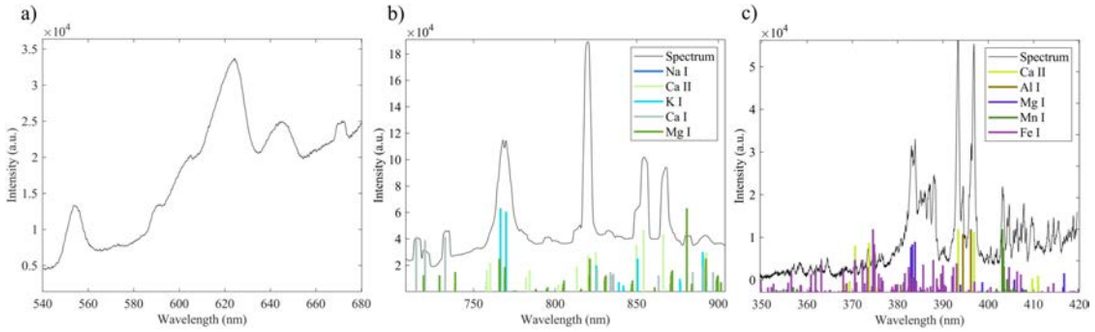

FIG 19 Most notable species in the OES spectra from the SSAB ladle furnace for a) CaO band from 550–560 and 590–625 nm, b) 700–900 nm, and c), 350–420 nm.

FFS | TOWARDS FOSSIL-FREE STEEL

These applications played a crucial role in advancing the Process Metallurgy research unit's (MET) research on fossil-free steelmaking as experts in process monitoring. Both topics have successfully acquired EU funding due to the efforts made in the FFS project, allowing MET to further develop the methods towards environmentally friendly steelmaking.

PUBLICATIONS AND THESES

Pauna, H. et al. (2022) Hydrogen plasma smelting reduction process monitoring with optical emission spectroscopy: Establishing the basis for the method, Journal of Cleaner Production, Vol. 372, 133755.

Pauna, H. et al. (2022) Optical emission spectroscopy as a tool for process control of steelmaking burners, 8th International Congress on the Science and Technology of Steelmaking.

REFERENCES

[1] Aula, M. et al. (2015) Optical Emission Analysis of Slag Surface Conditions and Furnace Atmosphere during Different Process Stages in Electric Arc Furnace (EAF), 55(8), 1702–1710.

FFS TOWARDS FOSSIL-FREE STEEL

CONTRIBUTORS

Joonas Ilmola, Oskari Seppälä, Joni Paananen, Jari Larkiola
Material and Mechanical Engineering Research Unit,
University of Oulu

3.12 Hot rolling and models for new carbon-free steels

BACKGROUND AND DESCRIPTION

Every year, digitalisation is playing a bigger role in the steel industry. Models for predicting metallurgical phenomena, rolling mechanics, and microstructure have commonly been used in the development of novel steel grades. These individual models may predict certain phenomena thoroughly, but input values are usually based on an assumption or a "good guess". To produce reliable boundary conditions for these models of individual phenomena, a virtual rolling mill is developed. This model complex computes the whole process of the hot strip mill from roughing to accelerated water cooling on a run-out table. Strip location and temperature evolution is calculated continuously as presented in Figures 20 a and 20 b. Thermal and thermo-mechanical (rolling stands) boundary conditions are in accordance with the process layout. Input data for the model are automatically read from raw process data. Rolling parameters are calculated using a coupled ARCPRESS model developed by the authors, which calculates normal and frictional shear stress distributions in the roll gap to predict roll forces and displacements of the work roll surface. Recrystallisation is considered when calculating the flow stress of the rolled strip. Phase fractions during water cooling are also calculated. The virtual rolling model minimises the need for parameter speculation, as all the parameters are calculated throughout the process. All the input values are read from actual process data, and the metallurgical and mechanical state of the strip are computed throughout the process. The virtual rolling mill is based on state-of-the-art phenomenological models and experimentally studied metallurgical and physical phenomena, along with the thermomechanical response of the actual rolling process.

20 a

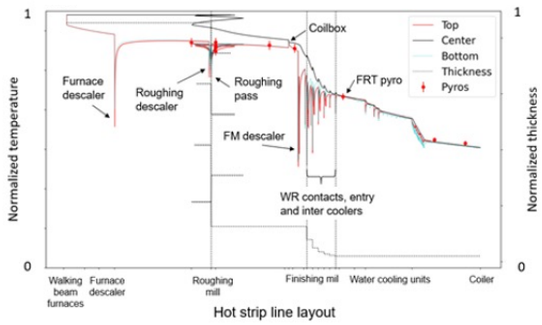

20 b

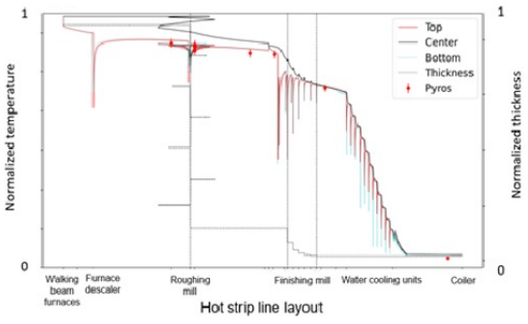

FIG 20 Simulated temperature paths over a hot strip rolling line in the virtual rolling mill.

MATERIALS AND METHODS

The hot strip rolling process contains many metallurgical and physical phenomena. To produce high-quality steel strips with the desired mechanical properties, the Thermomechanically Controlled Process (TMCP) must be managed. This requires a deep knowledge of thermomechanical physics and physical metallurgy. Plenty of research knowledge is available on these phenomena, so the main issue is not the lack of research information. Individual phenomena regarding metallurgy and rolling mechanics are well known, and advanced individual models have been developed to study them. The problem is to combine the individual models in a coherent model complex. In this study, the models have been combined in such a complex, called a virtual rolling mill.

The virtual rolling mill can obtain boundary conditions for each phenomenon in the process and couple all the separated models together. This enables all physical and metallurgical phenomena to influence each other similarly, as in a real process. The virtual rolling mill can be used to calculate any steel grades.

RESULTS AND DISCUSSION

Figures 21 a and 21 b show a contour plot of temperature, RX fraction, grain size, and cumulative strain in roughing and finishing rolling processes. The charts are centred for a better comparison between rolling passes. The change in thickness is caused by the rolling pass. Temperature, process time, and thickness values in the following results are normalised due to business secrets. These metallurgical phenomena are calculated simultaneously with the temperature evolution calculations presented in Figures 20 a and 20 b.

21 a 21 b

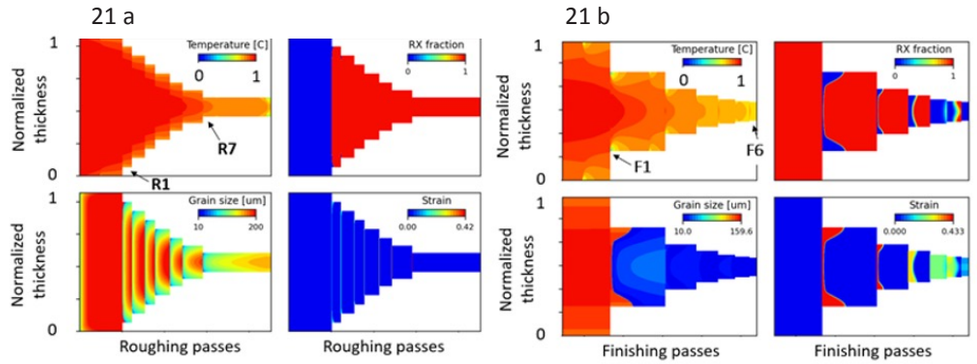

FIG 21 Temperature, RX fraction, grain size, and cumulative strain in roughing and finishing rolling.

For validation, data from 12,300 produced hot strips were gathered and simulated with the virtual rolling mill. The strips were randomly chosen and contained multiple different steel grades. The temperature errors between measured and calculated CBT and FRT temperatures are depicted in Figure 22. A comparison between measured and calculated roll forces for roughing "R" (87,094 passes) and finishing "F" (74,652 passes) rolling passes is also shown in Figure 22.

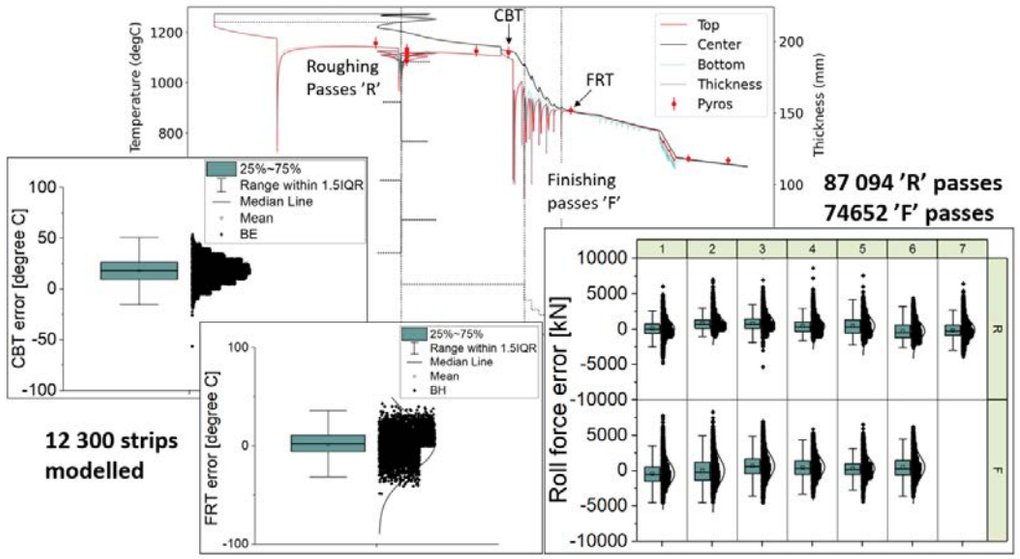

FIG 22 Validation of temperature calculations and roll force prediction of virtual rolling model.

PUBLICATIONS

Ilmola, J., Seppälä, O., Pohjonen, A., and Larkiola, J. (2022) Virtual rolling automation and setup calculations for six stands FEM finishing mill, IOP Conference Series: Materials Science and Engineering, 1270, 012060

Ilmola, J., Paananen, J., Seppälä, O., Pyykkönen J., and Larkiola, J. (2023) Phenomenon Based Model for Virtual Hot Strip Rolling, Thermec conference, (Accepted)

Ilmola, J., Paananen, J., and Larkiola, J. (2023) Effect of work roll surface warming on hot strip temperature development in industrial scale virtual rolling model, Numiform conference (Accepted)

Seppälä, O, Pohjonen A., Mendonça J., Javaheri V., Podor R., Singh H., and Larkiola J., (2023) In-situ SEM characterization and numerical modelling of bainite formation and impingement of a medium-carbon, low-alloy steel, Materials & Design, 230, 111956

FFS TOWARDS FOSSIL-FREE STEEL

CONTRIBUTORS

Markus Partanen, Kimmo Tapojärvi, Janne Pajala, Saku Puhakka, Tommi Hiltunen, Seppo Ahola I Tapojärvi

Timo Mäenpää, Antti Tikanmäki, Siva Ariram, Miikka Huusko, Juha Röning
University of Oulu Biomimetics and intelligent systems group (BISG)

3.13 Autonomous material handling

BACKGROUND

Emission-free solutions must be developed in the process industry. The electrification of material handling is one step towards this goal. Autonomous material handling is part of the digitisation of processes and provides an opportunity to improve the safety, quality, and efficiency of processes and reduce the burden on the environment. New solutions are being developed and are coming onto the market in the transition to electrical operation of heavy equipment. The goal is to save energy and personnel costs and improve safety.

SOLUTION, METHOD

Portable sensor system

Controlling autonomous vehicles can be accomplished with less data than needed for VR reconstruction. For this purpose, BISG-Robotics has developed a modular sensor system that can easily be mounted on different platforms. The sensor system is weatherproof for use in diverse conditions. The sensor system can be operated as part of an autonomous vehicle or as a stand-alone device using a battery. The sensor system consists of the collection of different sensors to collect multimodal data for later use. Sensors include 3D LiDAR, a stereo camera and GNSS/IMU. Using data acquired from these sensors, it is possible to create a 3D LiDAR reconstruction from the environment.

FIG 23 Portable sensor system developed by BISG.

The portable sensor system has an aluminium profile frame which can be easily modified to fit the current need of sensor setup and mounting options. A compact and waterproof casing is mounted to the frame, which is used as a modular unit for the control computer, and the components that are necessary, e.g. a voltage regulator, a USB hub, and a Raspberry Pi HQ Camera module. The portable sensor system is equipped with Ouster OS0-128 LiDAR, Xsens MTi-G-710 GNSS/INS, a RealSense T26 tracking camera, and a D435 depth camera. Using additional mounting brackets and magnets, the system can be attached to any magnetic surface, including the frame of heavy equipment vehicles. It is thus possible to collect the necessary data for VR reconstruction using actual vehicles, without the need of an additional data collection vehicle. Using magnetic mounting, it is easy to test different mounting points for the sensor system to achieve the best results.

FIG 24 Portable sensor system mounted on the front of a car.

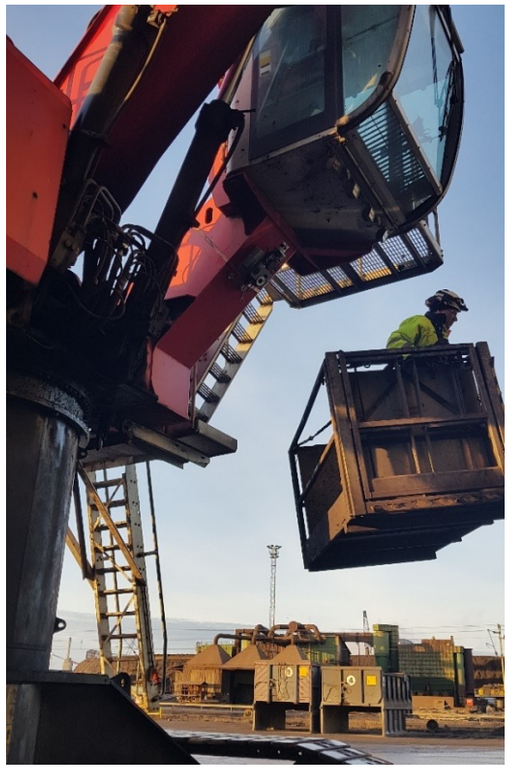

FIG 25 A portable sensor system mounted on a material handling machine.

SSAB EUROPE RAAHE

24.09.2021 Installation and measurement data, SSAB Europe Raahe recycling steel terminal:

FIG 26 A portable sensor system for material handler.

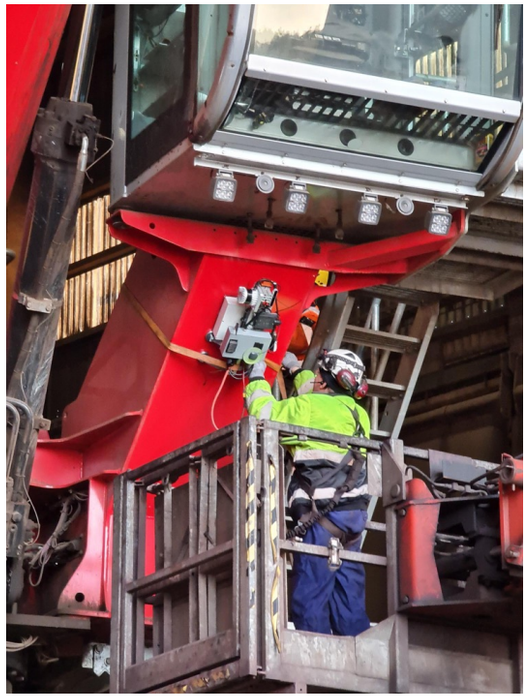

FIG 27 Mounting the portable sensor system on the material handler

Before the installation and measurement day, a 3D model (rough model) of Mantsinen's Material Handler machines was used as a starting point. The model was transferred to BISG's simulator, where the positioning of the sensors was examined before installation. Tapojärvi provided BISG with image material and rights, which could be used to see what information was available about the device, and what the interface was like. BISG prepared the sensor hardware for attachment to the Material Handler. The measuring equipment was prepared to record the data provided by the material handler as well. This happened with the aid of the cloud.

FIG 28 Mounting the portable sensor system on a Mantsinen 70R material handler.

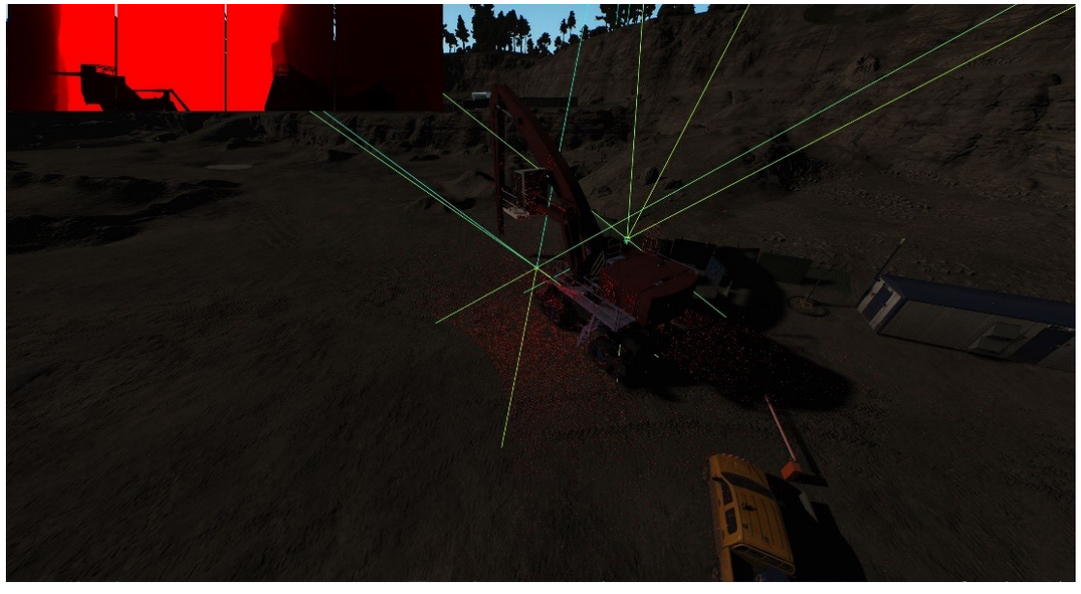

FIG 29 Visualisation of sensor placement in BISG SIM.

The University of Oulu Biomimetics and Intelligent Systems Group (BISG) had their portable sensor system mounted on Tapojärvi's Mantsinen 70R Material Handler to collect data and to see how sensors performed during metal recycling. The data collector system was mounted on the material handler's frame underside of the cabin using magnets. This ensured that the device's field of view was the same as the machine operator's view. For the autonomous operation, two distinct datasets were collected. The first was from the outside, with a material handler driving a metal pile and loading the metal onto a container. The second was from the inside of the recycling terminal, with a machine picking different types of steel from storage bins to a transport container to create the desired mix of recycled steel. The data were analysed during the following months.

The Mantsinen 70R Material Handler is a versatile piece of heavy machinery that is known for its practical design and robust capabilities. In Raahe, it is used for material handling. It features an elevated cabin, positioned approximately seven metres off the ground, which gives the operator an elevated view for safe and efficient control. The Material Handler is equipped with tracks, which offers enhanced stability and manoeuvrability across various terrains.

With an extended reach of approximately 20 metres, the machine is suitable for tasks that require access to elevated or hard-to-reach areas. The machine's tool system is connected via a universal joint, allowing flexible movement during material handling. In Raahe, the machine can handle multiple metal piles from one position. The machine is powered by a 24 V electrical system, which offers a great platform for automation equipment.

Automation challenges

The automation of the Material Handler presents several challenges that require careful consideration and innovative solutions. Understanding and overcoming these obstacles is crucial for ensuring the successful implementation of automation technology.

1. Elevated positioning

One of the primary challenges arises from the machine's elevated position. With the cabin situated approximately seven meters off the ground and the swing ring at four metres, the height differential poses a challenge. Ensuring that the sensors are appropriately positioned and aligned becomes paramount, especially those aligned with the main boom's direction. The need for elevated sensors introduces complexities to their design and deployment.

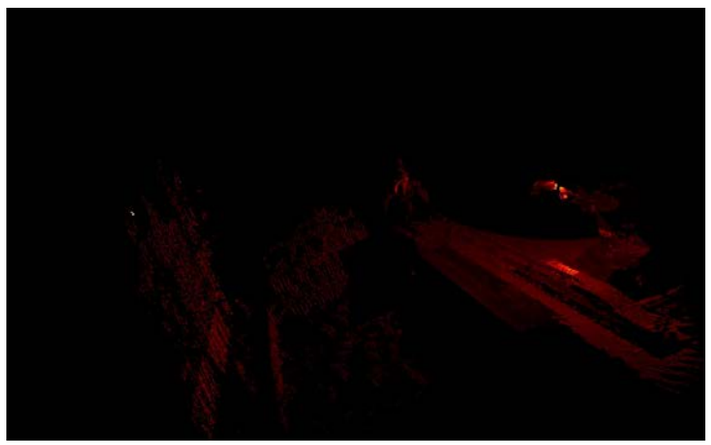

FIG 30 Point cloud from inside the material handling terminal, with a railing next to the machine, and the handling tool visible.

2. Rigid undercarriage

The undercarriage of the machine is rigid, which means that while the machine is in motion, the sensors mounted on the undercarriage will maintain their orientation relative to the tracks. These sensors could be used for autonomous driving of the boom machine from one place to another. These sensors can be closer to the ground than the sensors used for material handling and will not require such a high resolution. Sensors pointing to the sides especially can be low-resolution, attributing to the machine's incapability of moving sideways during normal operation.

3. Contamination by metal dust

Operating in an environment where metal dust is prevalent poses a challenge for automation. The presence of airborne particles can lead to sensor contamination, potentially compromising their accuracy and functionality. Developing protective measures or the use of specialised coatings to mitigate this issue is essential to maintain reliable sensor performance.

4. Low light conditions

In a relatively dark working environment, with most of the work lights positioned far away or oriented incorrectly for specific tasks like picking metal from storage bins or depositing it into containers, visibility becomes a concern. The implementation of effective lighting solutions or alternative sensing technologies that are less dependent on ambient light is essential to ensure accurate automation.

5. Unreliable odometry from skid steer machine

The unreliability of odometry data from the skid steer machine due to skidding presents a challenge for accurate motion tracking and control. The development of robust algorithms and sensor fusion techniques that can compensate for this uncertainty is crucial for precise automation.

6. Potential Radio Interference

The coexistence of Wi-Fi and communication radio systems introduces the potential for interference. Managing and mitigating this interference is essential to ensure reliable communication and data transmission, especially in critical automated operations.

Addressing these challenges requires a multidisciplinary approach, involving expertise in robotics, sensing technologies, control systems, and communication protocols. By tackling these obstacles head on, we can pave the way for the successful and efficient automated operation of the Mantsinen 70R Material Handler.

RESULTS

The implementation of automation technology in the Mantsinen 70R Material Handler has yielded promising results, showcasing the system's adaptability and capabilities. The following observations and achievements have been made:

The Ouster LiDAR, positioned beneath the operator's cabin, has demonstrated significant capabilities in detecting obstacles such as fences and even ground-level features like the railway tracks present in the material handling terminal. This presents an opportunity for further exploration of LiDAR applications in the automation process. Additionally, the LiDAR system provides competent results in identifying piles of metal, storage bins, and transport containers. Recognising critical components like the claw and boom of the machine from LiDAR datapoints to the versatility and adaptability of this technology. Furthermore, the LiDAR system's ability to detect high-visibility clothing at a distance opens opportunities for enhanced safety measures.

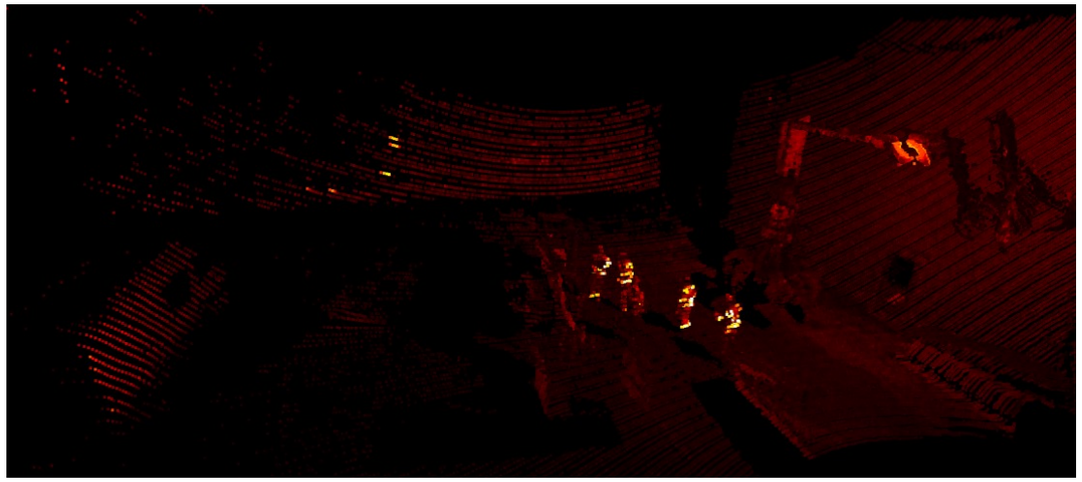

FIG 31 Point cloud, showing intensities. Note human figures with high-viz clothing and the recognisable claw.

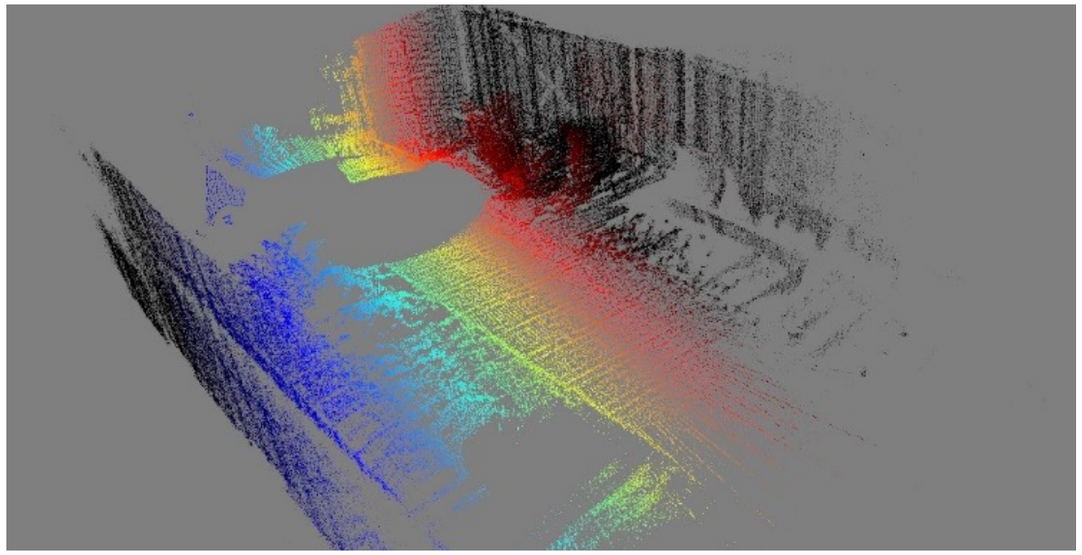

FIG 32 Point cloud from material handling terminal generated with a simple ICP.

Localisation within the terminal showcases the potential for refined precision in machine operations. If localisation is conducted utilising only the LiDAR sensor, specific features such as numbers above storage bins or additional reflectors need to be implemented for good results. The controlled nature of the terminal provides an opportunity for the installation of safety sensors on doors, augmenting the overall safety of operations. A system for reading the numbering above storage bins for accurate material tracking and handling could be achievable with the aid of machine vision.

Challenges persist in grabbing random sized and shaped pieces of metal from storage bins, indicating a need for further sensor integration or technological solutions. The consideration of side blind spots, given the skid steer machine's limited sideward movement, implies that a minor blind spot at the sides of the machine may be acceptable. Although some Can Open messages are present in the machine and are potentially valuable in the automation process, the lack of available documentation presents a challenge for integration and customisation.

KEMI MINE

30.8.2023 Visiting the operating environment day, Outokumpu Chrome Kemi mine:

FIG 33 Drone flying inside the Kemi mine during the scaling operation.

For the Kemi's underground mine, the same sensor setup was used to collect the data. At first, BISG installed the sensor equipment on the roof of the Hilux, and the journey to the tunnel was followed through level 350 to the scaling site. The scaling as a working phase was explained, and the scaler introduced the scaling machine.

Three distinct datasets were collected. The first and second were collected with the sensor system mounted on top of a SUV during normal driving inside the mine. These datasets were used to determine the possibility for the machine to autonomously move from one scaling target to the next. The third dataset was collected with the scaling machine. The data collector was mounted on the protective steel frame in front of the cabin. The data collector was below the operator's field of view but pointed reasonably well in the same direction as the operator was looking. Data were collected from one scaling operation, starting with the removal of loose rock and ending with piling the rock for pick-up. During the scaling operation, a drone was flown near the machine to capture videos from different viewpoints to aid in planning the final sensor placement. These datasets were analysed to determine the performance of LiDAR and cameras in the underground mine during machine operation.

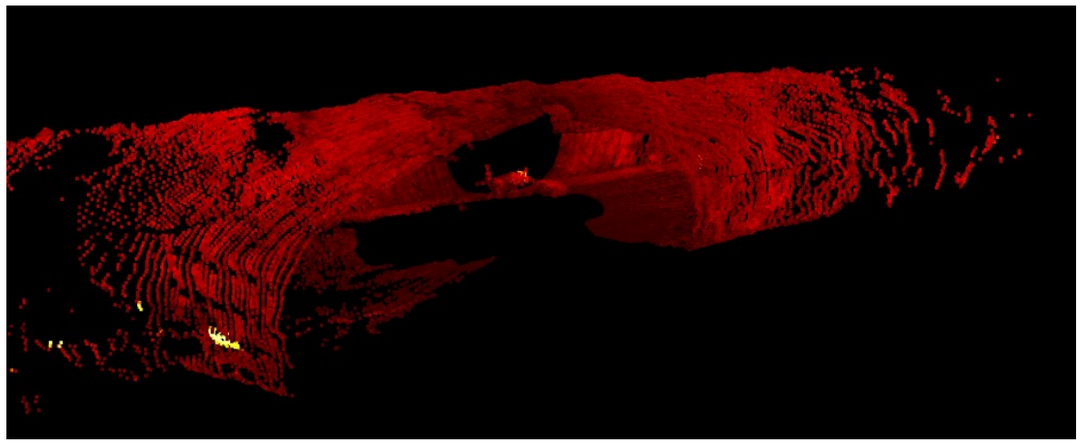

FIG 34 LiDAR point cloud with a portable sensor system mounted on top of the Hilux.

Automation challenges for scaling machine

The implementation of automation technology in the scaling machine presents several distinctive challenges. Navigation through low-ceiling tunnels requires precise control and obstacle avoidance to prevent collisions and ensure safe operation. The dark, wet, and dusty conditions pose a risk to the sensors. Protective measures and advanced cleaning mechanisms are required to maintain reliable sensor performance. Falling debris and loose rocks in the scaling environment present a significant damage risk to sensors. The implementation of robust shielding and protective measures is imperative to ensure sensor integrity during the scaling process. In the limited area of operation, the implementation of safety sensors to detect and respond to the presence of personnel or other machinery is critical to prevent accidents and ensure safe operations.

The strategic positioning of sensors to detect the surrounding features in all directions is crucial. Achieving optimal coverage while avoiding interference and obstruction is a complex spatial planning challenge. For navigation in the tunnels, the accurate detection of reflectors along the tunnel pathway can be used for robust localisation algorithms. In addition, the different tunnel labels can be used for loop closure during the initial mapping phase.

During the scaling process, the implementation of autonomous capabilities that can seamlessly switch between two distinct scaling tools demands robust tool-changing mechanisms and precise control algorithms. The coordination of visual inspection with autonomous scaling operations requires seamless integration between the vision system and the probing mechanism for the accurate assessment of scaling requirements.

FIG 35 RGB camera image during scaling operation.

SLAM for tunnel mapping

Even with basic SLAM algorithms utilising distance information, the machine successfully generates a reliable map of the tunnel network. The addition of intensity data, especially in the presence of installed reflectors, can further refine the localisation accuracy. Labels on the tunnel walls contribute to effective loop closure in the mapping process.

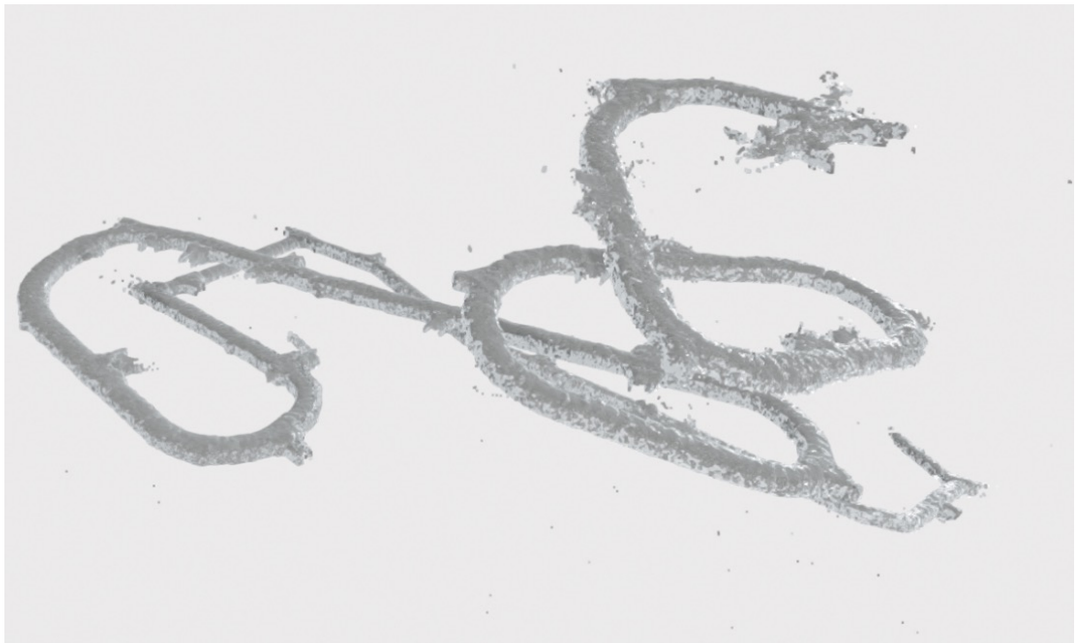

FIG 36 Generated map if the route is driven with Hilux from the maintenance hall to the scaling target.

Optimal sensor placement

The top of the machine is clear of other equipment and near the area of interest, allowing the possibility to mount the main LiDAR, ensuring unobstructed data capture and improved perception. At the current frame rate of 10 frames per second, there are limitations in detecting falling debris in real time. However, the detection of larger chunks of debris after a fall event could be utilised. The LiDAR system proves effective in detecting high-visibility clothing and large objects such as vehicles, providing an additional layer of safety and operational awareness.

Autonomous scaling operations

The machine demonstrates the potential for autonomous scaling by following the wall with the claw and autonomously detecting falling debris. The operator can oversee automated operations through a remote camera and LiDAR feed, providing instructions or taking manual control when necessary. Post scaling, rocks are organised for pickup. The LiDAR scan data from before scaling prove useful in identifying loose rocks on the floor, ensuring a thorough clean-up process.

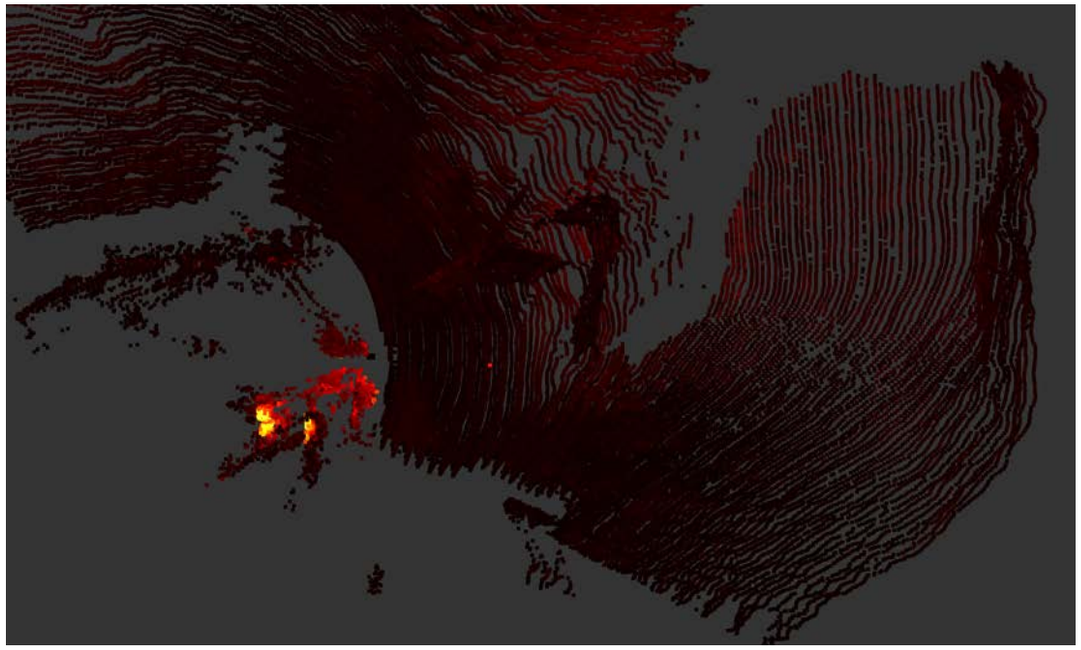

FIG 37 Point cloud from a portable sensor system mounted on the scaling machine.

By enabling autonomous movement between scaling targets and combining it with remote operation capabilities, the machine optimises worker resources, allowing them to engage in other tasks during machine repositioning. Different camera feeds, including infrared and RGB, offer valuable additional data to geologists for rock type determination, facilitating informed decision making during scaling operations.

FIG 38 An RGB camera image from the scaling machine during the final piling of the loose material.

FFS TOWARDS FOSSIL-FREE STEEL

CONTRIBUTORS

Thomas Kurtén, Erik Degerstedt I Nordkalk
Henrik Saxén I Åbo Akademi

3.14 Fossil-free lime

BACKGROUND

In line with the EU's ambition to be climate neutral by 2050 and therefore SSAB's target of producing fossil-free steel via Hybrit, Nordkalk has an opportunity to play an essential part in this ecosystem. Nordkalk is well suited for this purpose due to the availability of raw materials, production, logistics, and technology expertise. To achieve the ambitious goals, Nordkalk has established its own project, Towards Fossil-free Lime (FFL), as an integrated part of Nordkalk's corporate roadmap eLIMEnate, which was launched in Nordkalk 2020. FFL focuses on three different areas: raw material; technology; and fuel and energy.

SOLUTION, METHOD

Due to the complexity of the project, Nordkalk chose investigation as a method to broaden our knowledge of the field of fossil-free lime production. This includes a deeper understanding of the production of fossil-free lime production as a further implementation in various applications. Nordkalk has chosen full-scale analytics, as well as laboratory testing, as methods to confirm the project hypothesis.

Communication between partners in the FFS has been of huge importance for the clarification of intermediate targets and project goals. Continuous follow-up has altered the project goals, and the project targets have therefore been bound to change, yet they have given a broader implementation perspective and understanding of the areas of development.

PROJECT MANAGEMENT

The project has been managed with project meetings. The complete project group is gathered monthly to follow up progress and make sure that the whole project group has the latest information. For overall progress and follow-up, a steering committee, consisting of the CEO and relevant division director of Nordkalk, has been formed. The Steering Committee meets at the request of the project manager.

To deliver the project scope as expected, coordination meetings with SSAB are held. SSAB coordinates the alignment of the work of Nordkalk with SSAB.

For the weekly and biweekly follow-up, the project core team is invited to a planning meeting. These meetings ensure the project runs according to plan. The daily follow-up is mainly via email or phone calls.

RESULTS, FINDINGS, OUTPUT, AND IMPACT

Carbon capture

The chemical reaction of lime production is :
$CaCO_3$ + Energy → CaO + CO_2 (1)

As the aim for Net Zero and reaching the 1.5 oC target of the Paris Agreement, we need to reduce CO_2 emissions. The project aims to stop the use of fossil fuels, and Nordkalk also wishes to evaluate carbon capture as an option. The fuel change, also known as pre-combustion carbon capture, only eliminates a third of the emissions from a limekiln. This means post-combustion carbon capture will be required to eliminate the process gases.

Nordkalk has evaluated the advantages and disadvantages of different technologies.
This comparison can be seen in Table 6.

Product specification and limestone properties

Excellent quality lime is crucial in steel manufacturing. Nordkalk therefore wishes to ensure that there is suitable limestone for steel manufacturing purposes. Steel-grade limestone is low in impurities, especially sulphur, and has high reactivity and slag enhancing properties.

Nordkalk examined the whole value chain of the limestone so that the unnecessary shipping of products unsuitable as kiln stone would be decreased. In the big picture, this would reduce the use of fossil fuels, as fewer shipments would be needed, and efficiency and power consumption would be reduced.

A study was conducted to optimise the handling of the stone in the quarry and to follow the whole handling route. The aim was to decrease the amount of fines originating in the shipment.

The specification of the EAF is received, and the major focus is generally on low impurities but a higher carbon content. Carbon content is used for stirring in the melt, as carbon is oxidised to carbon oxide, creating gas bubbles.

Additionally, we have deepened our knowledge of the effect of raw material properties on slag attributes. This work has been performed both theoretically and empirically.

TABLE 6

	Absorption (Amine washing/scrubbing)	Absorption (Amine-free)	PSA (Pressure Swing Adsorber)	Adsorption	Cryogenic distillation	Membrane separation	Hydrate-based separation
Advantage	Standard technology (with many variations of amine-based absorber agents)	Lower energy needs for regeneration	Relatively common materials like adsorbants, zeolits, activated carbon silica gel, alumina, or synthetic resins	Reversible process	Mature technology	Well-known technology for separation of gases	Low energy need
	Sorbents can be generated numerous times	Low or no environmental impact from sorbent		Absorbent could be recycled	Adopted for many years in industry for CO_2 recovery	No need for steam for regeneration	
	High efficiency	High efficiency		High efficiency		High efficiency	
		Can handle a wide range of low-concentration flue gases				Low temperature process	
		No steam for regeneration is needed, only electricity				Low energy consumption per separated tonne of CO_2	
Disadvantage	Sorbent degradation may have an environmental impact	New application, still only in pilot phase	Needs at least 70% CO_2 – concentration	Requires high-temperature adsorbent	Only viable for very high CO_2 concentration	Operational problems may include low fluxes and fouling	New technology with a need for more research and development
	Needs steam 3 bar at 130 °C Saturated for the recovery of the absorber				Conducted at a very low temperature	Still only in the pilot stage for CO_2 separation	

No further investigation during the project was conducted.

Heat generation / fuel alternatives

Screening of heating alternatives

In the FFL project, it was decided that the evaluation of different heating alternatives would be started on a broad range of alternatives, not excluding any known option. This approach was taken to logically narrow the pool of alternatives and enable the later tracking of the reasoning behind the choices made.

The original list of heating methods consists of

- Solid biomass fuels, dried and ground to fine powder
- Gaseous fuels, either natural-gas-based or synthesis gas from biomass gasification
- Liquid biofuels
- A reference case for electrical rotary kiln calcination.

Solid biomass

In solid biomass evaluation, the study started by collecting the existing information from previous discussions with suppliers. In principle, fuel pre-treatment can be done in two ways, either from moist raw material through drying and milling or directly from dry raw material through milling. The economic evaluation of the different process stages resulted in a calculated investment cost on top of the anticipated fuel price. Cases were made for both dry raw fuels and moist fuels.

Biomass drying requires a large amount of available low-cost heat, but during the process, it was seen that the residual heat from the kiln process was limited in both temperature and volume, and drying needed a supplementary source of heat. This could be the combustion of the prepared fuel dust material.

Liquid biofuels

An estimation for receiving liquid fuels and a biofuel storage tank was compiled, also accounting for the fuel feeding revamp on the kilns. Preparations for the possible intake of fuel shipments will create a notable share of liquid biofuel investment. Cases were calculated with several different liquid biofuel options suitable for the kiln process.

Gaseous fuels

As the current fuel is coke oven gas (COG), a fuel change with the smallest effect on kiln systems will be to use other gaseous fuels. These include methane gas (logistics in liquefied form, LNG/LBG), synthesis gas from biomass gasification, and hydrogen.

Biomass gasification with fluidised bed technology results in a lower heating value of the gas than is used in the current setup. This would either reduce production capacity or require changes to the fuel dosing system. Syngas is also preferably fed hot into the kiln, as gas cleaning would otherwise be needed, and the heating value of the gas would be reduced due to the loss of heat capacity (condensation and temperature decrease). Gas cleaning is an additional investment.

During the supplier screening, it was found that some of the fixed bed gasification suppliers were no longer available, and some new suppliers were found with new technological solutions. The possibilities of waste and sludge gasification were also explored, but within the scope of conversion to biofuels, these options were not considered further, more than taking possible future process adoptions for flexibility into account.

Hydrogen was reviewed. The change into hydrogen air, enriched air or oxycombustion would result in investing in a new kiln with technology with flue gas recirculation. The kiln supplier already has such a solution in engineering, but no actual units have been built yet. The hydrogen gas market and project development have been followed up during the project. Many projects are ongoing but with fewer references, and the actual future price level can only be estimated with a wide range. Hydrogen is therefore seen as promising, but it is difficult to predict, at least at this stage, and is possibly a high-cost fuel option. Development needs to be followed up.

Fuel selection

During the initial screening phase, the different fuel cost data and estimated investment costs for different fuel change options were collected and compared as total energy cost (fixed and variable costs). The overall costs were also compared in chart format, with columns representing the total energy cost constituting the various partial costs.

After the initial screening process, it was seen that the two most flexible and presumably economically most viable options would be solid fuel feeding and syngas production with a gasifier.

SME outsourced work of the process engineering of a fuel handling line was ordered. The result, datasheets for enquiring about equipment for the entire fuel handling line, including reception, drying, milling, and storage until the fuel dosing unit, was then used for the continuation of equipment enquiries and the equipment supplier's quotation work. Discussions with suppliers continued, and a price indication was received for solid fuel dosing and woody biomass gasification.

A result of fuel option selection work during the subproject is the choice of the future heating method that is the most viable option for long-term production in light of the current knowledge.

The heating method chosen is solid fuel feeding, with possibilities to use different raw materials within the chemical specification limitations set by the limekiln process. In addition to the local woody biomass streams available in Northern Finland, the possibility of new sources in the international biofuel market have been repeatedly raised. Keeping in mind flexibility for possible exotic raw materials ensures that lime production with biofuels has the best future potential.

After the project, we will have confirmed information about how to develop the heating method of the Raahe kiln. As a continuation, we have the possibility to proceed with detailed quotations and a solid investment cost for future fuel investment decision making.

Electrical heating

During FFL project meetings, there were discussions of the potential need for Mg-containing lime in future fossil-free processes. In the previous Decarbonate project, VTT had built an electrical rotary kiln with Kumera, which was proven to reach calcination temperatures and high CO_2 content waste gases. As the results of calcitic limestone calcination were encouraging, it was decided that within the project, it would be very interesting to test and prove the usability of an electrical calcination process in dolomitic lime production.

The lower calcination temperature of MgO versus the higher temperature of CaO, was anticipated to enhance the feasibility of a temperature-limited electrically heated calcination process. VTT kiln also has the possibility to accurately measure the different process parameters for future work.

Approximately one week of testing was performed, divided into two parts and two fineness grades of feed material. The best test points provided well-calcined dolime material with a relatively low residual carbonate content (non-calcined). Massive amounts of data and charts were produced as the result of testing, and these can then be used in the continued evaluation of electrical calcination feasibility studies.

The high temperature requirement of lime calcination limits the capacity (the possibility of full-scale lime production) and increases the investment need. Nevertheless, electrical heating is a very interesting option to follow, especially for products with a lower production capacity.

Electrical heating

Electrical heating was also discussed with a novel technology supplier, which develops electrical heating with multistep mechanical gas heating. The technology offers potential to achieve the high calcination temperatures needed for lime production, higher than can be achieved with resistive electrical heating, which is limited by resistor material temperatures. As the heating of calcined material would take place convectively, there is also potential for effective heat transfer onto the heated material. The technology is still in development, and it will still require development before a ready-to-use solution for calcination is on the market. This heating technology is also interesting and worth following up closely.

Plasma test

Nordkalk conducted a test with plasma. The trial setup was to compare calcination with plasma using two different grain sizes. Samples of 100 µm and 500 µm were sent to a trial plant. The calcination was done with plasma, and the samples were sent to Nordkalk. Nordkalk did not attend the trial and only received the samples to be tested. Reactivity tests were also conducted on the different samples. The results suggested that further development was needed to achieve the desired product quality.

Branding of new products

This project will start a new era in the lime industry. It will also mean potential new products. To understand the market take on this, including how to name the new product, a workshop was held. More work with branding will be done by Nordkalk, but outside the FFL project.

Raahe engineering scope

As a fuel switch is a necessity to achieve fossil-fuel-free calcination, an engineering scope was conducted. The aim for the engineering was to make a plan for fuel storage, transport, drying, and intermediate storage. The engineering suggested the use of a bunker with a feed system to a dryer. The required amount of energy for the dryer would be 5 MW. The dryer would use solid biofuel to dry the fuel to a suitable moisture. The parameters used for the fuel were received from the kiln manufacturer. The next step is to conduct a feasibility study on the basis of the conducted engineering.

PUBLICATIONS AND SEMINARS

Research seminars

Work on CO_2 reduction possibilities in the lime industry was presented at the FFS-TOCANEM joint seminar in Espoo on 17 March 2022. The presentation covered topics such as the CO_2 emissions from the lime calcination process, various alternative heating methods for providing the heat required for calcination reaction, the benefits of oxygen enrichment, ongoing work around electrification, and CO_2 emission reduction in the lime industry in Finland and Sweden.

Another occasion to present the ongoing work with similar topics was the Pohto course on 27 April 2022 in Vantaa. There, the same topics were discussed and presented for an audience of metals industry personnel.

Lime injection

The optimisation of the future process gave an indication that the injection of lime into the steel furnace would be of interest. Nordkalk and Åbo Akademi University conducted a collaboration master's thesis study to research particle size phenomena during injection. The aim was to better understand particle behaviour in a liquid-liquid solution.

The tests were conducted in Åbo Akademi's laboratory in cold conditions. To resemble the conditions of an EAF (Electrical Arc Furnace), oil with a lower density and higher viscosity was used with water. This recalls the slag and melt in the furnace. A schematic of the setup can be seen in Figure 39.

FIG 39

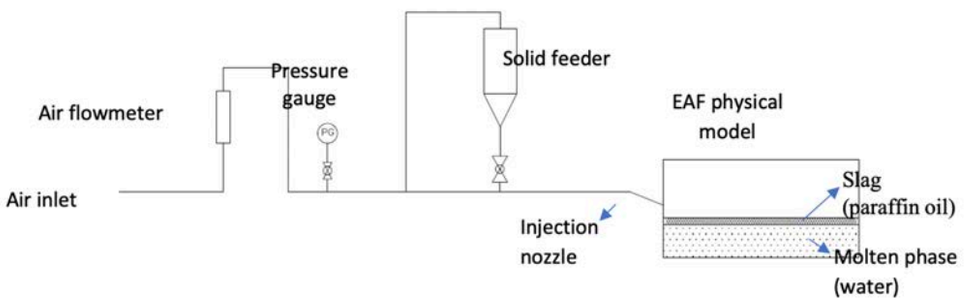

The results from the master's thesis produced a broader knowledge of injection and the necessity for a wider knowledge of particle size distribution. Further development work continues.
Final seminar (Oulu)

BLOG TEXTS

Lime in Steel – Nordkalk

Injection lime – for a more efficient steel manufacturing process and sustainable use of lime – Nordkalk

Carbon capture, storage, and utilisation in lime manufacturing – Nordkalk

Committed to setting emissions reductions in line with the SBTi – Nordkalk

Roadmap to eLIMEnate our climate emissions – Nordkalk

Lime and CO2 – What's the big deal? – Nordkalk

CLEAN ENERGY

FFS TOWARDS FOSSIL-FREE STEEL

CONTRIBUTORS

Robert Weiss, Jussi Ikäheimo, Mikko Lappalainen, Tomi Thomasson, Markus Hurskainen, Janne Kärki

4.1 Hydrogen production

Hydrogen production and storage at a carbon-neutral steel plant should be optimised to ensure the plant's competitiveness.

BACKGROUND

Hydrogen-based steelmaking (from hydrogen direct reduced iron, HDRI) is expected to gain ground in the Nordic countries. The clean electricity supply of electrolytic hydrogen production represents the dominant cost in the hydrogen value chain. This cost can be pushed down if the electrolyser can be operated mostly during periods of low power prices. It is essential to operate when renewable power or low-emission grid electricity is available. Different plant configurations, concerning unit dimensions and power supply options, should be considered because the resulting production costs can differ substantially. The plant configuration and operation should be carefully analysed to allow financial benefits from market price variations while minimising investments and ensuring green hydrogen targets.

The analysis also needs estimates of future power market prices. Exploiting historical power market prices may produce misleading results because the energy transition will profoundly affect the European power markets. New types of electricity conversion technologies are also appearing. The power market will therefore face significant changes, which in turn will affect the cost of electrolytic hydrogen. The FFS project therefore also included a study to estimate the behaviour of power prices.

SOLUTION, METHOD

A workshop was first arranged by VTT to define the future power market scenarios to be studied in the work and the data sources to be used. The open Backbone energy system model (Helistö et al. 2018) was used to model Northern European power markets and simulate market prices and the average emission intensities of power production. Backbone has previously been used in several research projects and has been validated against the commercial Plexos model. The advantages of Backbone are the possibility of flexibly including other energy vectors besides power, as well as material flows and the customisable temporal structure.

Backbone is a framework in which models for many different regions and scenarios can be built. This study used the model implementation of the Northern European energy system. The model includes the 13 countries shown in Figure 40. The study scenarios are based on the scenarios defined by the European Network of Transmission System Operators for Electricity ENTSO-E in their Ten-Year Network Development Plan (TYNDP) in 2020. Two scenario years, 2025 and 2040, were included.

FIG 40 Geographical scope of the Backbone Northern European model (Copyright VTT).

Power markets affect the operation of the steel plant, but the steel plant itself can also impact power prices. The energy system model therefore contains a surrogate model of the HDRI steel plant. The surrogate model is an approximation of the accurate model, which was used in the dedicated steel plant model. The linked runs of the power market and dedicated plant models were also performed. In this case, the surrogate model was iteratively updated based on the results of the plant model. As an accurate model, a novel and computationally efficient techno-economic power-to-x-plant optimisation model has been developed, including both plant unit configurations and renewable power procurement and energy market operations. Recently introduced EU rules for renewable fuels of non-biological origin, including green hydrogen, have also been implemented in the model. The model has then been applied to a HDRI plant located in Finland. Plant dimensioning has been carried out in several current and future power market and regulatory scenarios.

RESULTS, FINDINGS, OUTPUT, AND IMPACT

The Backbone Northern European model produced estimates of future Finnish power market prices and their variability. The price variability in the 2025 scenario was higher than in the historical years (2018–2019) used as a reference. In the 2040 scenario, price variability was significantly higher than in the historical years used as a reference. Simulated emission intensity values for Finland indicated that power production would be emissions free in the summer, and in the winter, less than 100 gCO_2/kWh most of the time. The linked model runs with the dedicated steel plant model converged well.

We predict a reasonable production cost for hydrogen direct reduced iron (HDRI) and hot briquetted iron (HBI), even decreasing in a future 2025–30 scenario. When the recently introduced EU rules for renewable fuels of non-biological origin are applied, the production cost increases by more than 10%. The rules also have a significant increasing effect on the required hydrogen storage. The flexibility of the HDRI shaft emerged as an important parameter. Flexibility strongly affected the required hydrogen storage, as well as the total production cost. The results are significant for the optimal design of future low-carbon steel plants.

REFERENCES

Weiss, R. and Ikäheimo, J. (2023) Flexible Industrial Power-to-X Production as Virtual Hydrogen Storage enabling Large Scale Wind Power Integration: A Case Study of future Hydrogen Direct Reduction Iron Production in Finland. In review and presented at the SDEWES2023 conference, Dubrovnik 24-29.9.2023.

Helistö, N., Kiviluoma, J., Ikäheimo, J., Rasku, T., Rinne, E., O'Dwyer, C., Li, R., and Flynn, D. (2019) Backbone: An Adaptable Energy Systems Modelling Framework. Energies 2019, 12, 3388. https://doi.org/10.3390/en12173388

ENTSO-E, TYNDP 2020 scenario building guidelines (2020) https://2020.entsos-tyndp-scenarios.eu/tyndp-2020-scenario-report/

Example: Pöyhönen J., Kovanen T., and Lehto M. (2021) Basic Elements of Cyber Security for an Automated Remote Piloting Fairway System. Presented at ICCWS 2021 – the 16th International Conference on Cyber Warfare and Security 25–26 February 2021, Tennessee, USA

FFS TOWARDS FOSSIL-FREE STEEL

CONTRIBUTORS

Andrei Wallin, Mikko Lappalainen, Tomi Thomasson I VTT

4.2 Operation of electrolysers in Nordic conditions

The ventilation requirements and HVAC options of an electrolyser system were studied to enable safe and reliable operation in Nordic conditions.

BACKGROUND

Waste heat from green hydrogen production can be recovered and utilised in suitable applications. In Chapter 4.2, VTT studied and developed a means to increase the waste heat recovery from electrolyser technologies. In this task, the focus of the work was on ventilation system sizing and waste heat utilisation possibilities within the electrolyser plant.

Accurate ventilation system sizing is necessary for hydrogen production, as an ATEX space (the space for equipment intended for use in explosive atmospheres) requires a constant high ventilation outdoor airflow rate to minimise the possibility of leaking hydrogen accumulating above the explosive limit, which is 4% at normal atmospheric pressure. Despite a dedicated cooling system, the electrolyser equipment causes a considerable heat load on the space, which needs to be removed to maintain the space temperature within limits.

However, estimating the ventilation and heating system sizing is challenging. The exact heat load profile of the electrolysis equipment varies, depending on the equipment provider and the operating strategy, meaning that multiple scenarios need to be evaluated. The portion of surplus heat from electrolysis equipment that is deposited in the space varies, depending on room temperature. Other aspects such as ambient temperature and solar radiation also need to be taken into effect for the study of the space's total energy balance. A dynamic simulation is therefore required.

SOLUTION, METHOD

The literature study explored hydrogen safety considerations and the waste heat utilisation of electrolytic hydrogen in Nordic conditions. Due to the high flammability of hydrogen, the primary measure for preventing explosions is to avoid the formation of flammable mixtures of hydrogen and oxidisers in any given scenario. This can pose special challenges during seasonally cold temperatures due to the high ventilation requirements for electrolysis buildings. On the other hand, a cold climate offers possibilities for the recovery and utilisation of waste heat from the electrolysis process.

Fortum provided the plant data and technical requirements for the analysis. The analysed system is shown in Figure 41. The housing contained the hydrogen production process components for waste heat calculations, which were the electrolyser and rectifier. The technical requirements included maintaining the indoor air conditions at specified ranges (10–40 °C, 5–85% RH), a minimum supply air temperature (3 °C) to avoid the risk of equipment freezing, and an outdoor airflow of 10 air changes per hour (ACH). In the housing, a smaller space was zoned as a non-ATEX space for rectifiers, and the rest as ATEX space for electrolyser equipment. An additional scenario with a unified space for the rectifier and electrolyser was also studied.

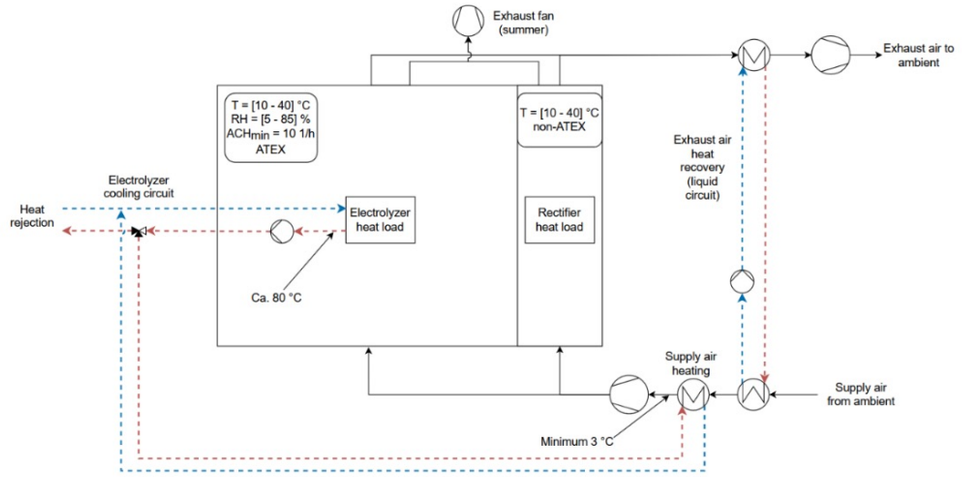

FIG 41 The studied system with utilisation of waste heat from exhaust air and the electrolyser cooling system.

VTT conducted a two-stage modelling for the task. First, based on provided manufacturer data and VTT's heat transfer modelling, a temperature-dependent model to estimate the waste heat availability of electrolyser equipment was created. The rectifier heat load on the space was modelled as constant, with different scenarios for air-cooled and liquid-cooled rectifiers. Second, dynamic simulations of the electrolyser housing's energy balance were performed with different parameters in IDA-ICE. The simulation was used to determine the required ventilation flowrates, as well as the heating system sizing and HVAC energy demand.

RESULTS, FINDINGS, OUTPUT, AND IMPACT

The key findings and practical implications of the study are the following:

1. For the electrolyser space, constant 10 ACH was found sufficient to maintain a space temperature below 40 °C under test year conditions (Figure 42). For the rectifier space, the air-cooled rectifiers resulted in extreme air change rates (constant 23 ACH and additional ventilation during summer) due to the small space available, favouring the liquid-cooled option. Using air-cooled rectifiers is more viable if there is a unified space with a single large air volume.
2. Increasing exhaust air heat recovery efficiency above 50% was found to bring diminishing energy savings, as supply air is heated only to the minimum temperature of 3 °C. While exhaust air recovery can cover most of the energy needed for supply air heating, additional heating is required during the coldest periods of the year.
3. Total electrolyser heat production by far exceeds the building heating demand. Supply air heating after exhaust air heat recovery can therefore be met with the waste heat from the electrolyser cooling system. In the absence of other uses for the electrolyser waste heat, the exhaust air heat recovery system can be omitted, and some of the waste heat can be used to completely cover the supply air heating demand.

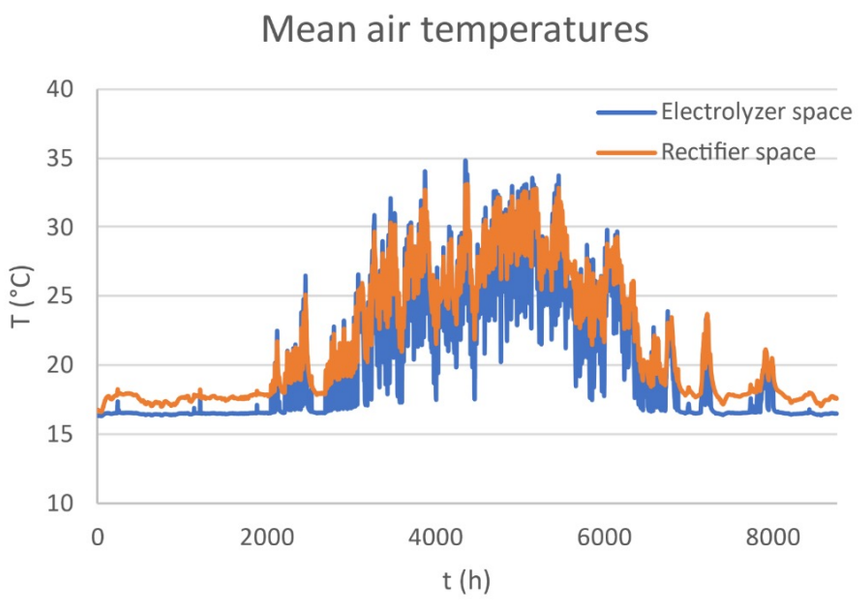

FIG 42 Simulated space temperatures with baseline assumptions.

WHAT ARE THE PERSPECTIVES AND FUTURE NEXT STEPS?

The possibility of utilising the waste heat in locations external to the site was excluded from this study, and case-specific valuation means this possibility can have an impact on whether waste heat should be used locally for supply air heating. Including the possible external heat utilisation or demand for analysis also makes studying heat utilisation from the dynamic operation of water electrolysers an interesting subject. In addition, to assess emergency ventilation situations in more detail, a more detailed modelling is required, allowing the development of a hydrogen concentration from a point source leakage to be assessed.

FFS TOWARDS FOSSIL-FREE STEEL

CONTRIBUTORS

Markus Hurskainen and Tiia Kanto I VTT

4.3 Techno-economic analysis of hydrogen transport using hydrogen carriers

Hydrogen carriers could enable renewable energy trade as hydrogen trade – but is it feasible?

BACKGROUND

The availability and cost of renewable electricity varies markedly between continents and countries. To date, there has been no cost-effective means of transporting renewable electricity over long distances to connect regions of low-cost production with high-demand centres. Given that a substantial portion of the demand for green electricity stems from the need for green hydrogen, utilising hydrogen as an energy carrier offers the potential to facilitate the trade of renewable energy across borders by transitioning from transporting electrons to transporting molecules. Ultimately, the feasibility of hydrogen trade will depend on whether lower hydrogen production costs can offset the cost of transporting the hydrogen from low-cost production areas to high-demand areas.

One option for hydrogen trading is through pipelines, but long-distance pipelines often face a significant challenge, as they already require a huge scale from the outset, giving rise to what is often called the “chicken-and-egg problem”. Moreover, transport distances can surpass the practical limits of pipeline transport.

Similar to CO_2, hydrogen trade could take place via ships. Gaseous hydrogen has a low volumetric density, which needs to be increased for efficient large-scale transport. While this could be done via pressurisation, transporting large quantities of pressurised hydrogen becomes impractical due to the weight and cost of containers.

This leaves two main options for large-scale hydrogen transport:

- **Liquefaction:** Hydrogen can be transformed into a liquid state by cooling it to -253 °C, significantly boosting its storage density to 70.8 kg/m3 (an 800-fold increase compared to gaseous hydrogen at 1 atm).
- **Hydrogen Carriers:** An alternative approach involves converting hydrogen into more convenient molecules such as ammonia, methanol, or liquid organic hydrogen carriers (LOHCs) and then releasing the hydrogen later when required.

Compared to pipelines, the utilisation of ships makes supply chains more flexible, as ships can serve several locations, and capacities can be easily scaled to increasing demand. Ship transport is also less affected by the transport distance. However, each of these options involves significant investment, required for hydrogen conversion and release steps, which also inevitably leads to marked efficiency losses. Thus far, no single carrier has emerged as superior to the others. Each carrier comes with its distinct advantages and drawbacks, and the choice is likely to depend on the case, e.g. capacity, transport distance, utility costs, and whether there is demand for heat. A Finland-specific analysis is therefore required.

SOLUTION, METHOD

First, a comprehensive review was conducted on the technology cost and performance, technology suppliers/developers, and health and safety aspects. Technology readiness levels and possible further development needs for large-scale deployment were then assessed. Subsequently, an analysis of the advantages and disadvantages of each option was carried out.

A techno-economic analysis was then performed to compare different hydrogen carriers for cases relevant for Fortum. The carrier options were compared for large-scale maritime hydrogen trade using an annual operation-based model, in which full load hours for each process were specified. The main result was the delivered cost of hydrogen (€/kg) considering all the process steps from hydrogen back to hydrogen (Figure 43). The costs were divided into different process steps to highlight their respective importance. Six carriers were studied: liquid hydrogen; ammonia; benzyl toluene; toluene; methane; and methanol.

As sensitivity cases, different capacities and transport distances were studied.

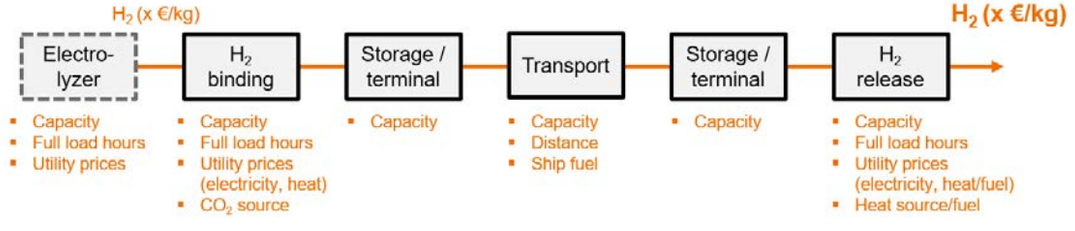

FIG 43 Description of the hydrogen carrier TEA model steps and the main input values.

RESULTS, FINDINGS, OUTPUT, AND IMPACT

Note: the results are preliminary, as the analysis is ongoing until the end of 2023.
Transporting hydrogen by ship was found to increase the cost of hydrogen markedly across all carriers. The investment costs related to the transport chain clearly surpassed those required for the electrolysers. Hydrocarbon carriers tend to lead to the highest costs, even when CO_2 is captured from a high concentration, low-cost source. With direct air capture (DAC), the costs would be markedly higher still.

While the differences in total costs for the other carriers were not too high, there were significant differences in cost structures. The respective competitiveness will therefore depend largely on scale, transport distance, the cost of utilities, and whether there is demand for heat. For example, given that the binding of hydrogen to LOHCs releases a huge amount of heat suitable for e.g. district heating, Finland is excellently positioned for the export of LOHCs.

Nevertheless, at a large scale, pipelines will probably be the most cost-effective option unless the transport distance is exceptional. However, in many cases, it may not be feasible to convert the hydrogen carriers back to gaseous hydrogen immediately at the port, meaning the benefits of terminal storage and more efficient inland distribution will need leveraging. Many of the carriers also find use as such, without ever converting them back to hydrogen.

FFS TOWARDS FOSSIL-FREE STEEL

CONTRIBUTORS

Kimmo Heikkinen, Merja Väänänen, Reko Rantamäki, Friedemann Hegge, Ari Kanerva, Tuomo Kiesi, Reetta Hurmekoski I Fortum E&P
Marko, Kari Ruusunoksa, Vuokko Laaninen I Fortum H2
Pasi Aarnio I Fortum Procurement
Tommi Johansson I Teollisuuden Vesi Oy
Risto Hautamäki, Markus Miikkulainen, Ari Suikki, Jorma Kuusela, Kari Ruusunoksa I Vahanen
Timo Nyman I Sweco
Leena Sovijärvi I Rejlers

4.4 Technical feasibility of H_2 plant

Fortum's feasibility assessment of a large H_2 production plant.

BACKGROUND

This feasibility study studied hydrogen production for a fossil-free steel plant planned for construction in Raahe on the western coast of Finland at SSAB's existing steel mill site. The new steel mill will replace an existing steel mill using blast furnaces. The idea of this investment is to reduce carbon dioxide emissions in the steelmaking process. The existing steel mill produces as much as 7% of Finland's total carbon dioxide emissions.

The new steel mill will use the direct reduced iron (DRI) process, where the iron ore is reduced in a hydrogen atmosphere. The process uses a lot of electricity because the furnaces are electric arc furnaces. Moreover, hydrogen is used in substantial amounts, and it is intended to be produced by electrolysis using fossil-free electricity.

SSAB aims to prove the process concept before making a decision to build a full scale DRI plant. There are several possible sites for the new DRI plant, and one of them is Raahe. Decisions concerning the site and results from concept verification are needed to proceed after this study, and they are expected during 2024. The hydrogen plant will be in operation in 2030 at the latest.

SSAB has reserved a greenfield site for hydrogen production. The site is adjacent to the existing plant area, in the southwest, and it is a peninsula, surrounded by the sea on both sides.

The study took into account the greenfield site conditions, as well as the requirements of the new steel mill. The aim of this study was to determine whether the process was technically feasible. The result of the study is described in this document and it also includes CAPEX and OPEX estimations of the plant to be used in economic feasibility calculations.

SOLUTION, METHOD

This feasibility study for an electrolysis plant to produce hydrogen was undertaken between May and November 2022. The plant is scheduled to be operational in 2030.

The study of 2,100 manhours produced a report covering all engineering disciplines, with 130 pages and 46 appendices.

The plant was designed to supply hydrogen to the SSAB steel mill using a DRI process. The technical availability of the plant was designed to be 90%.

Two technologies, pressurised and non-pressurised alkaline electrolysis, were chosen for this study because the efficiency of these technologies was the best at the time. Seawater (brackish) was chosen as a water source and heat sink, as its quality was better than that of the available fresh water. Reverse osmosis (RO) was chosen as the water treatment technology.
The heat recovery technology was not studied in this report.

The plant was placed on an SSAB property, Kuljunniemi, adjacent to the existing steel mill site.

RESULTS, FINDINGS, OUTPUT, AND IMPACT

The plant was found to be technically feasible, with some reservations that must be taken into account in further design:

- As the technology development is fast, and the project execution time is long, the electrolysis technology needs to be re-evaluated before the purchase of the equip ment.
- The stack size needs to be 10 MW or more, preferably 20 MW, otherwise the complexity of a plant of this size becomes a risk to operability and increases the plant's CAPEX and OPEX. This limits the number of potential OEMs.
- For water treatment, making feedwater out of se water is considered standard technology for the plant.
- The cooling water system is of great importance for the plant.
- The vent/flare arrangement of hydrogen needs to be verified to ensure plant safety. This study has already been started.
- Heat recovery was not studied, but it may affect this plant's profitability. However, a heat recovery study would require the involvement of SSAB and the Raahe municipality, which was at this stage against the customer's wish.
- The inspected property was considered suitable for building.
- The biggest problem to solve in civil engineering is the HVAC design of electrolyser buildings.
- The electrical system will be big, both in size and as an investment
- The automation system will be the same size as in a large-scale power plant. The technology used is normal process automation, except for the safety systems detecting hydrogen leakages.
- Safety and security issues in a plant of this kind are an extensive and multidisciplinary task.
- A time schedule for FEED and project execution was created. The timespan is from Q1/2023 until Q2/2028, assuming that no appeals processes were initiated for permitting (it is unlikely that there will be no appeals). Permitting will be critical, and it should begin in early 2023 to ensure the plant's start-up in 2030.

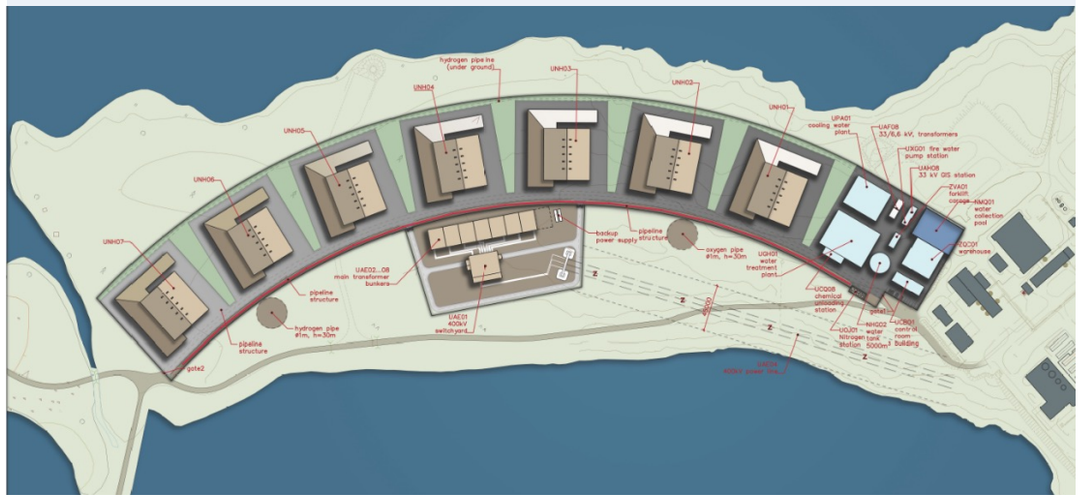

FFS TOWARDS FOSSIL-FREE STEEL

CONTRIBUTORS

Tommi Johanson, Miikka Lahdenperä, Maija Vidqvist, Silja Pitkälä, Jani Vuorinen I FFS/Fortum H_2/Water

4.5 Hydrogen production and water treatment

Water treatment plays a central role in H_2 production. Electrolysers require demineralised water with high volumes and flows. High volumes make demineralised water production a resource and cost issue but also a sidestream and waste issue.

This subproject aimed to gather understanding of the main process of H_2 production to a level and accuracy that allowed the optimal water treatment and control scheme to be developed.

Known and mature technology was to be compared with novel technology, promising a smaller footprint, smaller or no waste streams, and smaller overall CAPEX and OPEX while maintaining the high quality of the produced demineralised water.

Alongside the demineralised water process, wastewater and stormwater systems were predesigned for the SSAB Raahe site to an accuracy that allowed the achievement of a sufficiently accurate picture of the whole water treatment system. This work included a literature review, a site visit, design engineering, and the piloting of direct NF technology.

SOLUTION, METHOD

Current practices around electrolyser feedwater treatment and water quality requirements in electrolyser use were covered in the literature review. The review was divided into:

- a study of electrolyser feedwater quality
- water treatment technologies with the greatest potential for electrolyser feedwater treatment
- feed and process water treatment from lower-quality surface water and brackish water.

A water concept based on proven unit operations was created for the SSAB Raahe site. This included a site study, the creation of water balance, an inspection of the water infrastructure's current condition, future scenario modelling, and permitting issues.

A water treatment concept was created, covering:

- raw water and demineralised water treatment
- wastewater treatment
- stormwater treatment.

The raw water treatment process was based on chemical precipitation and ultra-filtration (UF), with demineralisation conducted with a two-stage reverse osmosis (RO) process, electro-deionisation (EDI), and a polishing mixed bed ion exchanger (MBIEX). This technology enables the use of brackish water from the Baltic Sea as raw water. The process is robust and tolerates alternations in raw water quality. A block diagram of the created concept is presented in Figure 44. The block diagram also includes the collection, balancing, and treatment of wastewater created from the raw water treatment and electrolysis process.

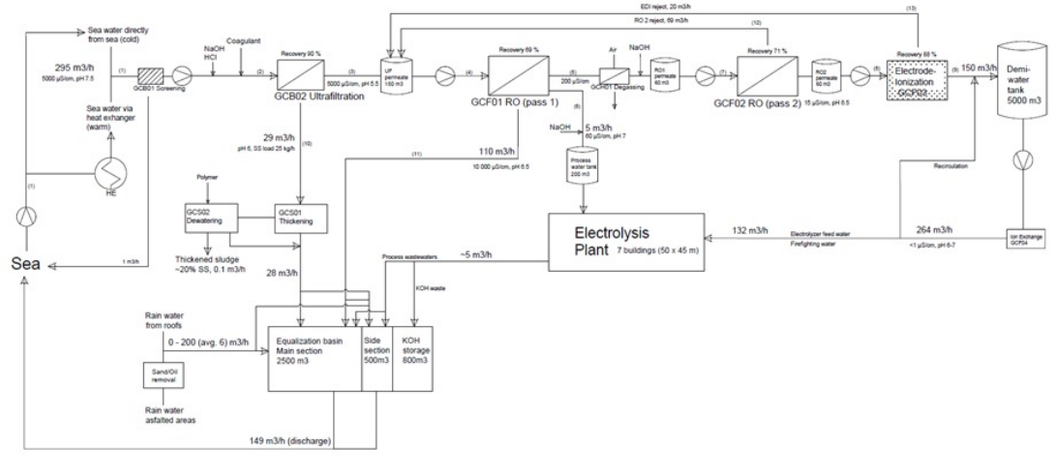

FIG 44 Water treatment process block diagram (Concept 1).

The wastewater treatment processes were based on the thickening of metal-organic sludge created by the precipitation of organic matter from raw water. If organics were not removed, they would foul the upstream RO membranes. The thickened sludge was further dewatered. The treated wastewater was returned to the sea.

The stormwater system was based on sand and solids removal and oil separation systems.

Conceiving this size of water treatment plant forces us to focus on resources in detail. Potable water is not an option because of its availability, cost, and sustainability. Water treatment processes relying on chemicals like NaOH and ion exchange resins are more vulnerable to availability and market disturbance issues. This steers the selection of the water treatment concept towards one using surface water as raw water and relying on electricity more than chemicals in demineralisation. Membrane technology-based demineralisation processes can also produce lower TOC concentration water than ion exchange processes. Table 7 shows the quality of the electrolyser feedwater.

Parameter	Units	Specification
Conductivity	µS/cm	<1
pH	-	6 - 7
Sodium	µg/l	<2
Chloride	µg/l	<2
Sulphate	µg/l	<2
Copper	µg/l	<1
Iron	µg/l	<5
Aluminium	µg/l	<5
Silica (as SiO_2)	µg/l as SiO_2	<20
Total Organic Carbon	µg/l as C	<200

TABLE 7 Quality targets for the electrolyser feedwater.

RESULTS, FINDINGS, OUTPUT, AND IMPACT

Three different concepts were created for comparison. The aim of the concept comparison was to a) minimise chemical use as much as possible and b) to minimise the volume of water treatment wastewaters, effluents, and sludges. With these goals, a concept with direct nanofiltration (dNF) and a concept with mechanical vapour recompression (MVR) were created. Block flow diagrams of these two concepts are presented in Figures 45 and 46.

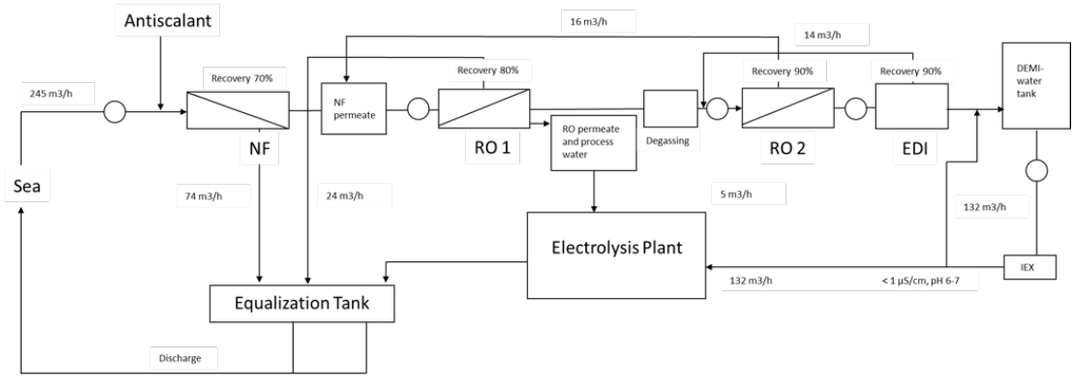

FIG 45 Water treatment process block diagram for concept 2 with dNF.

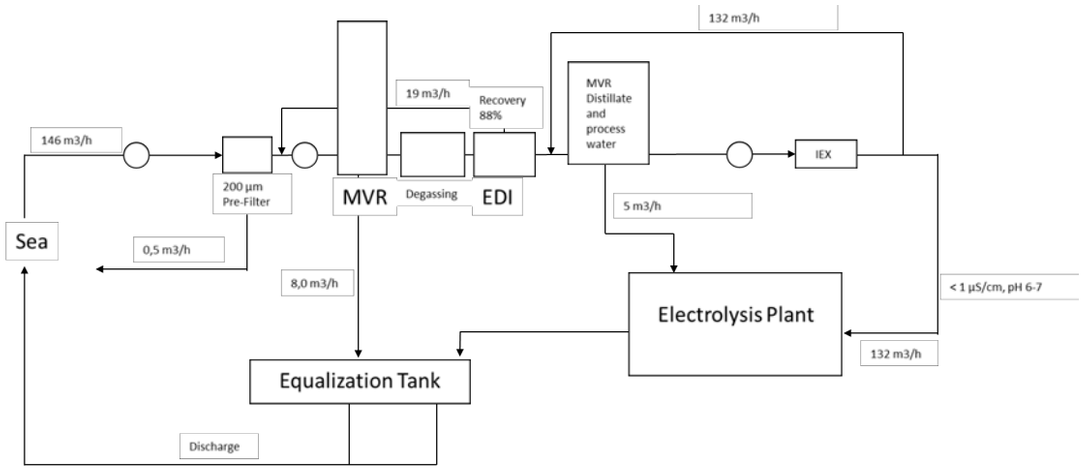

FIG 46 Water treatment process block diagram for concept 3 with MVR.

FIG 47 Raahe dNF Pilot equipment (Silja Pitkälä).

Table 8 summarises the concept comparison. Chemical use, electricity, operation, membrane/resin replacement and regular maintenance is included in total OPEX. The electricity price used was €60/MW, and the contingencies in CAPEX estimation were 25. It is noteworthy that a more detailed study of the use of waste heat from the electrolyser process was not made. A heat pump solution with a preheated feed to the MVR may reduce size of the MVR by as much as 20%.

All the concepts included similar stormwater and wastewater systems.

	OPEX (€/m3)	CAPEX (k€)
Concept 1	0,91	18 476
Concept 2	0,90	17 129
Concept 3	0,85	24 428

TABLE 8 Concept OPEX and CAPEX comparison.

The selected concept with precipitation and UF design work was taken further to the predesign stage, increasing the accuracy of CAPEX to +/- 10%. With this level of design process descriptions, detailed mass, and water balances, an engineering design to a higher detailed level was made for:

- **Water intake screening:** self-cleaning filters were primarily considered in the design.
- **Chemical precipitation:** based on the chemical precipitation tests (14.6.2022) with the sample seawater, a good coagulation result was achieved, both with ferric and aluminium coagulant. Ultrafiltration partially functions for organic removal without chemical precipitation, but chemical addition improves the removal percentage and decreases the fouling of membranes. In the design, both acid and base dosing options were considered in case the quality of feedwater or coagulant chemistry changed.

- **Ultrafiltration:** the pressure of feedwater on UF was increased to 3…6 bar with feed pumps. A back-washable, polymeric hollow fibre membrane module in a vertical installation was used in this project for the predesign and simulation.
- **Reverse Osmosis:** in the predesign, a recovery of 70% was used, which is typical for brackish water. Two separate passes of RO (filtrate of pass 1 was used as feedwater for pass 2) were required to achieve a sufficiently high total removal of ions.
- **Degassing:** the low pH of the RO feedwater led to carbon dioxide being mainly in the gaseous form and passing through the RO membrane for product water. To save the ion exchange capacity of EDI, additional carbon dioxide removal was required. This was achieved with degassing membranes.
- **Electro-deionisation:** the recovery in EDI was typically 88–94%, depending mainly on feedwater quality (e.g. hardness). The design was made with multiple parallel EDI stacks, in which the capacity of one stack was 2 m^3/h product (38 stacks per process line).
- **Ion exchange polishing:** the predesign consisted of 3 parallel and 2 series of ion exchange tanks. The first tanks in the series were filled with cation exchange resins, and the second were filled with anion exchange resins.
- **Effluent treatment process:** screening, ultrafiltration, and reverse osmosis produced rejects, which were directed to the equalisation tank.
- **Collection and balancing of effluents:** the equalisation basin (54.5 x 20 x 4 m) consisted of three sections. The main 2,500 m^3 section would be used in a normal situation to collect the discharge streams (except the one directed to the side section). The 500 m3 side section would be used for a quality check and the control of one or two selected streams, mainly UF and/or RO reject, and possibly process wastewater.

Part of the predesign work was to picture the road forward to the FEED phase

FFS TOWARDS FOSSIL-FREE STEEL

CONTRIBUTORS

Christopher Ridgewell, Marja Moisio, Matthew Pech, Matti Vuorinen, Patrik Pykälä-Aho, Sami Pasanen, Tommi Mäkelä, Ville Kortelainen I AW-Energy Oy

4.6 WaveRoller hydrogen hubs for fossil-free steel

Using wave energy to enable a fossil-free future.

BACKGROUND

The WaveRoller has several advantages for a green hydrogen system that will increase the efficiency of the system as a whole. First, the seasonal and daily variation between wave and wind and solar power differ, meaning wave energy is available and exploitable when other forms of renewable power are not. In combination with these power sources, wave power can plug the gaps in electricity supply and increase full load utilisation. Second, the technology houses a built-in hydraulic power storage which can smooth the electrical output and ensure the optimal utilisation of the various renewable resources applied for hydrolysis equipment. This stable power output also facilitates the use of higher efficiency and lower -cost alkaline (ALK) electrolysers instead of polymer electrolyte electrolysers (PEM). The full load hours will therefore be significantly improved, and the system will become more productive. As a result of these two main elements alone, it is foreseen that the integration of the WaveRoller will yield the optimal cost-benefit solution for green hydrogen production. Additionally, WaveRoller technology can be further adapted to pump and produce fresh water as a feedstock for the electrolysis process and for applications beyond the green hydrogen system itself.

A dedicated green hydrogen production facility requires the availability of multiple sources of renewable energy, access to efficient and economic transport and distribution through shipping, and adequate physical space for each system element. A combination of these elements is present in geographical areas where these opportunities would otherwise be less evident, especially considering the interlinkages between strong solar irradiation to make use of the most cost-effective new capacity renewable energy in solar PV and of a sufficient wave energy resource to balance the intermittency of production and unlock greater system utilisation. Countries such as Morocco, South Africa, Australia, Mexico, and Chile have vast potential for green hydrogen production.

Conceptual plans and a cost-benefit analysis have been produced for green hydrogen production facilities utilising solar, wind, and wave energy resources. The analysis examines small-, medium-, and large-scale plants. The transport of hydrogen to Finland from Southern Africa was considered, and associated costs denoted (levelised costs were evaluated for production and transport, and at the import site). Additionally, the potential for WaveRoller technology to produce water from the Baltic Sea for hydrogen production in Finland was assessed. Although found to be very low, the adjacent coastline in Norway was found to have strong potential for WaveRoller deployment. The potential for WaveRoller generation in Norway and exported through the Nordic grid to Finland was therefore examined as a case study.

SOLUTION, METHOD

The project was divided into the following subject areas and research tasks:

- Definition of power and water supply requirements for hydrogen electrolysis
- Description of water electrolysis technology and AEL and PEMEL characteristics. Description of power and water quality requirements and required technologies. Review of the technologies of leading manufacturers.
- Identified geographical areas with co-located renewable energy resources suitable for large-scale production and export of green hydrogen.
- Description of WaveRoller technology, its operating principles, and environment.
- Analysis of global power generation potential using WaveRoller. Potential in 2030 and in 2050. Analysis of potential impact for Finnish exports related to WaveRoller technology.
- WaveRoller sales potential and positive influence on Finnish economy.
- WaveRoller sales potential and positive influence on Finnish economy.
- Conceptual plans of electricity production for green hydrogen electrolysis using WaveRoller technology combined with wind or solar.
- Capability of wave energy (resource) to complement wind and solar power generation.
- Concepts for how WaveRoller can support freshwater supply for electrolysis. Electricity production/water pumping.
- Review of available methods for hydrogen transport, covering the whole transport chain i.e. pipeline vs truck, ammonia vs CH_2. Energy consumption of compression, liquefaction, Haber-Bosch. Required hydrogen storage capacity.
- Analysis of the potential to use secondary products of water electrolysis, i.e. waste heat and oxygen.
- LCOH analysis, cost contribution of different factors, i.e. energy, infrastructure, transport. Separate analysis also considering only electricity production of WaveRoller and its costs (LCOE).
- Assessing potential of WaveRoller technology for electricity production and/or water treatment in Baltic/Norwegian sea wave conditions.
- Case study on forming a PPA between electrolysis plant in Raahe and WaveRoller site in Norway.
- Cost-benefit analysis conducted for various project scales
- Case study on importing hydrogen from South Africa. Power generated using WaveRoller and PV plant.
- Report on concept and dimensioning of WaveRoller technology for providing water for hydrogen electrolysis.
- Modelling of standard RO plant production with wave energy.
- Study of optimal device scale for RO operation.

RESULTS, FINDINGS, OUTPUT, AND IMPACT

The main results from this project related to AW-Energy:

- Software tools to simulate the hydrogen production process to estimate project economics using a combination of wave energy, solar, and wind, with sales of compressed hydrogen, pure water and electricity were developed.
- The additional value provided by utilising wave energy were investigated and quantified. Utilising wind, wave, and solar as renewable energy inputs results in a significantly higher capacity factor for the hydrogen electrolyser compared to using only one or two input sources. It can also reduce the amount of hydrogen that needs to be purchased on the open market (and therefore depends on market prices).
- Wind and solar in the Namib desert region peaks in the summer months; wave energy peaks in the winter. Including wave energy in the mix therefore demonstrably increases process availability and reliability.

- It was found that wave energy strongly complemented solar and wind in Southern Africa, thus minimising the risk of the exhaustion of the hydrogen storage buffer, forcing a shutdown of the steelmaking process. This phenomenon was not observed in Northern Europe.
- In connection with this study, several factfinding visits were made to South Africa and Namibia. Several projects are currently underway in Africa to produce green hydrogen for domestic industrial needs and export as green ammonia. These projects are at various stages of development. It was noted that installations located close to the coastline faced a salty and corrosive atmosphere exacerbated by sub-sea sulphur eruptions. In addition, solar installations near the coast have reduced generation due to sea fog. It was noted that WaveRoller technology could complement these existing forms of generation.
- Cooperation agreements with local entities were established and significant progress was made on WaveRoller sales projects during the project.

Namibia

- (https://www.hydroreview.com/hydro-industry-news/oceantidalstream-power/aw-energy-signs-mou-to-produce-green-hydrogen-from-wave-energy-in-namibia/#gref

Spain

- (https://www.lne.es/economia/2023/10/14/duro-logra-2-17-millones-93319775.html)
- By 2050, the business opportunity for AW-Energy's WaveRoller technology was estimated to be EUR 167bn in the total addressable market, EUR 53bn in the serviceable addressable market, and EUR 8bn in the serviceable obtainable market.

Perspectives for the future:

- Since Russia's war on Ukraine, the electricity market has changed. This affects many of the assumptions in these financial simulations, so updated calculations are proposed as new energy market conditions emerge. The marginal pricing characteristics of the energy markets has meant that fossil gas generation has heavily influenced the electricity price. However, the accelerated rollout of renewables has changed this dependence. The price capture ratio of wind and solar has decreased, and energy storage has an increasing influence on the price in many markets. This tendency will probably increase. The increased electricity price and revenue for existing asset owners has initiated national claw-back schemes that have in turn dampened investment in new projects.
- The impact of expanding the fleet of solar and wind to the required capacity was not considered. Added site development costs are anticipated as sites become progressively more difficult to develop. The interaction of local people with the anticipated large rollout of the renewable generation infrastructure is unknown. This may become a material factor in the future and accelerate alternative forms of renewable energy generation

Proposed next steps:

- This study presented technology to increase the efficiency of an electrolyser and downstream plant. Simulations were conducted to study the quality of generated electricity with and without electrical energy storage. A full-scale demonstration of the methods and assumptions described in the study was proposed as an important next step. An array of WaveRoller-X with associated equipment would enable this. AW-Energy is currently developing several projects with different partners, and these are expected to proceed in the coming year. The Fossil-free Steel project partners are invited to participate in these projects to further the work presented here.
- Below are illustrations of the WaveRoller technology that will be deployed in the pilot projects.

REFERENCES

D307752 – Technical report – SSAB fossil-free steel

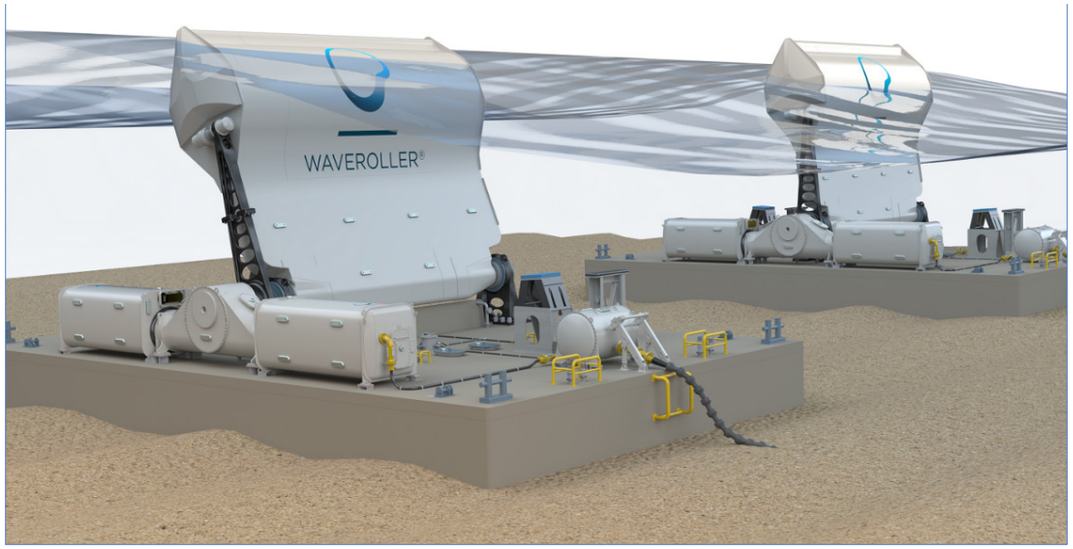

FIG 48 WaveRoller-C1 Array.

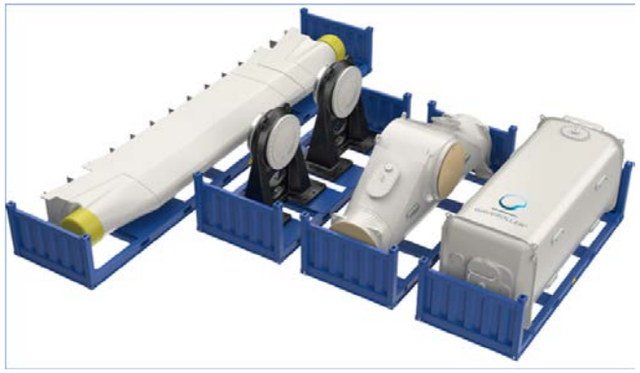

FIG 49 WaveRoller-C Logistics.

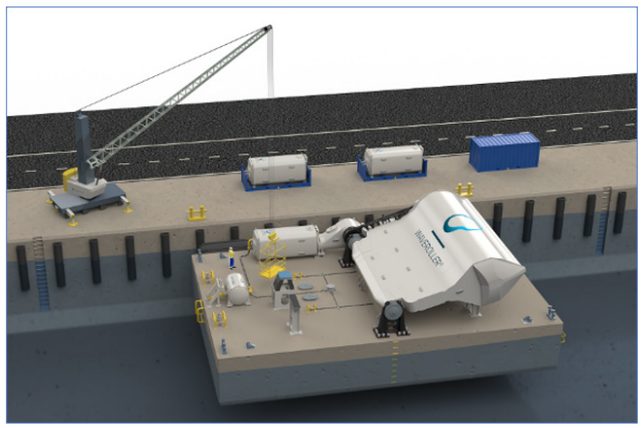

FIG 50 WaveRoller-C Assembly.

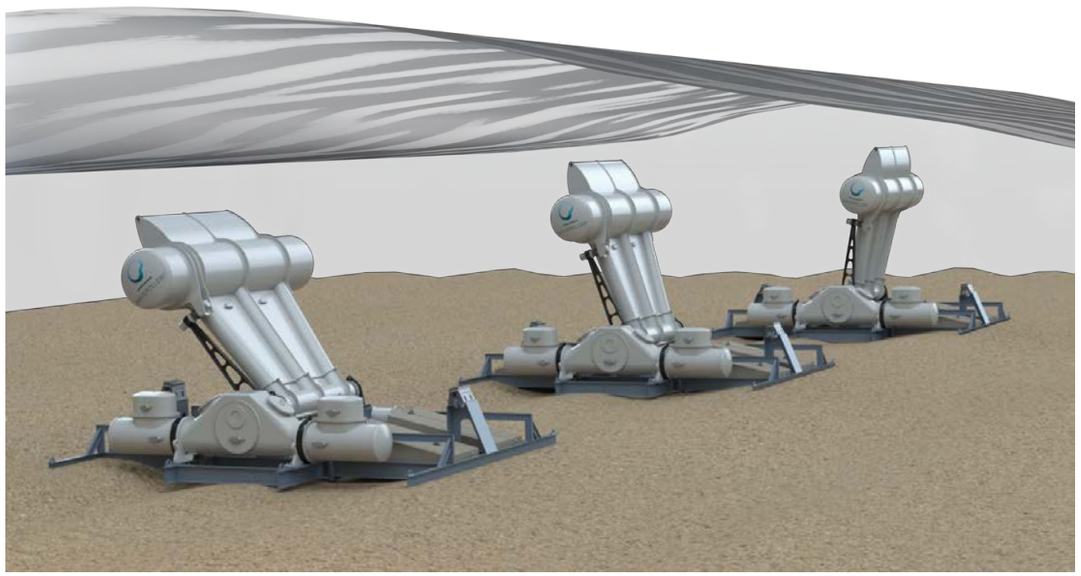

FIG 51 WaveRoller-X in operation.

FIG 52 WaveRoller-X Logistics.

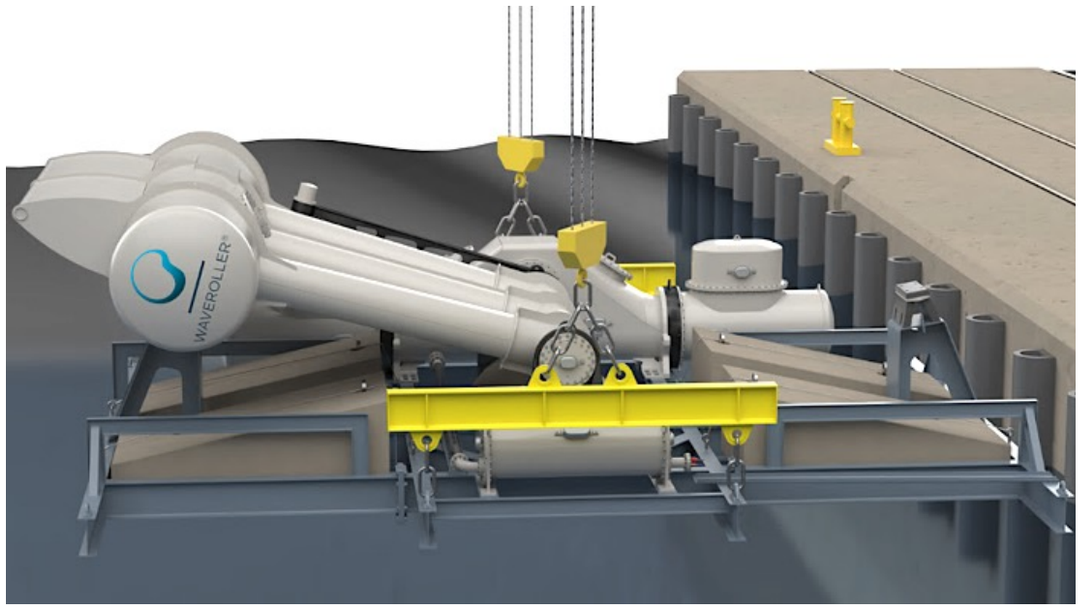

FIG 53 WaveRoller-X Assembly.

FFS TOWARDS FOSSIL-FREE STEEL

CONTRIBUTORS

Markus Hurskainen, Tiia Kanto, Jussi Ikäheimo, Jeremias Hopsu, Kirsikka Kiviranta, Jari Ihonen I VTT

4.7 Hydrogen logistics and supply

Hydrogen storage and transport infrastructure is key in enabling cost-effective green hydrogen value chains.

BACKGROUND

Although there have been many activities related to hydrogen production and electrolysers, the other vital pieces of the supply chain, namely storage and transport, have yet to receive similar attention. While electrolysers have the capability to adapt to the fluctuating output of wind and solar power plants, industrial applications utilising hydrogen typically require a relatively stable supply of hydrogen. In situations where electrolysers operate exclusively on intermittent renewable energy sources, storage between the electrolysers and the end-user becomes a necessity. Even if the electrolysers utilised grid electricity, hydrogen storage could decrease the costs by avoiding the running of the electrolysers at times of high electricity prices. While it is also conceivable to store electricity, it is more feasible to store molecules instead of electrons when the need is several hours or days. The most recent knowledge of different types of hydrogen storage and their applicability to Finland is therefore required.

In addition to storing, it will also be necessary to transport huge volumes of hydrogen. Hydrogen could be produced at locations where low-cost renewable electricity is available and transported to demand centres. Due to synergies, the optimal location for the electrolysers may not be at the end-user's site, where there may be no use for the waste heat and oxygen generated as a by-product or a lack of a high-capacity electrical grid connection. Furthermore, large electrolyser capacities also require space, which may be unavailable in close proximity to hydrogen demand sites. A more viable approach could be to install the electrolysers close to heat (and oxygen) demand centres and transport it to the demand site via a pipeline. Electrolysers could also be located next to new windfarms to avoid the need to build new electricity transmission lines, whose development has already been seen to have slowed down the development of new wind power projects.

However, pipelines are not the only option for transporting hydrogen. For smaller-scale users, compressed hydrogen can also be transported by lorries in gas cylinder containers. For large-scale users, more relevant options include liquid hydrogen and various chemical hydrogen carriers such as ammonia, methanol, and LOHCs (liquid organic hydrogen carriers). These could also enable the import – or more likely the export – of hydrogen from Finland by sea. An analysis of the characteristics of these technologies will shed light on their possible role as hydrogen transport and/or storage media for Finland.

Finally, most hydrogen supply chains will require the hydrogen pressure to be increased at some point. As the lightest element, even the mechanical compression of hydrogen presents some engineering challenges. On the other hand, the peculiar characteristics of hydrogen enable the utilisation of completely novel non-mechanical compression technologies. For the establishment of the hydrogen economy, it will therefore be important to assess the costs, performance, and market availability of large-scale compressors and the possibilities of novel compression technologies.

SOLUTION/METHOD

In the first phase, an extensive literature review of hydrogen compression, storage, and transport technologies was conducted. Various options were mapped, with a specific emphasis on large-scale technologies. The study included the gathering of the relevant performance and cost data required to assess the technologies' viability.

In the subsequent phase, the technologies that were identified as most relevant for Finland – hydrogen pipelines and lined rock cavern (LRC) storage – were then studied in more detail with a case study methodology using different simulation and modelling tools such as SpineOpt.

RESULTS, FINDINGS, OUTPUT, AND IMPACT

Hydrogen storage

Hydrogen has a high gravimetric energy density (142.0 MJ/kg) but a poor volumetric density (12.7 MJ/m^3), which makes the pre-processing of hydrogen before storage necessary. Depending on the desired properties of the hydrogen storage, different technologies can be applied. These technologies include compression, liquefaction, or binding hydrogen to other materials or substances. For example, the applied storage technology depends on the required storage capacity, duration, (dis)charging rate, purity of released hydrogen, and if the storage is for stationary or mobile purposes.

Storage technologies can be divided into physical and materials-based storage (Figure 54). Physical storage denotes the storage of hydrogen in its elemental form, either via compression or liquefaction, while materials-based storage comprises technologies where hydrogen is bound to other materials, either by adsorption or reactions with chemicals or (metal) alloys. Chemical carriers especially are expected to be scaled up in hydrogen transport. These chemicals are often widely traded and used bulk chemicals such as methanol or ammonia. Another type of hydrogen carrier is liquid organic hydrogen carriers (LOHC), which can be hydrogenated and dehydrogenated repeatedly without significant chemical losses.

The simplest and most common means for storing hydrogen is compression. Pressure vessels represent the traditional compressed hydrogen aboveground storage, ranging from small bottles to up to several hundreds of kilograms of hydrogen. For large-scale storage, the storage facility must be constructed below ground level, where the surrounding rock mass can provide support. Underground storage technologies include salt caverns, aquifers, depleted gas and oil fields, lined rock caverns (LRC), and pipe storage. The gas in the storage is divided into working gas and cushion gas, of which working gas represents the fraction that can be withdrawn from the storage once it is filled. Cushion gas, on the other hand, remains in the storage to ensure stability and reasonable compressor work. The ratio between working and cushion gas depends on storage technology. For example, aquifers may require up to 80% cushion gas, while pipe storage may have less than 10%. Depleted oil and gas fields, salt caverns, and LRC rank between this, with an approximately 50%, 30%, and 10% of cushion gas share respectively (Kruck et al. 2013).

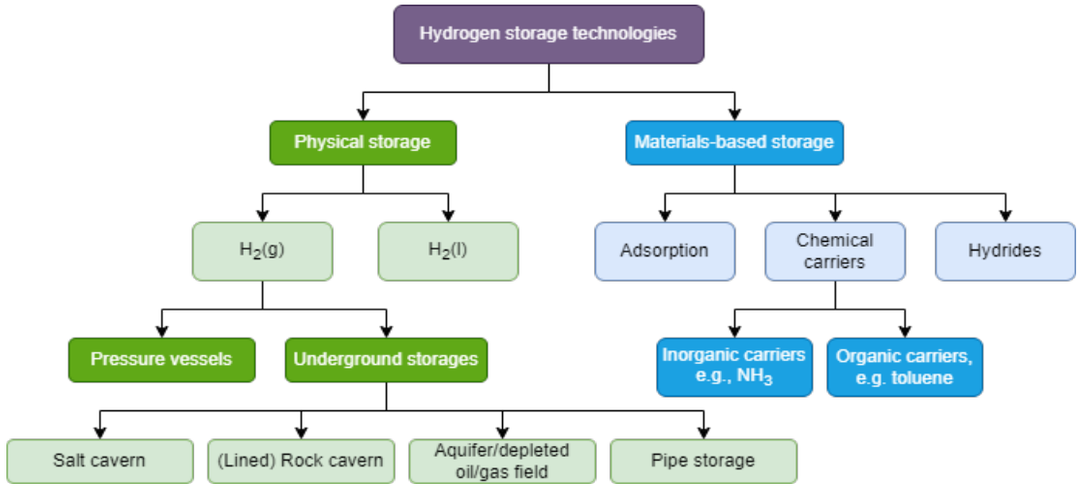

FIG 54 Hydrogen storage technology categorisation.

Hydrogen storage technologies differ markedly in terms of feasible hydrogen capacity ranges and the number of cycles they typically perform within a year (Figure 55). For example, pressure vessels and pipe storage are used in small-scale applications where the cycle durations are typically less than a day, while salt caverns, aquifers, and depleted gas and oil fields can be used for seasonal large-scale storage.

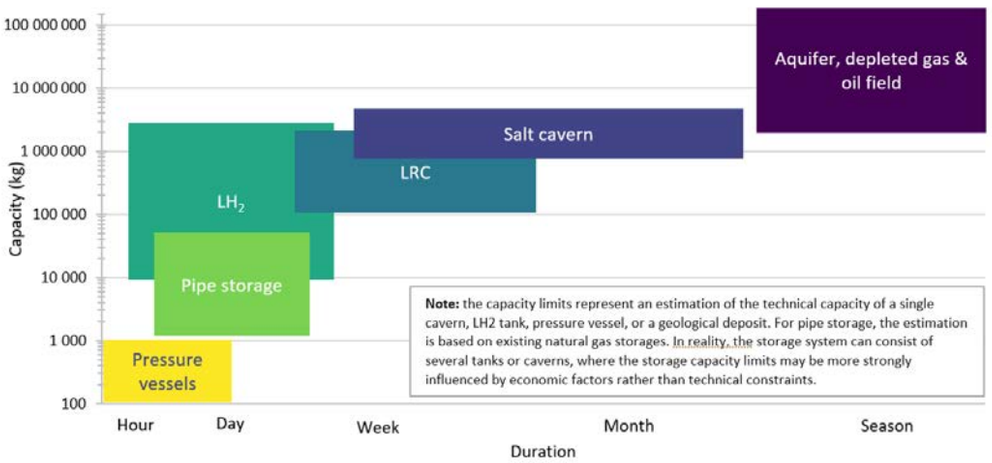

FIG 55 Indicative capacity and storing duration ranges for different hydrogen storage technologies.

As of today, large-scale underground storage of hydrogen takes place in salt caverns. A salt cavern is a solution-mined cavity which is suitable for storing gases due to their mechanical properties. Under compressive stress, rock salt becomes gas-impermeable, eliminating the need for additional sealing (Kruck et al. 2013). With a history dating back to the 1970s, salt rock reservoirs have been extensively employed for natural gas storage, exceeding 300 reservoirs in Europe alone. In the UK and the USA, salt caverns have been used to store hydrogen since the 1970s, providing decades of successful experience and affirming salt caverns' suitability for hydrogen storage. Salt caverns are estimated to have up to ten cycles (from empty to full and back to empty) over a year. With the discharging rate, the cycling properties outline the suitable use of storage – seasonal storage, for example, needs to perform 1–2 cycles a year, and the discharge rate can be slow, while energy storage that evens out daily fluctuations or provides grid frequency control needs a fast response time and multiple cycles.

In regions where porous rocks or salt formations are absent, a lined rock cavern (LRC) appears to be a sensible option. LRC storage is a steel-lined cylindrically mined cavern that is further secured with a pressure-transferring layer of concrete between the lining and the rock mass. The technology was developed in Sweden, initially for natural gas storage, but a pilot for the applicability of LRC as hydrogen storage is being conducted in Luleå between 2022 and 2024 by the HYBRIT consortium. LRC requires a uniform and hard bedrock such as granite or gneiss. The pressure range of LRC is contingent on the storage depth and quality of the bedrock, with estimates ranging between 20 and 250 bar. Notably, LRCs exhibit lower minimum pressure and a reduced fraction of cushion gas than salt caverns, as well as being estimated to operate more dynamically than salt cavern, with more annual cycles.

To the best of the authors' knowledge, there is no experience of storing pure hydrogen in aquifers, depleted oil or gas fields, or pipe storage. However, all the aforementioned technologies are used to store natural gas and are often mentioned in the literature as potential hydrogen storage technologies. Yet the chemical and biological reactions that can take place in such natural storage (including salt caverns) are largely unknown. Experiences with town gas storage indicate that hydrogen can be converted into methane at a relatively fast pace, necessitating purification or even ruling out certain technologies. In addition, hydrogen storage in porous media, i.e. aquifers and depleted oil and gas fields, poses significant limitations to operability, as they are capable of only one annual cycle y.

A summary of the storage technologies discussed in this study is presented in Table 9. The preferred option for large-scale hydrogen storage is a salt cavern due to its low cost and simple construction compared to other technologies. However, the lack of suitable geological formations in Finland rules out salt caverns, as well as aquifers and depleted oil and gas fields. Among the studied technologies, the only feasible option for large-scale storage of hydrogen therefore appears to be LRC, as the Finnish bedrock consists largely of crystalline rocks, for which the technology in question has been developed. Liquid hydrogen storage still plays a minor role in global hydrogen storage, limited to special applications requiring liquid hydrogen, such as the space industry. The liquefaction of hydrogen only to store it on site with subsequent regasification is not regarded as feasible. At a medium scale, pipe storage could be applied within a very short time frame, as the structure is essentially the same as in hydrogen transmission and distribution pipes, but costs are relatively high. For the smallest scale, pressure vessels represent mature technologies.

While LRCs are associated with higher investment costs than salt caverns, LRC enables faster charging and discharging rates and does not suffer from hydrogen contamination, which may prove to be a major advantage.

	Salt cavern	Aquifer/ Depleted oil/gas field	Lined rock cavern (LRC)	Pipe storage	Pressure vessel	Liquid hydrogen
Scale	Large	Large	Medium–Large	Medium	Small	Medium
Storage timespan	Medium–Long	Long	Short–Long	Short–Medium	Short–Medium	Short
(Cycles per year)	(<10)	(1–2)	(>10)	(>10)	(>10)	(>10)
Investment cost [€/kg H_2]	10	n.a.	50	460	400–500 (Type I)	60***
Pressure range [bar]	60–180	39–53** 150–170** 110–280**	10–250	5–100	<200 (Type I) <300 (Type II) <700 (Type III, IV)	atmospheric
Example storage* volume [m^3]	500,000	n.a.	40,000	6,000	n.a.	4,700
Example storage useful H_2 [t]	4,000	n.a.	680	45	n.a.	340
Hydrogen contamination	yes	yes	no	no	no	no
Geological requirements	high	high	moderate	minor	none	none

* From (Kruck et al. 2013)
** Natural gas storage in Hähnlein (Germany), Stenlille (Denmark), and Rheden (Germany). The first two are aquifers; the third is a depleted natural gas field (Kruck et al. 2013).
*** Does not include the liquefaction plant.

TABLE 9 Comparison of hydrogen storage technologies

Hydrogen pipelines

For large-scale energy transport, hydrogen pipelines provide an appealing alternative to energy transport via power grids. In 2021, the global hydrogen pipeline network spanned a total length of 5,209 km, with Europe taking the lead in planned and announced additions. Projections indicate that Europe is set to witness an expansion of more than 1,900 km in pipeline length between 2022 and 2026, with Denmark, the Netherlands, and Italy leading the way (GlobalData 2023).

Several hydrogen pipeline initiatives are currently underway in Finland and are being developed by Gasgrid Finland Oy, the Finnish transmission system operator for gas. These initiatives include: 1) the Nordic Hydrogen Route, designed for cross-border hydrogen transport in the Bothnia Bay Region; 2) the Nordic–Baltic Hydrogen Corridor, which aims to enable hydrogen transmission between Finland, Estonia, Latvia, Lithuania, Poland, and Germany; and 3) the Baltic Sea Collector, which plans an offshore hydrogen pipeline connecting Finland, Sweden, and Germany (Figure 56). All these pipelines are scheduled to become operational by 2030. Furthermore, Gasgrid Finland's first hydrogen transmission infrastructure demonstration project is ongoing in Southeast Finland, with a plan to connect a chemical industry site that produces by-product hydrogen for a steel mill (Gasgrid Finland 2023).

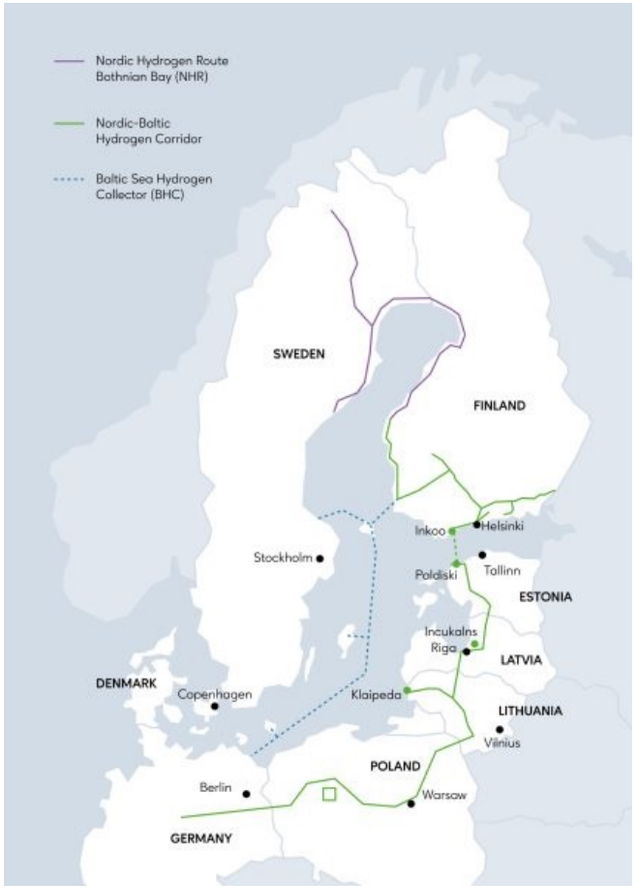

FIG 56 Ongoing hydrogen pipeline initiatives in Finland (Gasgrid Finland 2023).

Hydrogen pipeline transmission costs involve the pipeline itself, compressors, and compression energy. New pipeline investment depends on diameter and operating pressure, with larger diameters resulting in non-linear increases in steel use, labour costs, and capacity. The construction of a larger pipeline is therefore often more cost-effective than multiple smaller ones. Cost estimates vary widely due to factors like terrain, design pressure, cost scope, and fluctuating steel prices. Higher pressures require thicker pipelines, increasing costs and introducing uncertainty. New hydrogen pipelines can be 10–50% more expensive than natural gas pipelines. Transporting hydrogen over 1,000 km in Europe's planned network is estimated at €0.11–0.21/kgH2 (€3.3–6.3/MWh) (European Hydrogen Backbone 2022).

Hydrogen carriers and transport

Chemical hydrogen carriers are substances, either organic or inorganic, that contain hydrogen. The basic principle is to make hydrogen react with other agents like CO_2 or N_2, resulting in hydrogen-containing substances designed to yield more hydrogen per unit volume than elemental hydrogen. These carriers can be circular or non-circular. Circular carriers, exemplified by compound pairs like toluene and methylcyclohexane, can repeatedly undergo loading and unloading with hydrogen (Figure 57). On the other hand, non-circular carriers such as ammonia and methanol do not follow a closed-loop system, meaning the carrier material or compound is not regenerated for multiple cycles of hydrogen storage and release.

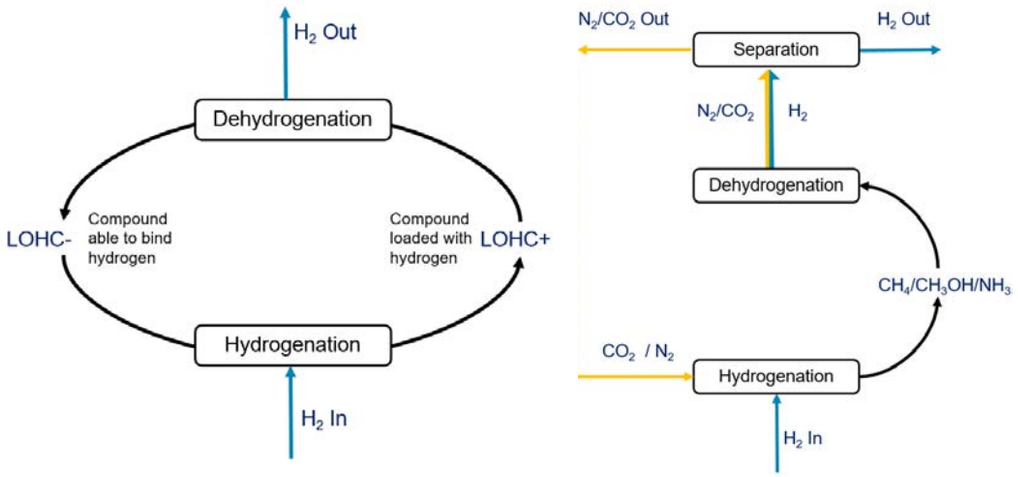

FIG 57 Difference between circular carrier (left) and non-circular carrier (right) concepts.

The ideal hydrogen carriers possess high hydrogen/energy density (kWh/m^3), are easily and safely handled (liquid at atmospheric conditions, low flammability, non-toxic, non-corrosive), environmentally friendly, stable with minimal storage losses and degradation, energy-efficient in hydrogen binding and release, cost-effective, and available in large quantities or have the potential for scaling up the production.

In this project, the considered hydrogen carriers were ammonia, methane, methanol, and three LOHCs (toluene, benzyl toluene, and dibenzyl toluene). Liquid hydrogen (LH2) was used as the benchmark.

As discussed earlier in this report, a major challenge in hydrogen storage and transport is the low energy density of hydrogen and consequently, large vessel volumes. However, converting hydrogen into more hydrogen-dense forms introduces another challenge, which is the conversion losses and energy input associated with conversions. The dehydrogenation of hydrogen carriers requires a thermal energy input corresponding to 25–40% of the lower heating value of hydrogen. The source of heat therefore has a significant effect on economic profitability and the environmental impact.

LH_2 avoids chemical conversion losses and the need for additional purification – re-gasifying hydrogen can utilise ambient heat, but liquefaction is both capital- and energy-intensive, and sustaining the cold environment, -253 °C, for LH_2 is challenging. Moreover, LH_2 is neither produced nor transported at large scales. Instead, NH_3, MeOH, and CH_4 are some of the most produced and traded chemicals globally, which facilitates their application as hydrogen carriers. Besides the existing large-scale infrastructure to transport these carriers, storage conditions are milder compared to LH_2. Some challenges and scaling needs are present with all carriers, however; NH_3 reconversion back to H_2, known as ammonia cracking, is not yet proven at a large scale. Similarly, commercially available steam reformers for MeOH are small. Both MeOH and methane production using (biogenic) CO_2 sources and green hydrogen still require capacity upscaling and catalyst research to improve process performances. It is also noteworthy that the feasibility of synthetic MeOH and CH_4 also depends on technological advances in the field of carbon capture.

LOHCs benefit from their diesel-like features, making them generally compatible with existing infrastructure. They experience no losses during storage and transport, have low toxicity, and can be handled in ambient conditions. On the other hand, LOHCs have lower hydrogen content than the other carriers discussed here. Like other carriers, LOHCs require a significant energy input in dehydrogenation (25–35% of the lower heating value of hydrogen). Of the three LOHCs covered, benzyl toluene (BT) seems to perform best in a cold climate.

As a result of the hydrogen carrier assessment, no superior carrier could be identified. The optimal solution depends on various case-specific requirements, e.g. transport distance, volume, required purity, and transport starting point and destination. However, some indicative heuristics have been created in several reports; intracontinental distances (up to ~3,000 km) typically advocate for pipelines, but this depends largely on capacity. For waterborne transport, LH_2 and LOHC appear to be feasible for short to medium distances – LOHC for smaller volumes, and LH_2 for large volumes. Having the highest hydrogen density, ammonia is favoured when transport distances are long, and volumes large.

Compressors

Various compressor technologies for hydrogen gas exist. They can be divided into two categories: mechanical and non-mechanical compressors. In mechanical compressors, mechanical energy is directly converted into gases' potential/pressure energy. Most commercial hydrogen compressors are mechanical compressors. They are also applicable for other gases, whereas non-mechanical compressors are specific to hydrogen gas properties. Currently, all non-mechanical hydrogen compressors are mostly in the research stage.

Mechanical hydrogen compressors include reciprocating piston, diaphragm, linear, liquid, scroll, screw, vane, and centrifugal technologies. Reciprocating piston and diaphragm compressors are the most widespread technologies due mainly to their maturity and suitability for various applications.

Non-mechanical hydrogen compressors include cryogenic, metal hydride, electrochemical, and adsorption compressors. Cryogenic, metal hydride, and adsorption compressors are thermally driven, making them attractive for waste heat applications, but they tend to have very low efficiency. An electrochemical compressor is a potential technology for compressing hydrogen due to its high efficiency. It resembles PEM (Proton Exchange Membrane) technology in fuel cells or electrolysers, as hydrogen protons are forced through a membrane by supplying electrical power. A full list of the main advantages and disadvantages of all hydrogen compressor technologies is shown in Table 10.

	Compressor technology	Pros (+)	Cons (-)
Mechanical compressors	Reciprocating piston compressor	Maturity, large range of flowrates, high discharge pressure	Contamination (lube oil), embrittlement, many moving parts, maintenance need, thermal transfer management, noise
	Diaphragm compressor	Maturity, power efficiency, high throughput, low cooling requirement, purity of compressed H_2,	Diaphragm failure/durability, complex design
	Linear compressor	Compactness, reliability, efficiency	Necessity to control piston displacement, necessity to operate at resonant conditions
	Ionic liquid compressor	Efficiency, energy consumption, weariness and service life, material costs, low noise, no gas contamination, moving parts, number of moving parts	Corrosion, leaks, cavitation
	Centrifugal compressor	Maturity, efficiency in optimal design conditions, less vibration and noise problems vs reciprocating	Low pressure ratio for H_2, durability of the impeller with H_2 (due to increased impeller speed)
	Screw compressor	Flowrate capacity, capacity controllability, reliability	Low discharge pressure, load-bearing capacity of the shaft
	Scroll compressor	Noise level, compact design, efficiency, fewer moving parts vs reciprocating piston	Complex design, repairability, manufacturing cost
	Vane compressor	Efficiency, compact design, low noise and vibration, maintenance	Low discharge pressure
Non-mechanical compressors	Cryogenic compressor	H_2 density, volumetric efficiency, gravimetric and volumetric capacities	Energy intensity, management of thermal insulation, vacuum stability of insulated vessels
	Metal hydride compressor	Thermallv-driven. no moving parts, compact design, safe, no noise, high-purity H_2	Efficiency (limited heat transfer), weight, cost
	Electrochemical compressor	Operation cost, high-purity H_2, no moving parts, very high compression efficiency (low to moderate pressures), ability to function as H_2 purifier	Manufacturing challenges, sealing, cell resistance, H_2 back diffusion
	Adsorption compressor	Thermallv-driven. no moving parts, no noise, no sealings, adsorbent cost	Thermal conductivity of adsorbents, thermal management, low-temperature (cryogenic) operation

TABLE 10 Main advantages and disadvantages of different hydrogen compressor technologies.

Several potential hydrogen compressor manufacturers with high flowrates (>10,000 m^3/h or >1,000 kg/h) were found. Only centrifugal and screw compressor technologies could compress these large flowrates. Both technologies feature a rotating mechanism that enables high rotational speeds. No single technology is capable of compressing hydrogen with a high flowrate and high discharge pressure, as Figure 58 shows. Most compressor technologies are either suitable for a high flow capacity or a high discharge pressure, but not for both. The reciprocating piston compressor seems the best trade-off. Metal hydride and scroll compressor technologies, which are characterised by a low flow capacity and low discharge pressure, have other properties (such as low noise or thermal drivability) that make them suitable for some niche applications.

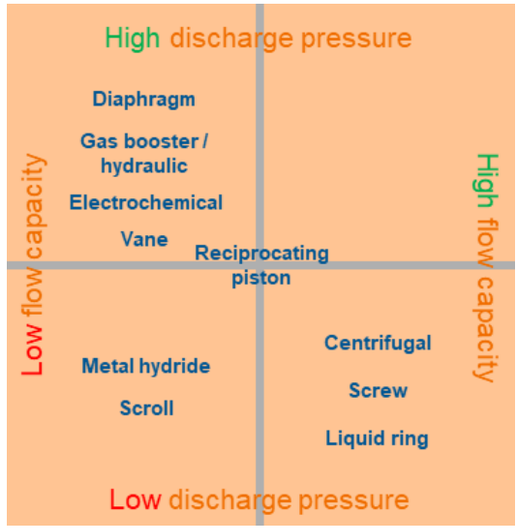

FIG 58 Suitability of different hydrogen compressor technologies for high/low flowrates and discharge pressure levels.

Hydrogen compressor efficiency data are relatively scarce. The data are gathered from literature and are shown in Figure 59. A relatively large spread of efficiency values can be seen for some technologies (such as for the reciprocating piston compressor: ~45–90%), but the main differences between the technologies can be observed. Electrochemical and centrifugal compressor technologies represent the highest end by exceeding even 90%. The very low overall efficiency of the metal hydride compressor stands out clearly from all other technologies.

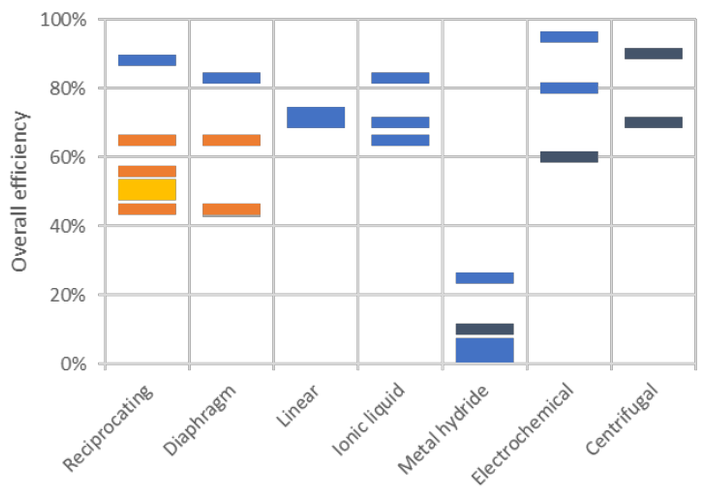

FIG 59 All the identified literature data for hydrogen compressor efficiencies. Different colours represent different sources (Sdanghi et al. 2018, EFRC 2022, Khan et al. 2021, Cornish 2011, DoE 2009).

Cost data were sought both from the literature and manufacturers. In general, decreased suction pressure, increased discharge pressure, and increased flow capacity increased the cost of hydrogen compressors. Figure 60 shows specific costs (€/[kg/h]) for <100 and >100 kg/h capacities, indicating quite significant economies of scale until a capacity of 1,000 kg/h. The operating and maintenance cost of hydrogen compressors is typically 4–5% of the capital expenditure per year.

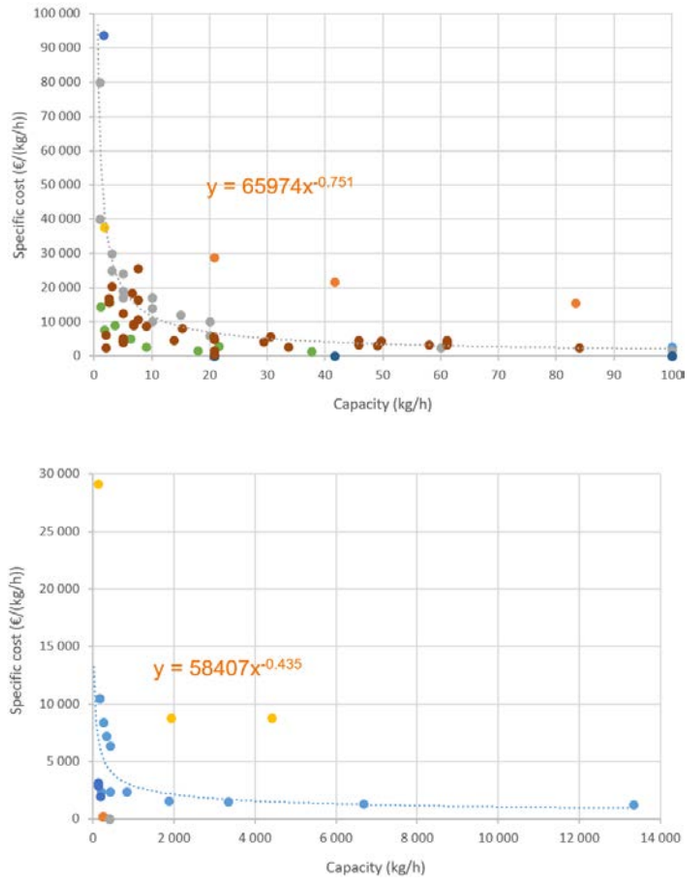

FIG 60 Specific costs of hydrogen compressors for <100 kg/h (left) and >100 kg/h (right) capacities (Sdanghi et al. 2018, Khan et al. 2021, Cornish 2011, Christensen 2020, Ulleberg & Hancke 2019, IEA ETSAP 2014, Minnuo 2023, Dawkins et al. 2022, Weinert 2005.)

To summarise, various compressor technologies and manufacturers for H_2 already exist. However, no technology can achieve very high pressure and flowrates at the same time. For the largest flowrates, reciprocating, centrifugal, and screw compressors with capacities >10,000 Nm³/h are available. When small flowrates and high pressure are required, the electrochemical H_2 compressor is a promising non-mechanical technology, as it has high efficiency and gas purity, low noise and vibration, and no moving parts.

Case study: Using electrolysers to accelerate wind power in areas with limited power transmission capacity

Finland is currently experiencing a rapid pace of construction for new wind power capacity. The installed capacity of wind power reached 6 GW in 2023, and by 2030, the installed capacity is expected to exceed 20 GW (Fingrid 2023A). With the increase of weather-dependent electricity production, the power system will occasionally experience shortages of transmission capacity, and as large wind power sites are located in remote areas, the projects may experience delays if the transmission capacity additions take place at a slower pace than wind projects aspire to progress.

Co-locating hydrogen production with wind production could provide multiple benefits for wind power operators, local communities, and society at large. From the perspective of the power grid, bringing electricity consumption closer to production allows lighter sizing and additional investments in power transmission capacity, which can make good overall economic sense. In this case, the need for hydrogen transmission increases if hydrogen consumption sites are located at a distance from production. Energy transmission in the form of molecules instead of electricity has certain advantages: if the end use of energy is in hydrogen, power lines also transmit the fraction of energy that will be lost in electrolysis (~35%). Moreover, the electricity transmission infrastructure requires more land area than pipelines (Fingrid 2022). This could favour hydrogen pipelines from not only the economic but also the environmental and landscape perspectives and increase the social acceptance rate.

Wind power has experienced decreasing capture prices due to the cannibalisation effect, and this trend is likely to continue as the cumulative wind (and solar) power capacity increases. The demand flexibility of electrolysis could mitigate the cannibalisation effect and provide an off-taker for the produced electricity. On the other hand, hydrogen producers can hedge against electricity price volatility though power purchase agreements (PPAs), as the electricity price is the most important contributor to the hydrogen production cost.

For local communities, hydrogen production and further use close to wind power production brings employment and tax revenues. As the current wind power production and future capacity additions are outside metropolitan areas, largely in areas that suffer from migration loss and unemployment, it would be more socially sustainable to help municipalities with large wind power potential to benefit from it by extending a wider segment of the hydrogen value chain and its associated jobs to these municipalities.

Oulujärvi, Northern Ostrobothnia

In the areas around Oulujärvi, more than 6 GW of new wind power capacity is being planned by 2030 (Fingrid 2023B). Currently, there is no connection capacity for new production in the main grid in the area. New capacity will be built in the coming years, and it is realistic to assume that a significant fraction of the planned wind power capacity will not materialise. However, the planned production capacity additions are unprecedented, and at this scale, transmitting energy in molecules instead of electrons could be justified. Theoretically, 6 GW of installed wind power capacity could produce approximately 23.5 TWh of electricity annually, using the 2019 wind speed data for the area. If that electricity were fed to an electrolysis process that con-

sumed 52 kWhel/kgH_2, this electricity could be converted to roughly 450,000 tonnes of hydrogen. According to European Hydrogen Backbone, this would correspond to hydrogen transmission with a DN900 pipeline with a capacity of approximately 80% (European Hydrogen Backbone 2021). Figure 61 illustrates the wind projects being planned in Northern Ostrobothnia and around Oulujärvi. Hydrogen produced in the area could be transmitted to Oulu. Hydrogen is currently used in the city, and there is potential to increase use through new applications: large point sources of CO_2 could be utilised to produce synthetic methanol or methane, for example. Additionally, there is a large harbour, and the planned Nordic Hydrogen Route hydrogen transmission pipeline passes through Oulu, which will provide a connection with large users all the way to Northern Sweden by 2030.

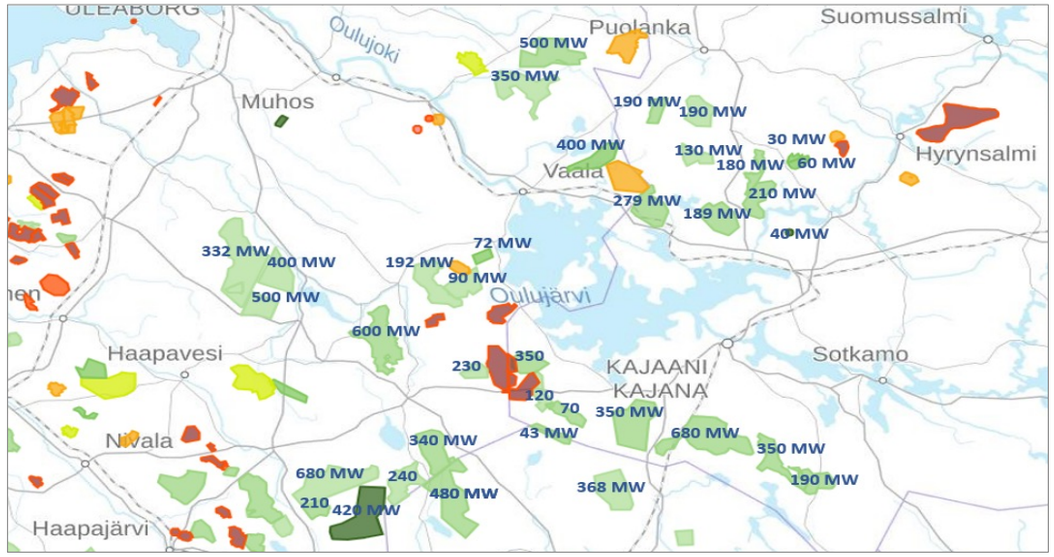

FIG 61 A screen capture of planned wind power projects from Fingrid's Grid Scope map, with manually added planned wind power capacities.

Targeting a smaller area, 1.9 GW of new wind power capacity is planned between the Vaala and Paltamo municipalities alone. Again, not all the projects in the pipeline will materialise, but assuming roughly 35% of the planned capacity will eventually be built, this would equate to 730 MW of new wind power capacity. Using 2019 wind speed data and assuming a 150 m hub height for the windmills, the average electricity output of such a site would be 340 MW. The duration curves from the perspective of power transmission needs are presented in Figure 62. If an electrolysis capacity of 400 MW were installed to utilise all the available wind power production and excluding 20% of the least windy hours, the system could produce 46,000 tonnes of H_2 a year. By comparison, the total consumption of hydrogen in Finland today is approximately 150,000 tonnes per year (Laurikko et al. 2020). If further converted to higher value products, this would equate to e.g. approximately 258,000 tonnes of green ammonia, exceeding Finland's current ammonia consumption. By directly converting electricity into hydrogen at the wind power production site, the maximum transmission need in the main grid can be reduced by 55%, which is illustrated in Figure 62. This in turn allows a decrease in the required installed power transmission capacity by an equivalent capacity. As with a hydrogen pipeline, this amount of hydrogen is modest, and would correspond to a DN500 pipe using less than a quarter of its capacity. Using EHBs investment cost data (European Hydrogen Backbone 2021), the levelised cost of transporting hydrogen for 130 km would be approximately €0.8/kgH_2. The total cost of production and transport would equate to €4.0/kgH_2, assuming a total capital investment of 1,000 €/kWe for the electrolyser plant and an electricity price of €40/MWh. If the pipeline was later utilised at 75% capacity, the levelised cost of transport would decrease to €0.3/kgH_2.

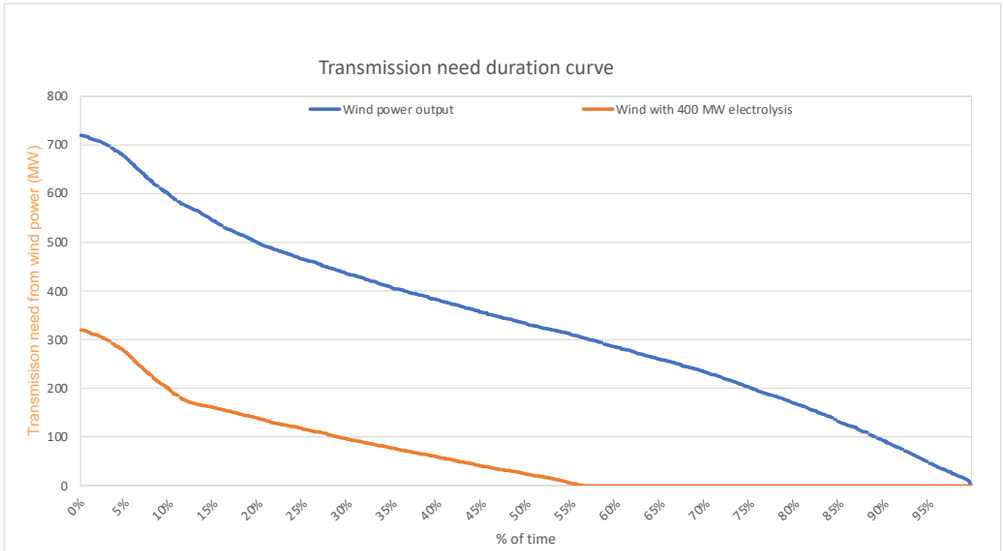

FIG 62 Electricity transmission need without (blue) and with (orange) hydrogen production connected to wind power production.

Disclaimer: The estimations were performed at a very granular level and contain significant uncertainties, both in wind power capacity and production estimations, as well as in hydrogen production and transmission costs. Instead of an attempt to display a realistic or desired development in the area, this preliminary case study should be treated as an opening for a wider discourse on the potential and extent of the integration of variable renewable electricity and hydrogen production, particularly in regions that are not in the immediate vicinity of large industrial sites.

Case study: Utilisation of waste heat from electrolysers: where should electrolysers be located?

To enable the role of hydrogen in the energy transition, it is very important to take advantage of the by-products of the electrolysis process. One important by-product is the waste heat from electrolysis. In countries where there are district heating networks, distributing the collected waste heat is especially easy. An obvious problem is that the locations of hydrogen demand and heat demand do not always coincide. At least one of the energy vectors should therefore be transported. This work studied the techno-economic feasibility of exploiting the waste heat in an existing district heating system when the hydrogen demand was not co-located with the heat demand.

The study focused on a DH system of a typical medium-sized Finnish town. Several system attributes may affect the economic feasibility of heat integration, such as the magnitude of hydrogen demand, the types of production units available for heat generation, the heat demand profile, fuel prices, etc. In addition, the option for transporting heat instead of hydrogen exists. The effect of only a subset of all the attributes was studied. Figure 63 illustrates the system composition. Heat production was allowed by biomass and oil boilers, biomass-fired CHP, and heat pumps in addition to the electrolysis plant. Hydrogen was transported to the usage site via a dedicated pipeline.

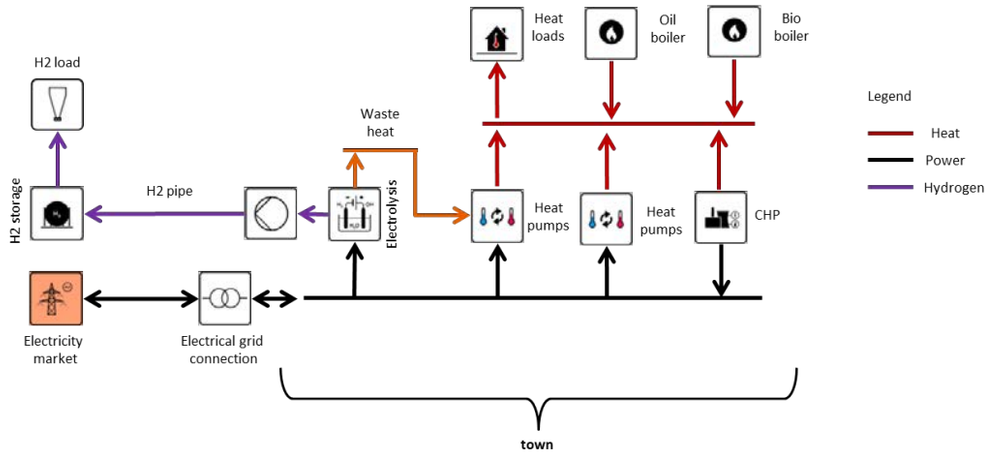

FIG 63 Illustration of the different components and energy flows in the studied system.

The SpineOpt model was used for the economic analysis of the district heating system and the electrolysis plant. The model is based on the optimisation of total system costs, including fuel, taxes, variable operation and maintenance costs, and electricity purchases.

In the base scenario, 100 MW of hydrogen demand was served by the electrolysis, whereas the peak heat demand of the district heating system was 450 MW. As Figure 64 shows, the maximum economic transport distance in this scenario was 128 km. High electricity prices reduced the gains of heat integration (Constrained market scenario), whereas the increased role of the biomass boiler in the system had a limited effect. Halving the magnitude of served hydrogen demand (small plant scenario) reduced the transport distance to 80 km. Hydrogen transport displays significant economies of scale.

The study found that the additional flexibility offered by the inherent hydrogen storage in the transmission pipe was rather modest, corresponding to only less than one hour of hydrogen demand in the base scenario with a 128 km pipeline. It is very likely that larger dedicated hydrogen storage would be built to offer more flexibility.

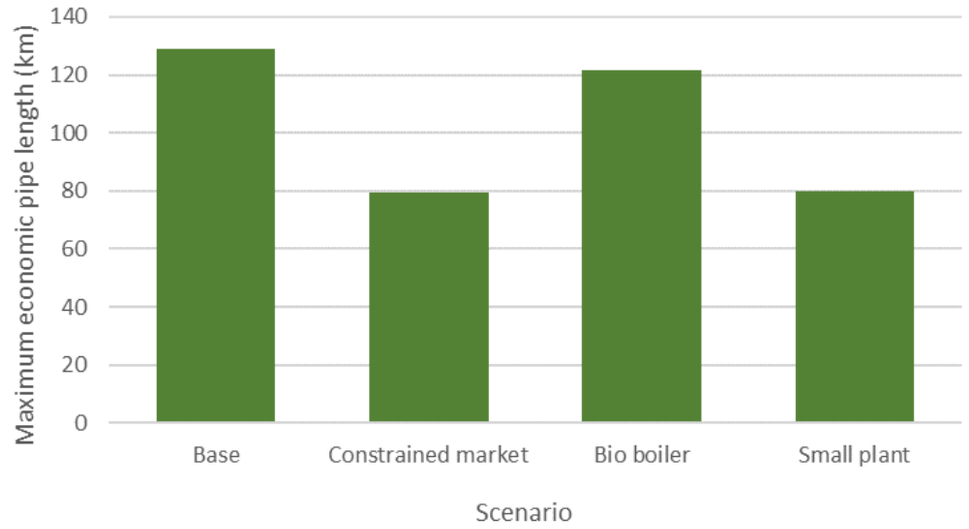

FIG 64 Maximum economic hydrogen transport distance in different scenarios.

Co-locating the electrolysis with hydrogen demand and transporting the waste heat was also considered. A steady-state model was used to dimension the district heating pipe: in the base scenario, a DN400 size pipe was cost-optimal. The cost of the district heating pipe proved to be 34% higher than the cost of the hydrogen pipe. In addition, the long delays and cooling of the pipe complicated the scheduling of the electrolysis plant. However, given the large uncertainty in the hydrogen pipe cost, it was impossible to rule out the heat transport option as more expensive.

The analysis is ongoing, and more detailed results will be reported later.

REFERENCES

Christensen, A. (2020.) Assessment of hydrogen production costs from electrolysis: United States and Europe

Cornish, A. J. (EPC). (2011) Hydrogen fueling station cost reduction study: Survey results and analysis of the cost and efficiency of various in-operation hydrogen fueling stations

DoE (2009) Energy requirements for hydrogen gas compression and liquefaction as related to vehicle storage needs, Department of Energy, USA.

Dawkins, J., Ash, N., and Suvendiran, K. (2022) Cost reduction pathways of green hydrogen production in Scotland EFRC (2022) Hydrogen compression: Boosting the hydrogen economy, European Forum for Reciprocating Compressors

European Hydrogen Backbone (2021) Analysing future demand, supply, and transport of hydrogen. Available at: https://ehb.eu/files/downloads/EHB-Analysing-the-future-demand-supply-and-transport-of-hydrogen-June-2021-v3.pdf

European Hydrogen Backbone (2022) European Hydrogen Backbone: A European hydrogen infrastructure vision covering 28 countries [online]. Available at: https://ehb.eu/files/downloads/ehb-report-220428-17h00-interactive-1.pdf

Fingrid (2022) Energian siirtoverkot vetytalouden ja puhtaan energiajärjestelmän mahdollistajina, [Energy transmission grids as enablers of the hydrogen economy and clean energy system] Mid-term report. In Finnish. Available at: https://gasgrid.fi/wp-content/uploads/Fingrid-Gasgrid_Valiraportti_Energian-siirtoverkot-vetytalouden-ja-puhtaan-energiajarjestelman-mahdollistajina.pdf

Fingrid (2023A.) Kantaverkon kehittämissuunnitelma 2024–2033 [Development plan for the national electricity grid]. In Finnish. Available at: https://www.fingrid.fi/globalassets/dokumentit/fi/kantaverkko/kantaverkon-kehittaminen/fingrid_kehittamissuunnitelma_luonnos_26.6.pdf

Fingrid (2023B) Grid scope map. Available at: https://www.fingrid.fi/en/grid/grid-connection-agreement-phases/grid-scope/ (Accessed 11 October 2023)

Gasgrid Finland (2023) Website https://gasgrid.fi/en/projects/ (Accessed 11 October 2023)

GlobalData (2023) Hydrogen Pipelines Length and Capital Expenditure Forecast by Region, Countries, Companies and Projects, 2023–2027 [online]. Available at: https://www.globaldata.com/store/report/hydrogen-pipelines-length-and-capital-expenditure-projects-analysis/

IEA ETSAP (2014) Hydrogen production & distribution

Khan, M. A., Young, C., Mackinnon, C., and Layzell, D. B. (2021) The techno-economics of hydrogen compression: technical brief

Kruck, O., Crotogino, F., Prelicz, R., and Rudolph, T. (2013) Overview on all Known Underground Storage Technologies for Hydrogen [online]. Available at: https://hyunder.eu/wp-content/uploads/2016/01/D3.1_Overview-of-all-known-underground-storage-technologies.pdf

Laurikko, J., Ihonen, J., Kiviaho, J., Himanen, O., Weiss, R., Saarinen, V., Kärki, J., and Hurskainen, M. (2020) National Hydrogen Roadmap for Finland, Business Finland, ISBN 978-952-457-657-4.

Minnuo (2023) Website https://mncompressor.com/gas_compressor/hydrogen compressor/?gclid=EAIaIQobChMIwL MrzY_QIVTY9oCR3D2QQVEAAYASAAEgJ2avD_BwE (Accessed 2 March 2023)

Sdanghi, G., Maranzana, G., Celzard, A. and Fierro, A. (2018) Review of the current technologies and performances of hydrogen compression for stationary and automotive applications. Renewable and Sustainable Energy Reviews, 102, November 2018, pp. 150–170, 2019, doi: 10.1016/j.rser.2018.11.028 Ulleberg, Ø and Hancke, R. (2019) Techno economic calculations of small scale hydrogen supply systems for zero emission transport in Norway

Weinert, J. (2005) A near term economic analysis of hydrogen fueling stations

FFS TOWARDS FOSSIL-FREE STEEL

CONTRIBUTORS

Krista Kuutti and Sari Rautiainen I VTT
Samuli Urpelainen and Mika Huuhtanen I University of Oulu

4.8 Proof-of-concept for selected liquid hydrogen carriers

Improving the feasibility of hydrogen transport and storage by enabling efficient hydrogen release with novel catalysts

BACKGROUND

Stationary onsite hydrogen storage using liquid hydrogen carriers enables variable operation of electrolysers according to electricity prices. Hydrogen carriers also enable efficient and safe transport of hydrogen over long distances. Liquid organic hydrogen carriers (LOHC) store hydrogen by chemical bonding to the carrier molecule, such as toluene or benzyltoluenes. While the hydrogenation of the carrier to store the hydrogen is a well-established technology, hydrogen release by dehydrogenation is currently used only in a handful of industrial-scale examples.

The dehydrogenation catalyst is at the core of the process: hydrogen release from LOHC occurs on a heterogeneous metal catalyst at elevated temperatures (150–400 °C). The stability and activity of the catalyst are crucial for a feasible process: the catalyst should withstand several catalytic cycles without deactivation. Furthermore, the formation of by-products is detrimental to the purity of the released hydrogen, and the selectivity of the reaction is therefore extremely important. Platinum catalysts are the most extensively studied catalysts for the process thanks to their high activity and selectivity. However, due to the high price of the metal, it is crucial to minimise the amount of platinum used and maximise the efficiency of the metal.

In this task, novel efficient catalysts for releasing hydrogen from liquid organic hydrogen carriers were developed in collaboration with VTT and the Max-Planck-Institut für Kohlenforschung (Germany). The catalysts were tested in a continuous laboratory-scale hydrogen release process at VTT. An extensive catalyst characterisation was conducted by the University of Oulu.

SOLUTION, METHOD

The goal of the task was to develop novel methods for the preparation of stable and active hydrogen release catalysts. However, the conventional catalyst preparation using solution methods produces large amounts of waste, as solvents and precursors are used. Mechanochemical synthesis methods such as ball milling are simple, reproducible, and scalable methods which are attracting growing interest in catalyst synthesis (Amrute 2021). The novel catalysts were prepared in collaboration with Prof. Ferdi Schüth's group at the Max-Planck-Institut für Kohlenforschung in Mülheim, Germany. For comparison, conventional impregnated catalysts were prepared based on previous work at VTT (Aakko-Saksa 2020). In both cases, platinum was supported on metal oxides in the form of nanometre-sized particles. The effect of support and dopant was also studied.

The catalysts were used in the dehydrogenation of methylcyclohexane (MCH) into toluene, which is one of the most promising LOHCs and is used on a commercial scale by the Chiyoda Corporation in Japan. The catalysts were tested in a continuously operated laboratory-scale reactor at atmospheric pressure in the laboratories at VTT. The reactions were carried out in the gas phase, and online GC analysis was used to determine the conversion of MCH and the amount of released hydrogen. Process conditions were studied using statistical methods, and the various preparation methods, supports, and active metals were compared.

The catalysts were characterised using both standard laboratory techniques and large-scale synchrotron radiation facilities (such as the Canadian Light Source, CLS, and MAX IV Laboratory, MAX IV). The nanostructure of the catalysts was determined using transmission electron microscopy (TEM) coupled with an energy dispersive X-ray spectrometer (EDS). The surface chemical composition was analysed using X-ray photoelectron spectroscopy (XPS). To reveal the minute differences in the atomic structure of the catalysts, synchrotron-based high-energy X-ray diffraction (XRD) was employed at CLS. MAX IV was used to study the catalyst behaviour in operando conditions using the state-of-the-art ambient pressure XPS method. The specific surface areas of the ball mill and wet impregnation synthesised catalysts were measured and compared to determine the preparation method's effect on pore sizes. The fresh and used catalysts were characterised using Diffuse Reflectance Infra-Red Spectroscopy (DRIFTS) to determine the adsorbed surface compounds. The determination of the types and characteristics of surface species allows e.g. deactivation mechanisms to be identified.

RESULTS, FINDINGS, OUTPUT, AND IMPACT

Optimal reaction conditions for the MCH dehydrogenation experiments were determined through the design of experiments analysis on MODDE software based on experiments with a varying MCH feed rate and reactor temperature. The optimised conditions were then used in catalyst comparison experiments. A comparison of the prepared catalysts in the MCH dehydrogenation reaction showed that monometallic platinum catalysts supported on titania or spinel outperformed the other catalysts. Furthermore, it was found that the synthesis method affected the stability of the catalysts; Figure 65 illustrates that the ball mill synthetised catalyst had a stable MCH conversion, whereas the conventional wet impregnated catalyst was fully deactivated during the experiment.

The characterisation results show the differences between the catalysts prepared using ball milling and conventional wet impregnation methods. The characterisations were performed as prepared catalysts (prior to the reaction) and spent catalysts (after running the reaction) to also elucidate the mechanisms of deactivation and the effects of the reaction conditions on the structure and composition of the catalyst. The HE-XRD results showed the structural differences between the catalysts prepared using the different methods, and the operando APXPS results could show and confirm the active phase of the catalyst. It was found that pore sizes and volumes differed quite a lot when the ball mill and wet impregnated catalysts were compared. The surface compounds were similar in both cases, and only some minor differences could be detected.

Based on the methods developed in this task, a patent application was filed for the novel catalysts for LOHC dehydrogenation. Furthermore, the results will be published in leading scientific journals. During the task, two research exchange visits were made from VTT to the Max-Planck-Institut für Kohlenforschung in Mülheim, Germany, to gain expertise in mechanochemical catalyst preparation methods. Moreover, state-of-the-art research infrastructure like the instruments at MAX IV (Figure 66) were successfully employed in the research of LOHC dehydrogenation, elucidating the role of the catalyst in the hydrogen release process.

REFERENCES

Aakko-Saksa, P., Vehkamäki, M., Kemell, M., Keskiväli, L., Simell, P., Reinikainen, M., Tapper, U., and Repo, T. (2020) Chem. Commun., 56, pp. 1657–1660 and patent FI128885B.

Amrute, A., De Bellis, J., Felderhoff, M., and Schüth, F. (2021) Chem. Eur. J. 27, pp. 6819–6847.

Y. Sekine, and T. Higo (2021) Recent Trends on the Dehydrogenation Catalysis of Liquid Organic Hydrogen Carrier (LOHC): A Review, Topics in Catalysis, 64 (2021) pp. 470–480

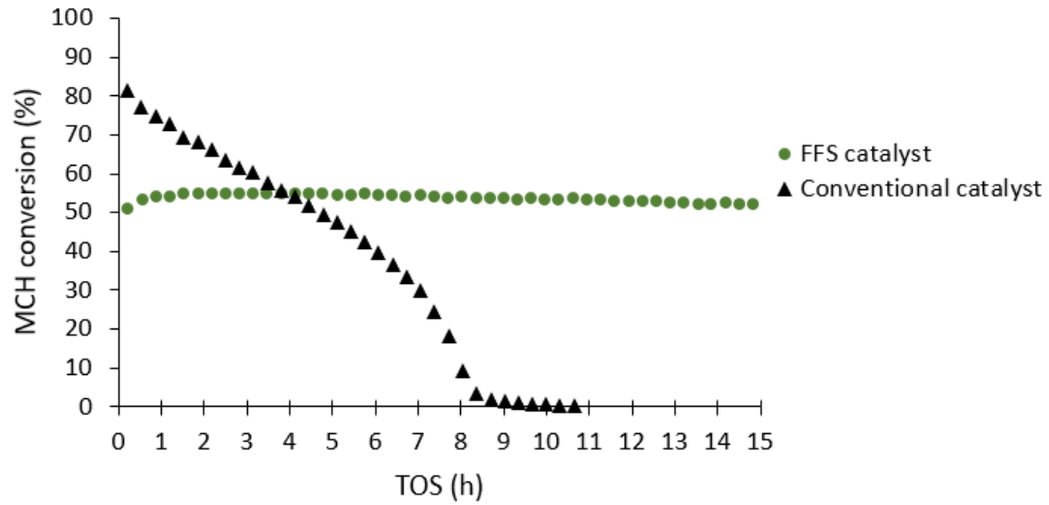

FIG 65 Comparison of the novel FFS catalyst with a conventionally prepared one in the dehydrogenation of methylcyclohexane at VTT.

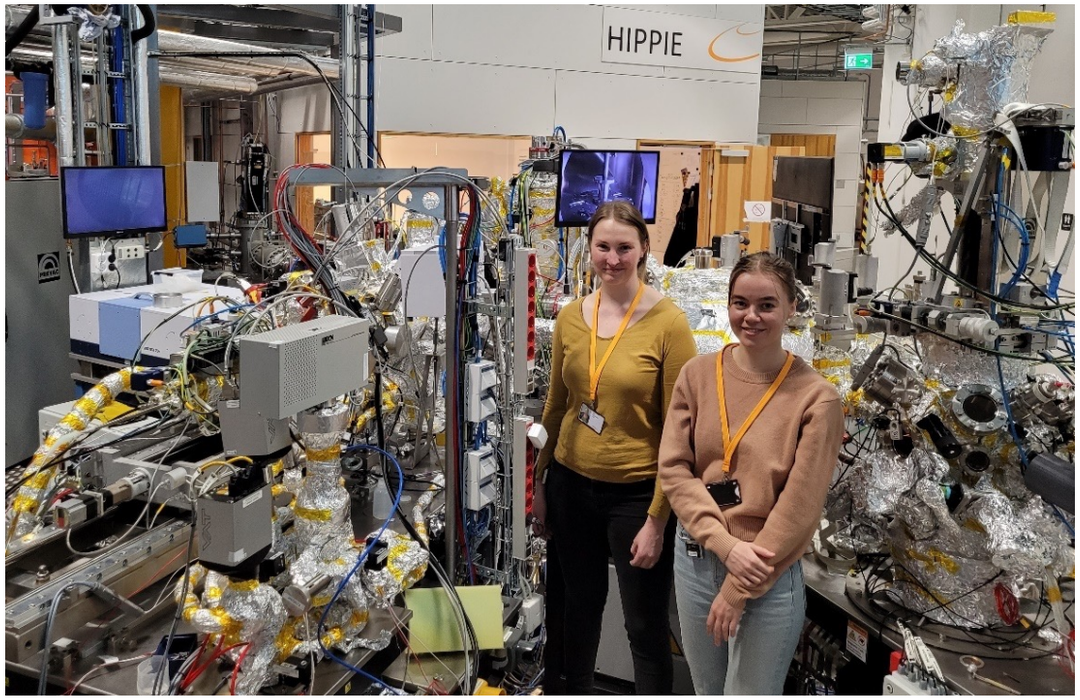

FIG 66 Sari Rautiainen and Krista Kuutti visiting MAX IV in Lund, Sweden, for the characterisation of the developed catalysts. Photo by Samuli Urpelainen.

FFS TOWARDS FOSSIL-FREE STEEL

CONTRIBUTORS

Juho Peltola, Vesa Hahto, Marko Huttunen, Juho Kauppinen, Harri Luomala, Jouko Kukkonen, Toni Pikkarainen, Robert Weiss I VTT

4.9 Hybrid burner development for industrial kilns and furnaces

Electrically assisted combustion could provide a straightforward and retrofittable solution for the decarbonisation of high-temperature heat for industrial kilns and furnaces. Electrification reduces fuel consumption and can enable the use of low-calorific fuels. The system should also be able to operate dynamically with respect to the level of electrical assistance, thereby operating as a flexible electrical load at an industrial scale.

BACKGROUND

In addition to the H_2-DRI process and electric arc furnace, fossil-free steel requires high-temperature fossil-free heating solutions for processes like rolling mills and refractory heating. Electrical assistance could be used to elevate waste gasification gas combustion to the temperatures required by the processes, or it could be used to reduce combustion fuel consumption when fuel is expensive, or its availability is limited.

The economic feasibility of the hybrid burner was evaluated with a simplified dynamic optimisation of a hypothetical 1 MW natural gas burner against historical (2013–2020) hourly price data and a hypothetical "2030" energy market scenario. The assumptions are that the burner can use electricity to offset up to 50% of fuel power and has the option of participating in the frequency containment market (FCR-N) by providing a symmetric flexible load. When operating in the FCR-N market, the burner operates at 25% electricity share to allow load balancing in both directions. The electricity price data are the hourly Finnish wholesale price, and the cost of CO_2 emissions and fuel taxes are assumed to be zero.

Figure 67 presents the realised annual operating hours for the electrical heating based on economic optimisation. Based on market conditions, the burner can either use the electric heating to minimise fuel consumption by replacing 50% of it with electric heating, or the hybrid burner can be contracted to symmetric FCR-N as a flexible load. If neither electrified operation mode is profitable, the electric heating is turned off. The results show that historically participation in the FCR-N market has been the main driver of the use of electricity, but as volatility in the electricity market increases (2020 data and "2030" scenario data), the balance shifts to the exploitation of low electricity spot prices instead of the FCR-N market.

Figure 68 shows the financial savings and emissions reductions based on the optimisation for each year. The average annual saving from the electrification of the burner is approximately €40,000/MW, and the average reduction in fuel consumption and thus direct GHG emissions is approximately 20%. These results indicate that the savings may be able to offset the increased CAPEX of the hybrid burners, while simultaneously reducing greenhouse emissions. If CO_2-allowance costs of fossil fuels are increased, or more expensive fuels are to be used, the electrified solution becomes even more attractive.

The key requirements for flexibly operating a hybrid burner are to be able to maintain the burner's heating characteristics, to quickly alter the relative shares of the energy sources, to maintain acceptable emissions performance, and a flue gas composition that is suitable for the targeted process.

To advance the adoption of hybrid burners in industrial use cases, the goals of the present work were to construct and commission a prototype hybrid burner at the VTT BioRuukki piloting centre in Espoo and conduct an experimental campaign to gain experience of the operation and performance of such a burner. The experimental data were then to be used to validate the CFD models of the protype burner and then use these CFD models to scale up the concept to industrial scales.

Because of delays in the construction and commissioning of the prototype burner, an extension of the project end date to the end of this year was applied for and granted. The work therefore continues, and the present report documents the current state of the work.

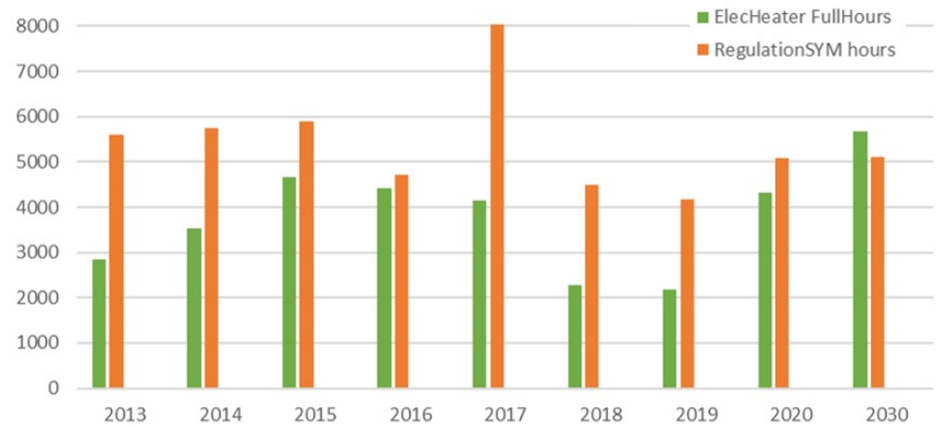

FIG 67 The number of annual operating hours of the electric heating of the hybrid burner is active, based on the simplified economic optimisation of a hypothetical hybrid burner in the Finnish Energy market. Orange bars indicate hours contracted to the FCR-N market, and during these hours, the electric heater operates at an average of half of its maximum capacity. Thus, in terms of electricity use, two hours of FCR-N contracted hours represents one hour of use of the full electric heating capacity.

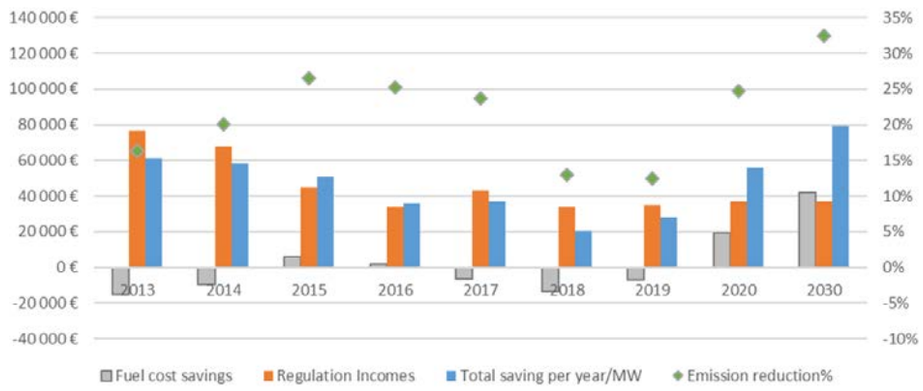

FIG 68 Results of simplified hourly economic optimisation of a hypothetical hybrid burner in the Finnish Energy market compared to a similar unelectrified burner.

SOLUTION, METHOD

The prototype burner was to be installed in the pre-existing combustion chamber at the VTT BioRuukki piloting centre. Previously, a burner was installed that was used to burn the product gases from gasification and pyrolysis pilot equipment at BioRuukki. The combustor part of the new hybrid burner was designed and provided to the project as an in-kind contribution by Andritz. It was designed as a replacement for the pre-existing product gas burner. The main differences are the addition of a 300 kW LPG burner to allow the independent operation of the burner and larger, insulated, and heat-resistant secondary gas channels for the hot and high-volume gas emanating from the electric heaters.

The layout of the installation is shown in Figure 69. VTT was responsible for the electric heating part and control parts of the hybrid burner. The required electric power supply components were provided as an in-kind contribution to the project by ABB. Commercial heating elements (Leister LE 10000 DF-HT type) were used. Six 15 kW heaters were installed in parallel for a total electric heating capacity of 90 kW, and the hot side of the heater plenum was attached to the burner's secondary gas inlet. The maximum gas outlet temperature of the heaters was 900 °C.

An important part of the operation of a hybrid burner is that because the gas is used as the heat transfer medium for the electric heat, the gas mass flow should remain high, even when the fuel feed is decreased. This leads to an increase in the flue gas oxygen level and an increase in NO_x emissions as well. Flue Gas Recirculation (FGR) is an obvious way to counteract this effect and provide an additional control method for the flue gas oxygen. In the protype hybrid burner, flue gas can be mixed with the gas flow into the heaters. In addition to the effect on heat transfer and emissions, the testing of the operation of the heating elements in the flue gas atmosphere is also a target.

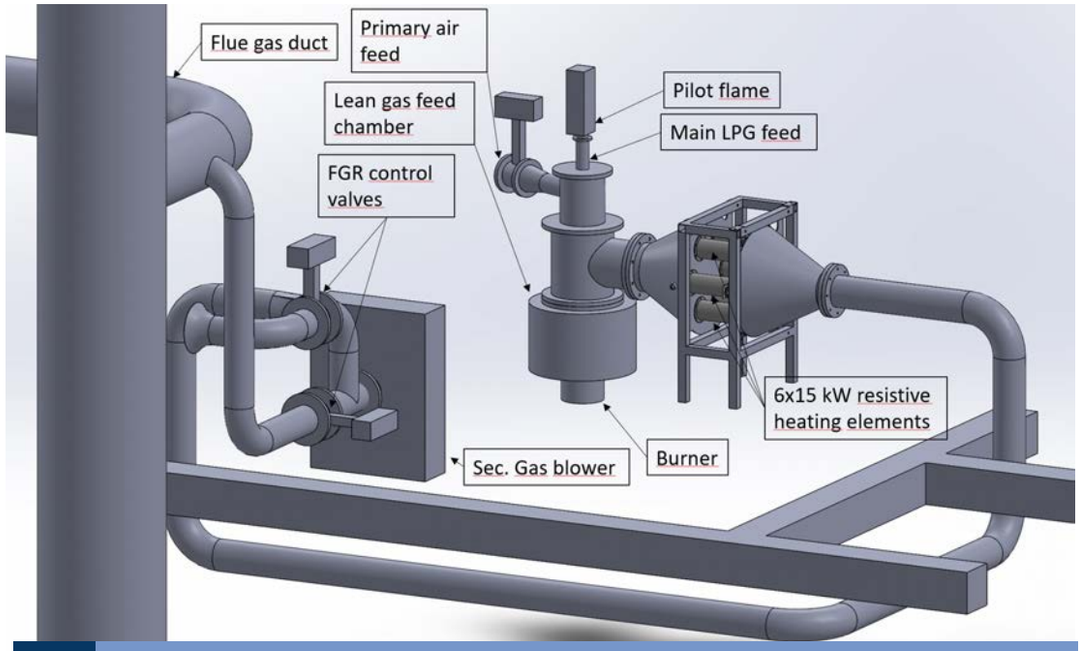

FIG 69 The layout of the prototype burner installation at BioRuukki.

Figure 70 shows the layout of the combustion chamber and planned measurement locations. The burner is installed in the ceiling of the combustion chamber. On the side wall, there are two measurements ports, which are used for the visualisation of the flame with a camera and to measure temperature, heat flux, and gas compositions with probes. At the end of the combustion chamber, there is a continuous temperature measurement, and at the outlet, there are oxygen and NO_x measurements. The installation of the prototype is ongoing, and as such, no experimental results can be reported at this stage, but the expectation is that the experimental campaign will be conducted before the end of the year.

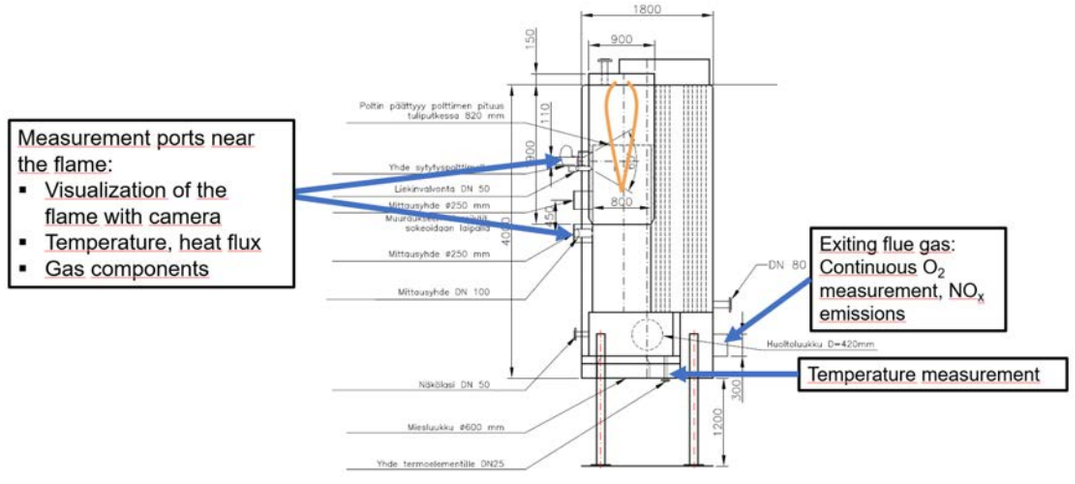

FIG 70 The combustion chamber and planned measurements.

Because of the delays in the burner commissions, it was impossible to wait for the experimental results before starting the CFD modelling. The prototype and scaled-up version of the burner were therefore simulated without a foreknowledge of how the hybrid burner behaved. Once the experimental results are available, they will be compared to the simulation results, and the reasons for possible differences will be investigated with additional simulations and experiments.

The CFD simulations were carried out with ANSYS Fluent software (version 18.1) with sub-models developed at VTT for gas firing. Model predictions included the simulation of flow, gaseous combustion, and heat transfer and emissions of CO and NO_x. Homogeneous combustion of hydrocarbons was treated with a global scheme in which CO was an intermediate species. A simplified reaction rate equation was adopted for CO oxidation. The Eddy Dissipation Concept (EDC model) was employed to account for turbulence–chemistry interaction.

RESULTS, FINDINGS, OUTPUT, AND IMPACT

CFD simulations of the prototype 300 kW burner

Simulation results are shown for six different operational points to compare the heat transfer and emissions performance. Table 11 lists the presented cases. "LPG" is the burner operating as a normal burner without the preheating of the secondary air at fuel power of 300 kW. The predicted heat transfer to the walls within the computational domain is 222 kW, CO emissions are low, and NO_x emissions are 260 mg/m³n, dry 6% O_2. When 30% of the fuel is replaced with electric

heating (“LPG hybrid”), the predicted overall heat transfer to the walls and flue gas flow does not change significantly, but the NOx emissions increase by an order of magnitude due to increased peak temperatures and high oxygen levels. Outlet O_2 is 8,0 vol-%. When operated with lean gas (200 °C, LHV 6.5 MJ/m3n) at a fuel power of 300 kW, the flue gas flow increases by 40%, and the adiabatic temperature drops by 500 °C. The predicted heat transfer to the walls decreases by 14% compared to the LPG case. The predicted NO_x emissions are low, but it should be noted that fuel NOx, which may be a factor with lean gas, was not included in these simulations.

	1. LPG	2. LPG hybrid	3. Lean gas	4.Lean gas hybrid	5. Lean gas hybrid 2	6. Lean gas hybrid 3
Fuel + El. input	300 kW + 0 kW	210 kW + 90 kW	300 kW + 0 kW	300 kW + 90 kW	300 kW + 110 kW	210 kW + 90 kW
T 2’ry, C	25	900	25	900	1100	900
Heat to walls	222 kW	219 kW	192 kW	268 kW	290 kW	224 kW
FEGT	552 °C	586 °C	610 °C	~ 680 °C	~ 690 °C	~ 580 °C
CO	< 1 w-ppm	< 1 w-ppm	< 1 w-ppm	< 1 w-ppm	< 1 w-ppm	< 1 w-ppm
NO_x	90 mg/MJ	645 mg/MJ	25 mg/MJ	78 mg/MJ	150 mg/MJ	71 mg/MJ
	146 w-ppm (actual)	1020 w-ppm (actual)	29 w-ppm (actual)	92 w-ppm (actual)	177 w-ppm (actual)	109 w-ppm (actual)
	260 mg/m3n, dry 6 % O2	2690 mg/m3n, dry 6 % O2	60 mg/m3n, dry 6 % O2	185 mg/m3n, dry 6 % O2	350 mg/m3n, dry 6 % O2	240 mg/m3n, dry 6 % O2
O_2, exit	2.0 vol-%	8.0 vol-%	4.1 vol-%	3.0 vol-%	3.0 vol-%	4.7 vol-%
Flue gas (m3n/h)	342	352	480	468	468	360
Tad	1,950 °C	1,950 °C	1,450 °C	1,850–1,900 °C	1,900–1950 °C	1,850 °C

TABLE 11 The operational parameters of the presented simulation cases and their predicted heat transfer rates and emissions at the outlet of the combustion chamber.

When the electric preheating is used to elevate the adiabatic temperature of the lean gas combustion (“Lean gas hybrid”) for a total heat input of 390 kW, the wall heat transfer increases to 268 kW, 21% above the initial LPG cases for the additional 33% energy input. NO_x emissions remain lower than in the LPG case. In hybrid mode, the electrical heating also replaces the LPG pilot flame used in non-hybrid lean gas combustion, further reducing CO_2 emissions. In the prototype, the heating elements are capable of a gas temperature of 900 °C, but heaters up to 1,100 °C are also readily available. If they were used (Lean gas hybrid 2), the adiabatic temperature of the LPG operation could be recovered. Combined with the high flue gas flow of the lean gas cases, this results in a 31% increase in the heat transferred to the walls for a 40% increase in total energy input. Finally, the 300 kW total energy input lean gas hybrid case (Lean gas hybrid 3) is a close match with the original LPG case: total wall heat transfer is up by 1%, and emissions performance is also very similar, indicating that a lean gas burner with electrical preheating could provide a drop in replacement for existing LPG/NG burners.

A more detailed view of the combustion behaviour is provided in the temperature contour plots of Figure 71 and axial wall heat transfer and the incident radiation plots in Figure 72. In the cases that predicted similar total heat transfer rates – 1, 2, and 6 – the length of the flame is similar. The non-hybrid lean gas case differs radically from the other cases in flame shape, and the LPG pilot flame is clearly visible in the middle of the burner. The higher total energy input and flue gas flow cases 4 and 5 have longer flames that reach beyond the 1,900 mm refractory lined part of the combustion chamber. The refractory is also clearly visible in the axial wall heat transfer profiles in Figure 72. A variable for the heat transfer characteristics of each case that is perhaps easier to interpret is the incident thermal radiation plot. Here we can see that the LPG and LPG hybrid cases are as close as they were for the total wall heat transfer, but close to the burner, the 300 kW lean gas hybrid (6) does not quite match the thermal radiation output of the LPG cases, an effect masked by the total heat transfer numbers by the refractory lining in this configuration.

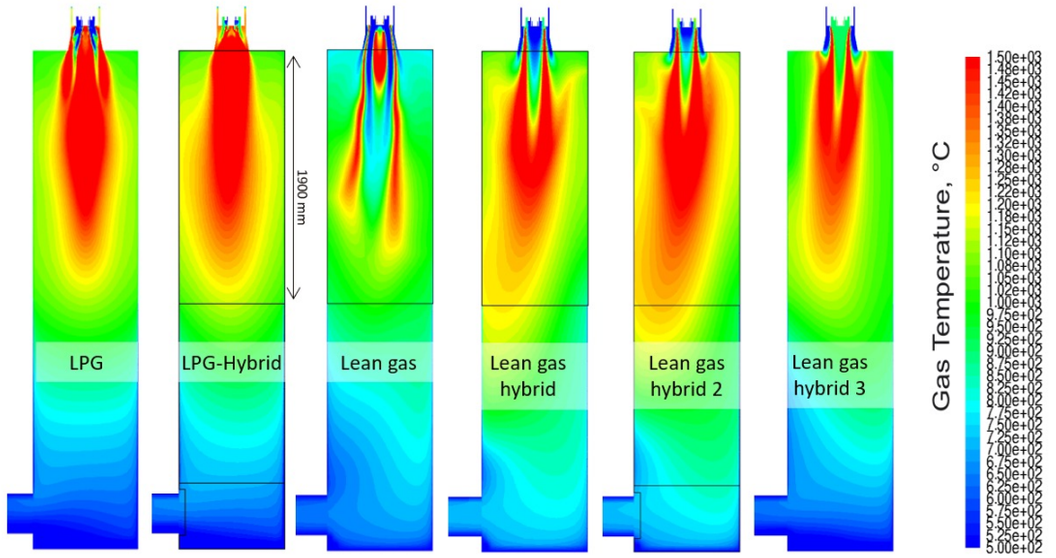

FIG 71 Contour plots of the gas temperature in the CFD simulations of different operational points of the prototype hybrid burner.

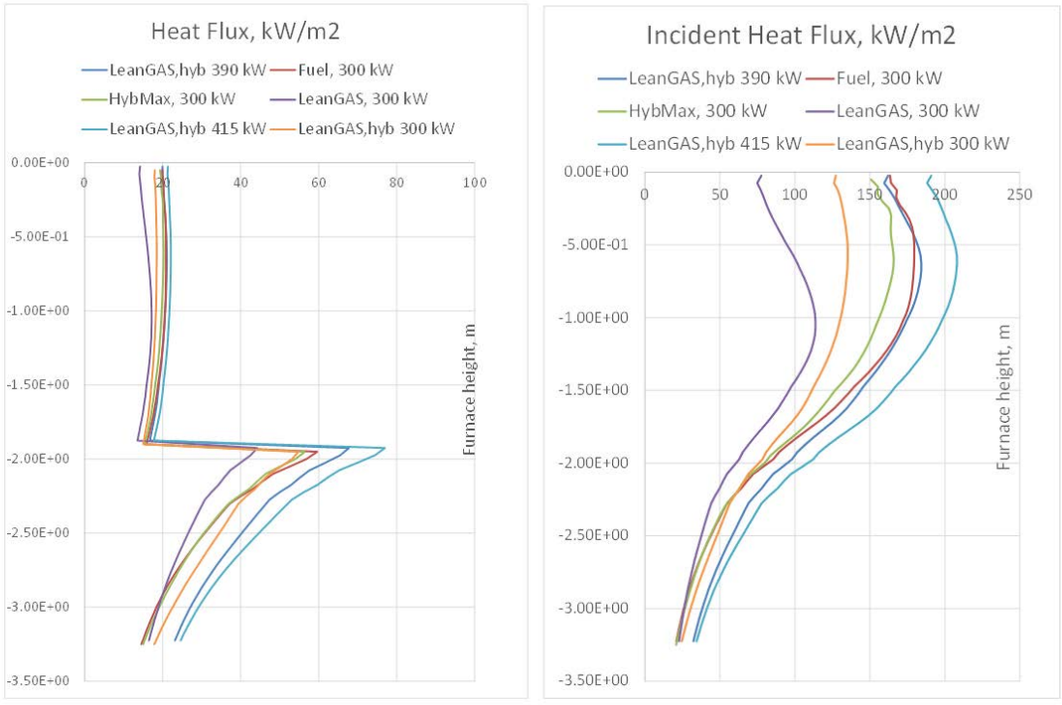

FIG 72 Axial distribution of simulated wall heat transfer and wall incident radiation in the various operational modes of the prototype hybrid burner.

CFD simulations of a hybrid burner scaled up to 4.8 MW

As the next step, the hybrid burner was scaled up from 300 kW to 4.8 MW. Two of these burners were placed on opposite walls of a computational domain (Figure 73) that roughly resembled a drastically simplified rolling mill furnace in a steel mill. The floor had a fixed 400 °C temperature, and the rest of the walls were adiabatic. The distance between the opposite burner walls is 12 m, and the height of the furnace is 3 m.

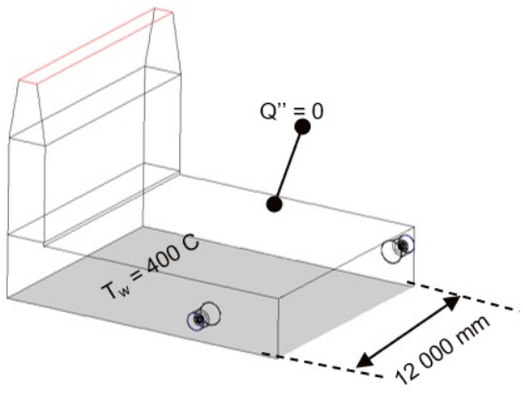

FIG 73 Computational domain for the scaled-up CFD simulation, with two 4.8 MW hybrid burners.

The results are presented for four different operational points, each with a 9.6 MW energy input. The operational points are listed in Table 4 . The first case is the pure LPG combustion case. The predicted heat transfer to the bottom wall is 6.6 MW, and the NO_x emissions are 408 mg/m3n, dry 6% O_2. When 30% of the LPG-provided energy is replaced with electric heating, the heat transfer to the wall is increased by 3%, but the NO_x emissions increase again by an order of magnitude, and flue gas oxygen is 8.0 vol-%. The oxygen level can be controlled by introducing FGR, which drops it to 2.9 vol-%, and the NO_x emissions also decrease to the same level as they were in the pure LPG case. If the LPG is replaced with lean gas and electric pre-heating, the predicted wall heat transfer increases by 4.5%, and the predicted NO_x emissions increase by 45%.

	Fuel (LPG)	Fuel Hybrid	Fuel Hybrid +FGR	Lean Gas Hybrid
Fuel + El. input	9.6 MW + 0 MW	6.7 MW + 2.9 MW	6.7 MW + 2.9 MW	6.7 MW + 2.9 MW
T2'ry, C +(FGR)	25	900	900	900
O_2, exit	2.0 vol-%	8.0 vol-%	2.9 vol-%	4.7 vol-%
Flue gas flow (m3n/h)	10,950	11,275	10,810	11,540
Tad	1,950	1,950	1,950	1,850
FGR, %	NA	NA	29 %	NA
Heat to bottom wall	6.6 MW	6.8 MW	6.8 MW	6.9 MW
CO	<1 w-ppm	<1 w-ppm	<1 w-ppm	<1 w-ppm
NO_x	140 mg/MJ	995 mg/MJ	145 mg/MJ	175 mg/MJ
	228 w-ppm (actual)	1,568 w-ppm (actual)	237 w-ppm (actual)	270 w-ppm (actual)
	408 mg/m3n, dry 6 % O_2	4,140 mg/m3n, dry 6 % O_2	425 mg/m3n, dry 6 % O_2	595 mg/m3n, dry 6 % O_2

TABLE 12 The operational parameters of the presented simulation cases and their predicted heat transfer rates and emissions at the outlet of the combustion chamber.

Figure 74 shows the contour plots of the gas temperature and incident thermal radiation for the same four 9.6 MW cases, and it is possible to see more differences in the distribution of the thermal radiation than was visible in the total heat transfer rates, which were similar for all cases. Overall, the incident radiation distributions are still qualitatively similar, and drawing conclusions about how significant the differences are would require simulations of more realistic furnace configurations. At the same time, the design of the hybrid burner could be modified to address the issues identified in those simulations.

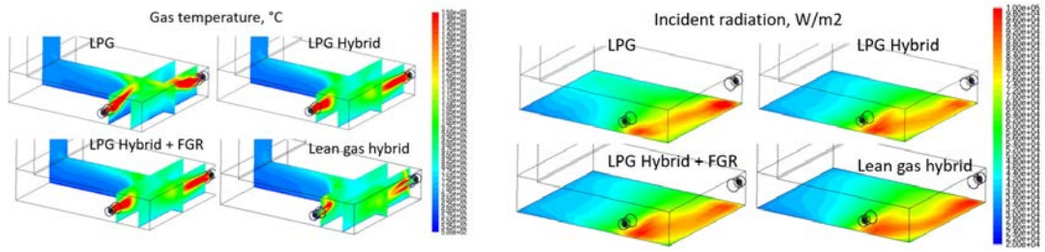

FIG 74 Gas temperature and incident thermal radiation contour plots in different operational points in the up-scaled CFD simulation with two 4.8 MW hybrid burners.

Thus far, the simulations indicate that a hybrid burner could work either as a flexible means of utilising electricity to offset fossil fuel use when the cost of electricity is low to minimise the use of expensive or limited-availability non-fossil fuels or to boost low-calorific fuels so that they can act as a replacement for fossil fuels in high temperature processes.

It should be noted that the experimental campaign still to be carried out in the project will provide validation data for the CFD simulations presented here, which may alter the conclusions directly or lead to changes in the CFD modelling approach that may affect the current conclusions.

In further upscaling studies, the focus should be on more realistic furnace configurations, which would allow more meaningful investigation of the differences between the various operational modes and design choices in the burner itself. These design choices are not limited to their influence on the combustion behaviour of the burner but also to layout restrictions of real industrial furnaces, which have a significant impact when the retrofit ability of the concept for the existing processes is evaluated.

FFS TOWARDS FOSSIL-FREE STEEL

CONTRIBUTORS

Samuli Urpelainen
Nano and Molecular Systems Research Unit, University of Oulu
Mika Huuhtanen
Environmental and Chemical Engineering Research Unit, University of Oulu

4.10 Photocatalyti utilisation of organic streams in hydrogen production

BACKGROUND

Photocatalytic hydrogen evolution reactions offer a pathway towards sustainable hydrogen production without the use of electricity. The same catalysts that have been shown to photo-catalytically split water have also shown potential for breaking down organic molecules and have also been proven to be applicable in e.g. water purification. However, the catalysts are most often active in the UV range of the electromagnetic spectrum, and to efficiently take advantage of these catalysts, it is important that they can be operated under sunlight, e.g. in the visible part of the spectrum as well. Furthermore, organic hydrogen carriers and the organic waste and sidestreams originating in hydrogen carriers can also pose new threats to the environment. It is therefore important to develop novel solutions for water purification and ideally combine organic degradation with the utilisation of the hydrogen bound to the molecules.

In this task, catalyst materials were developed and tested for organic waste degradation and hydrogen production. The proposed catalyst materials were extensively characterised using a state-of-the-art methodology, both at laboratory scale and at large-scale synchrotron radiation facilities such as the MAX IV Laboratory in Lund, Sweden. Furthermore, a sustainability analysis was conducted to estimate the overall viability of the potential catalyst materials from the perspective of the entire value chain. At the beginning of the project, a thorough literature analysis of various types of photocatalyst materials was performed.

MATERIALS AND METHODS

In this task two types of catalysts were considered: rhodium (Rh) supported on titania (TiO_2) nanoparticles; and purely nickel (Ni) -based catalyst materials. The materials were chosen based on the excellent photocatalytic activity of TiO_2 in the UV range, with Rh dosing increasing the visible light absorption and thus shifting the activity towards the visible range. The Ni-based nanoparticle catalyst on the other hand offers a possible cost-effective and critical raw-material-independent catalyst material that could be deployed cheaply at a large scale. The Rh/TiO_2 catalysts were prepared using the wet impregnation method, while the Ni catalysts were procured from a commercial supplier and subjected only to vacuum annealing, significantly boosting their hydrogen production efficiency.

The Rh/TiO_2 catalysts were tested both for water purification (using diuron, a herbicide and emerging pollutant) and hydrogen evolution reactions, as well as the Ni catalysts for the hydrogen evolution reaction. The tests were performed using a white light vertical reactor, as well as a desktop visible light photoreactor with single narrow band wavelength light sources, as well as a white light. The catalysts were studied using standard laboratory techniques for micro and nanostructure determination (transmission electron microscopy, TEM, with energy dispersive X-ray spectroscopy, EDS), atomic/molecular structure determination (X-ray diffraction, XRD), and for surface chemical composition, using x-ray photoelectron spectroscopy (XPS).Furthermore, the Ni-based catalysts were extensively studied using state-of-the-art in situ/operando ambient pressure XPS (APXPS) at the MAX IV Laboratory to reveal

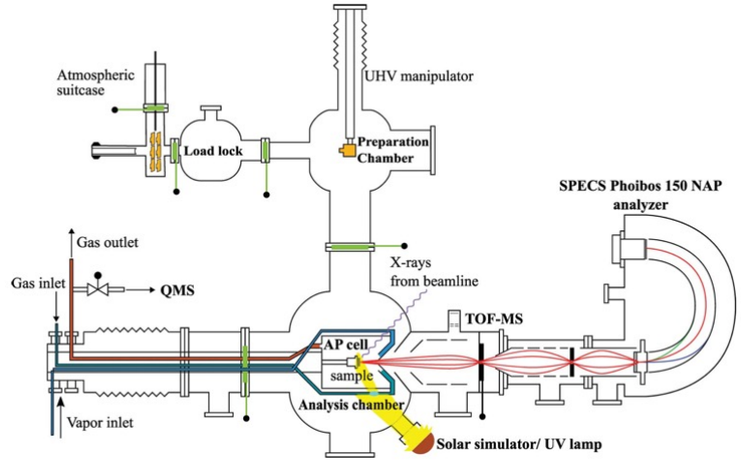

FIG 75 The photocatalytic APXPS setup at MAX IV. From A. Klyushin et al. J. Synchrotron Rad. (2023) 30, 613–619. CC BY 4.0.

the electronic and molecular level phenomena and reaction steps during the reaction itself to better understand the catalyst activity and tune its properties for higher efficiency. For this, an in-situ experimental system was developed in collaboration with the MAX IV Laboratory to study photocatalytic reactions using APXPS (Figure 75).

Sustainability assessment using LCA (life cycle analysis) and MCA (multicriteria analysis) -based approaches is ongoing. The materials and chemicals used, preparation conditions, and parameters were considered as indicators. The sustainability of the manufactured materials and preparation processes will be compared to evaluate the environmental, economic, and social aspects.

RESULTS AND DISCUSSION

The Rh/TiO_2 photocatalysts were shown to have significantly higher light absorption in the visible range of the spectrum. Furthermore, the catalysts showed improved efficiency for the photocatalytic degradation of diuron using visible light compared to pure TiO_2. The amount of Rh on the TiO_2 nanoparticle substrate was shown to affect the catalyst's overall efficiency. The characterisation results were critical in explaining the differences between catalysts with different amounts of Rh. The catalysts were also shown to be active in the hydrogen evolution reaction.

A photocatalytic sample environment for the APXPS system at the MAX IV Laboratory was designed and commissioned. The Ni-based catalysts were studied using the system, showing its capabilities. The APXPS results show that the method can be used to study the transient phenomena and intermediate steps in photocatalytic reactions in operando conditions, establishing a new method for the MAX IV user community. The results could also be used to elucidate the role of nickel carbonate in the photocatalytic reaction using the Ni-based

catalyst, as well as to give hints about the mechanisms of deactivation. The developed methods and new understanding of the photocatalytic reactions will be further used to develop a more efficient photocatalyst for hydrogen evolution wand waste degradation reactions. The results of the sustainability analysis will be reported by the end of the year.

PUBLICATIONS AND THESES

Quimbayo, J. M., Ojala, S., Urpelainen, S., Huuhtanen, M., Cao, W., Huttula, M., andKeiski, R. L. (2022) Nanostructured Photocatalytic Materials for Water Purification, In M. P. Shah, S. P. Bera, B. Y. Tore (eds). Advanced Oxidation Processes for Wastewater Treatment, Boca Raton: CRC Press.

Klyushin, A., Ghosalya, M., Kokkonen, E., Eads, C., Jones, R., Nalajal, N., Gopinath, C. S., and Urpelainen, S. (2023) Photocatalytic setup for in situ and operando ambient-pressure X-ray photoelectron spectroscopy at MAX IV Laboratory. Journal of Synchrotron Radiation, 30(3) pp. 613–619

Quimbayo, J. M., Sasikala Devi J., Ghosalya A. A., Huttula M. K., Alatalo, M., Urpelainen, S., and Ojala, S. Photocatalytic degradation of Diuron, submitted

Ghosalya M. K., Talebi P., Singh H., Klyushin A., Kokkonen E., Mansouri M. A., Huttula M., Cao W., Urpelainen S., (2024) Solar Light Driven Atomic and Electronic Transformations in Ni@$NiCO_3$/NiO Hybrid Photocatalyst Revealed by Ambient Pressure X-ray Photoelectron Spectroscopy, submitted

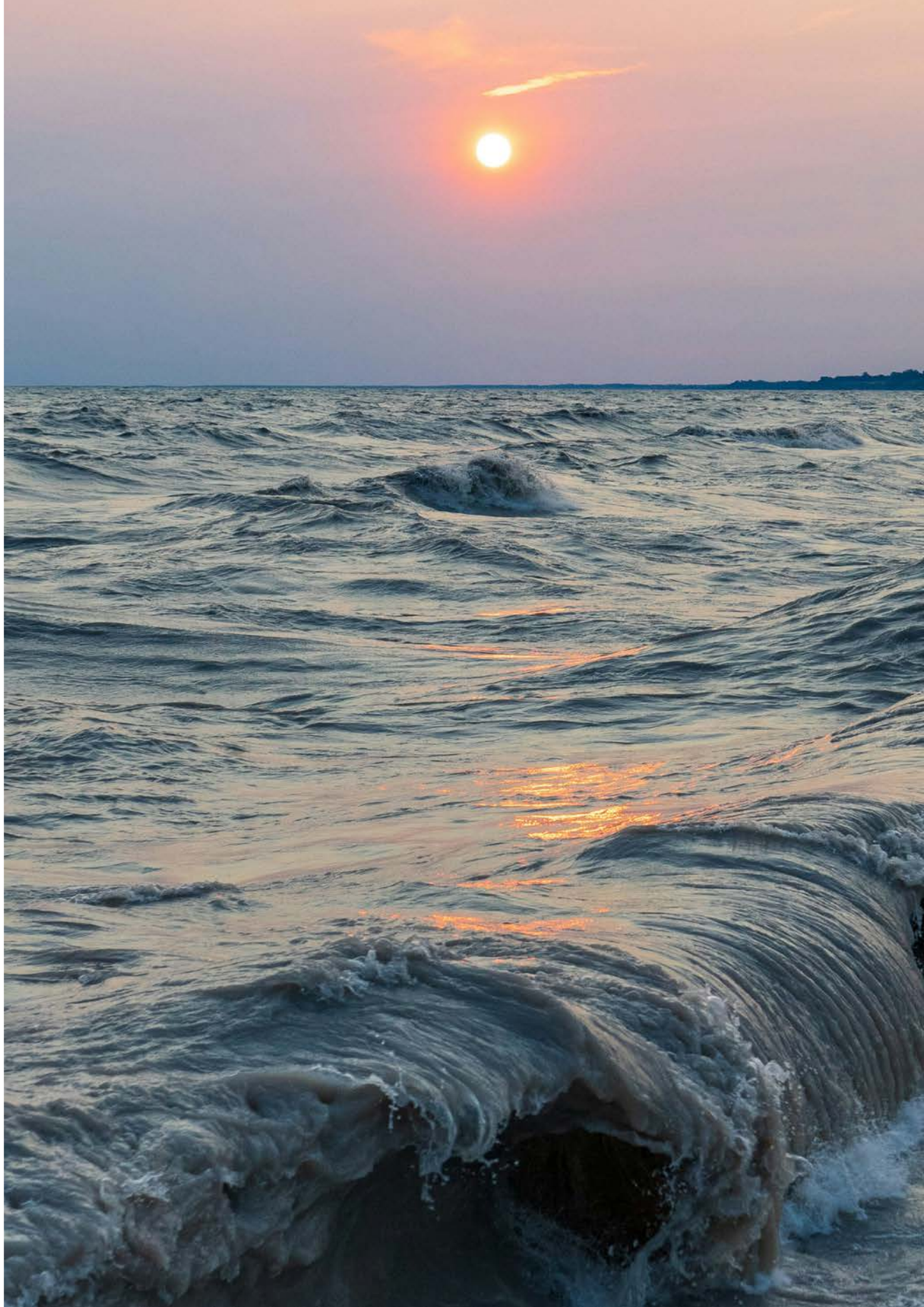

FFS TOWARDS FOSSIL-FREE STEEL

CONTRIBUTORS

Timo Paananen, Anne Seppänen, Kimmo Kinnunen Jarmo Lilja I SSAB
Mikko Raiko, Joakim Autioy, Vesa Helanti I Valmet

4.11 Biomass gasification for fossil-free reheating of steel slabs

BACKGROUND

The main content of Valmet's project is to develop its biomass and waste gasification technology so that it can be utilised in the steelmaking process to generate energy for process needs. SSAB has set as its strategic goal the development of a completely fossil-carbon-dioxide-free steelmaking process, and the utilisation of biomass and waste gasification is considered one of the most promising alternatives for replacing coke oven gas and liquefied natural gas in steel slab reheating. Fossil fuels for slab reheating creates approximately 0.25 million tonnes of fossil CO_2-emissions, which equates to roughly 6% of SSAB Raahe's total greenhouse gas emissions.

SOLUTION, METHOD

Multiple ideas were developed to tackle the heating requirements of slab reheating furnaces. The air gasification route investigated mature Valmet technology, and the advanced gasification route investigated a novel approach to gasification and its integration into an existing coke oven gas cleaning and storage system. In addition, by-product biochar from Valmet pyrolysis technology was considered as an option for an electric arc furnace biocarbon. This will be studied in FFS2. The next phase of the FFS project, the Advanced gasification route, was deemed too novel to be developed and implemented in the accelerated investment timeline. Air gasification faced multiple challenges to be a viable solution for slab reheating furnaces, ranging from capacity and flexibility requirements to gas quality.

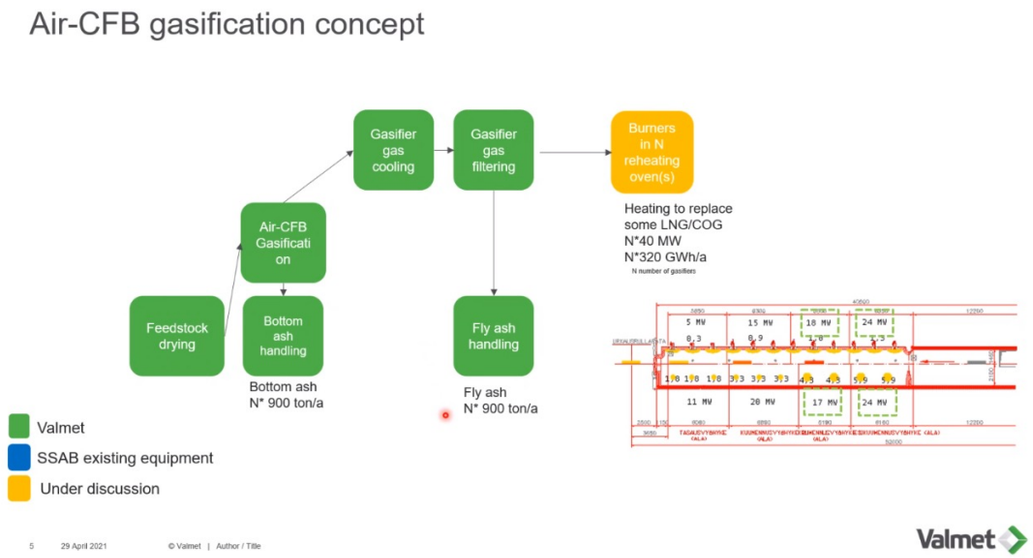

FIG 76 An example of studied scenarios for reheating of slabs at SSAB Raahe.

RESULTS, FINDINGS, OUTPUT, AND IMPACT

Th air gasification investigation presented many challenges and open questions concerning how to integrate gasification technology to work with reheating furnaces. The main challenges consisted of the low heating value of gasification gas, particle emissions' impact on slab surfaces, and the fundamental attributes of gasification technology, such as load flexibility and minimum capacity. The gasification investigation was performed as a desktop study, involving calculations and modelling. Most of the challenges remain as barriers for a swift implementation of air gasifier technology.

Advanced gasification and the utilisation of existing coke oven gas cleaning equipment was a conceptual exercise to understand how novel technology could be used to provide a "drop-in" gas to replace coke-oven gas and LNG. However, the technical readiness level and the change in SSAB's investment timeline made the gasifier concept undesirable.

Pyrolysis char utilisation in an EAF was tested at OU and was proven to have some potential. Feedback on the quality limitations and potential of pyrolysis char paved the way for new technology development. The further thermal processing of pyrolysis char may improve its suitability in EAF applications. Pyrolysis char utilisation is being continued in the FFS2 project.

FFS TOWARDS FOSSIL-FREE STEEL

CONTRIBUTORS

Juho Haapakangas, Susanna Airaksinen, Sonja Riikonen, Aleksi Laukka
University of Oulu
Anne Seppänen, Leena Määttä I SSAB Europe

4.12 Experimental study of scale formation with alternative reheating practices

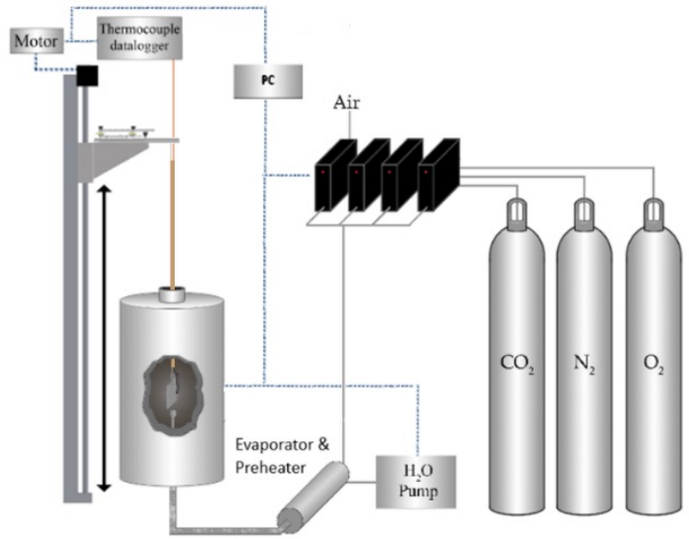

FIG 77 Overview of the TGA furnace used in oxidation tests.

BACKGROUND

Mitigation of CO_2 emissions is one of the major focal points of research in iron ore-based steelmaking. Currently slab reheating before hot rolling is the second largest source of CO_2 in steelmaking, succeeded only by the blast furnace process. In this task, two technological improvements to the current reheating practice, use of hydrogen as fuel gas and replacement of air with oxygen (oxyfuel), during slab reheating were studied regarding their role in the oxide scale formation on the surface of steels. The primary objectives were to study the oxidation kinetics and estimate scaling losses in both current and future reheating conditions, and secondly to estimate potential changes in the adhesion of the formed oxide scales to the steel substrate.

MATERIALS AND METHODS

Oxidation tests were performed using a tubular thermal gravimetric analyzer (TGA) depicted in Figure 77. Four of the most relevant steel grades were selected and provided by SSAB to be used in the oxidation tests. The test atmospheres consisted of N_2, CO_2, H_2O and O_2 in ratios simulating the industrial furnace. Four simulated combustion gas atmospheres were selected for the testing: 1) Methane – air; 2) Coke oven gas – air; 3) Hydrogen – air; 4) and 50:50 H_2-CH_4 mixture – oxygen. Oxidation tests were performed both isothermally at 1150, 1230 and 1300 °C, as well as in dynamic conditions by raising the temperature from 500 to 1180 °C. Oxidation kinetics were determined by continually measuring changes in sample mass during the tests. The structure and morphology of the formed oxides was studied with FESEM-EDS analyses.

RESULTS AND DISCUSSION

Oxidation of steel was notably increased in the future reheating conditions of "H_2 – air" and "H_2-CH_4 – oxygen" for all four steel grades. Differences in oxidation kinetics began to show above the temperature of 910 °C. The increase in oxidation rate correlated well with the increased content of water vapor in the gas atmospheres. There were also large differences between steel grades regarding the amount of oxidation increase. Water vapor clearly changes the oxidation mechanism of steel, which is evident from the significant changes in the pore structure development of the iron oxides in different gas atmospheres. The future reheating processes will notably affect the scaling losses for low carbon steels compared to the current industrial practices. No clear effect was seen from the oxidation gas atmosphere on the adhesion of oxide scales to the steel substrate, hence the future reheating conditions are not expected to cause de-scaling problems. The adhesion of the steel-scale interface was determined mainly by the content of silicon in steel and the heating temperature.

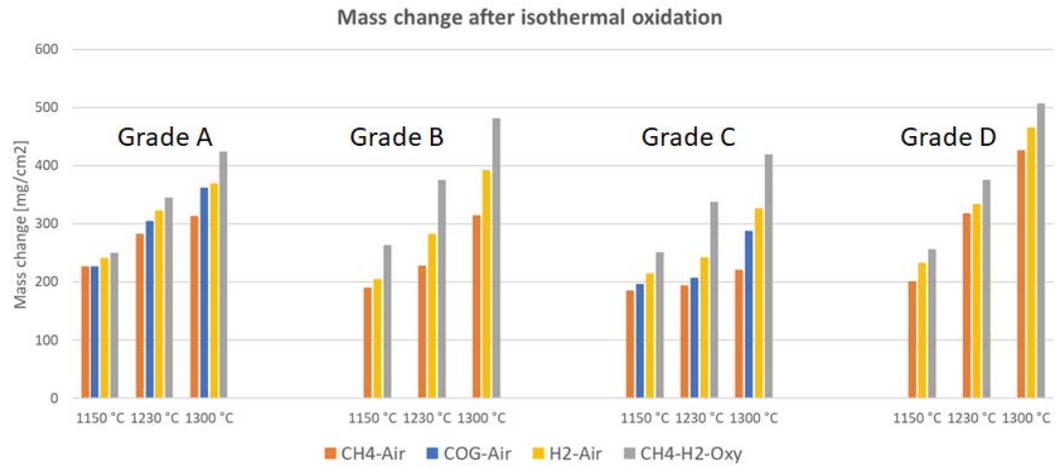

FIG 78 Total oxidation in isothermal tests.

PUBLICATIONS & THESES

Haapakangas J., Riikonen S., Airaksinen S., Heikkinen E.-P., Fabritius T. (2024) Oxide Scale Formation on Low-Carbon Steels in Future Reheating Conditions, Metals, 14(2), 189

Riikonen S. (2022) Towards fossil fuel-free carbon steel reheating furnaces: effects on oxide scale formation. Master's Thesis

FFS TOWARDS FOSSIL-FREE STEEL

CONTRIBUTORS

Markus Engblom, Anders Brink, Henrik Saxén I Åbo Akademi
Leena Määttä, Anne Seppänen, Kimmo Kinnunen I SSAB

4.13 Simulation of slab reheating

In the steelmaking process, reheating furnaces are important units that guarantee an appropriate and uniform temperature of the steel slabs before the hot rolling step. Today, the furnaces are operated using fuels of fossil origin – typically coke oven gas (COG) or natural gas (NG) – which must be replaced by non-fossil counterparts to decarbonise the steelmaking operation. Preliminary models were developed to describe the conditions in a pusher-type slab reheating furnace to characterise the present and potential future operation states, using simplified first-principles models and CFD modelling of the reheating furnace sections.

BACKGROUND

In steelmaking's green transition, fossil carbon (coal and coke) must be abandoned as a reducing agent and energy source, but this will have strong indirect implications for steel plants because of the simultaneous elimination of by-product gases (blast furnace gas, coke oven gas, etc.) that are efficiently integrated into the plants of today. Obviously, these gases should not be replaced by other fossil-based fuels. To assess the potential of using other energy sources in reheating furnaces, mathematical modelling can be applied to explore the feasibility of alternative solutions, including biogas combined with hydrogen or oxygen enrichment, or strong (electrical) preheating. This can reveal both overall limitations (e.g. insufficient energy supply, excessive gas flowrates) and violation of specific constraints (e.g. NO_x emissions that are too high) for proposed alternatives, providing guidelines on which options to explore in further detail.

METHODS APPLIED

The modelling was tackled with a twofold approach. First, the overall conditions of the various alternatives for the preheating were explored using the present conditions of the pusher-type reheating furnace LT-11 in Raahe, fired by COG, as a reference case. From the present operation practice, the heat input, off-gas temperature and residual oxygen ratio, and adiabatic flame temperature were set as requirements for the new alternatives, and the feasibility of different fuel mixes or preheating concepts was assessed, using overall material and energy balance calculations in combination with a simplified model of the conditions in the flame region. This efficient approach made it possible to study a broad range of alternatives, with the goal of finding feasible operational practices that should be explored in more detail.

More sophisticated studies of the conditions in the vicinity of the burners were undertaken by CFD modelling using ANSYS Fluent. The present operation practice based on COG in combination with preheating of the combustion air (to 350 °C) was first simulated for the wall burners. The burner geometry was modelled in detail, applying different formulations of the computational domain in front of the burner(s). The kinetic models of the combustion reactions were kept relatively simple to limit the computational effort. To study the potential future states of operation, the burner in the model had to be redesigned to prevent the gas flowrates becoming excessive, e.g. when exploring alternatives with strong gas preheating.

MAIN FINDINGS AND IMPACT OF THE WORK

The overall analysis revealed future alternatives that could be ruled out, as they could not satisfy the constraints set for the operation of the reheating furnace. For example, biogas is not a feasible alternative as such due to its insufficient heating value, which yields flame temperatures that are too low and high gas flowrates. Certain mixtures of biogas and hydrogen resulted in operation states within the feasibility limits, but the share of energy introduced by the biogas was modest, so this alternative may not be interesting. Furthermore, the alternative with higher shares of biogas in combination with oxygen-enriched air leads to problematic operation states due to excessive oxygen content in the air. Synthetic methane combined with hydrogen is naturally a feasible alternative because of its strong similarities with COG, but the gases must be of non-fossil origin to make the replacement meaningful.

Alternatives involving the strong preheating of the combustion air (and possibly also the fuel gas) were found interesting. Heating the air and biogas to 900-1,000 °C yielded a sufficient flame temperature and energy input, but the gas volumes increased excessively. Biogas combined with strong air preheating and oxygen enrichment can provide an energy input, flame temperature, and gas volume in parity with present operation states. The required share of power in the energy input may be up to 35%, so the electricity should be green to make the concept attractive. These alternatives require a fundamental redesign of the burners, which was beyond the scope of the present task. However, the activities at VTT on the development of hybrid burners may provide interesting solutions.

The results of the CFD-based studies undertaken confirmed the findings of the overall model, demonstrating the insufficient temperature of the flame region if biogas was used as the sole energy source (in addition to modest air preheating). Alternatives with strong preheating of the gases could yield sufficient temperatures in the flame region, but high gas flowrates would result in an excessive pressure drop in the burner and the dramatically changed conditions of the flame. After a (simple) redesign of the burner in the CFD model, where the gas channel cross-sections were increased, the strong preheating concept was found to give rise to similar thermal conditions in the simulated domain as in the reference case (Figure 79), indicating the solution's preliminary feasibility.

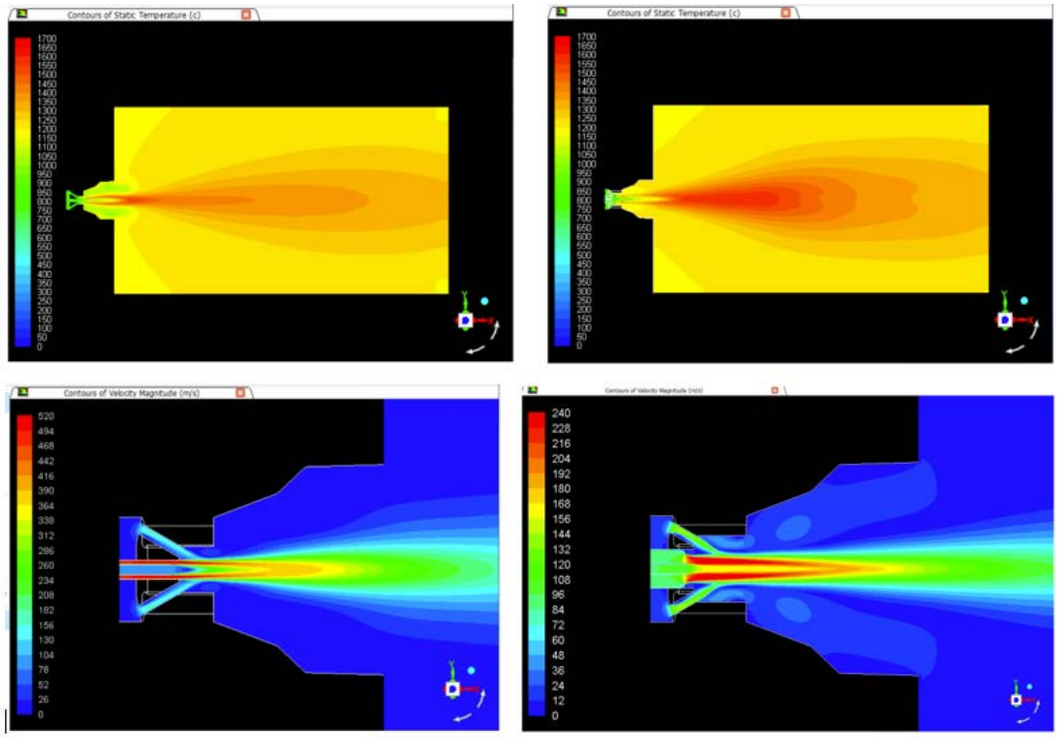

FIG 79 Simulated temperature fields (top row) and velocity fields (bottom row) for COG combustion with the original burner (left) and the redesigned burner for air and biogas preheated to 800 °C (right).

A more realistic simulation domain that included a section of the reheating furnace with two adjacent burners and the steel slabs below them provided estimates of the energy supply from the combustion gases to the slabs, including radiative and convective heat transfer. These results are still preliminary, and further work is required to assess the feasibility of different fuel mixes. The impact of the changed conditions on other important factors, such as NO_x emissions, must also be explored. The studies undertaken in the task also revealed the need for a thermal model of intermediate complexity (e.g. a zonal model) for a swift assessment of the feasibility of future states of operation, as well as for designing energy-efficient operation strategies.

REFERENCE

Saxén H., Brink A., and Engblom M. (2023) Modelling of steel reheating furnace. Intermediate report, Åbo Akademi University, May 2023

FFS TOWARDS FOSSIL-FREE STEEL

CONTRIBUTORS

Carl Haikarainen, Lei Shao, Henrik Saxén I Åbo Akademi
Jarmo Lilja, Kimmo Kinnunen I SSAB

4.14 Process integration for an optimal transition to sustainable steelmaking

A modern steel plant is a highly integrated industrial complex where the material flows are optimised, and by-products and energy are used efficiently. In the transition to sustainable steelmaking, the phasing out of key process units such as the blast furnace (BF) and coke plant will substantially affect the plant-internal flows and will have severe implications for energy integration and the process economy due to the lack of by-product gases in the new plant setup. In the worst case scenario, missing energy will have to be replaced by external energy from fossil resources. This makes it of utmost importance to design the transition properly by guaranteeing efficient energy and material use and integration in steel plants evolving towards sustainable operation. A further challenge is to make appropriate and timely decisions concerning investments to safeguard a smooth decarbonisation path.

BACKGROUND

The transition to sustainable steelmaking will occur in steps, and steelmaking companies have selected various paths to gradually decarbonise the steelmaking chain. The transition is complex because the replacement of traditional process units will lead to substantial changes in other parts of the plant due to an efficient integration of material and energy flows. The lack of such integration may endanger the efficiency of the forthcoming transition, leading to fewer environmental benefits and considerably higher costs than expected. To study the stepwise green transition in steelmaking, a model-based optimisation approach to the changes in the plant setup was made to guarantee an environmentally friendly and economically feasible path to hydrogen-based steelmaking.

APPROACH

Simplified models of the main units in an integrated steel plant acted as the starting point of the work, and these were written down in the Python Pyomo framework to allow efficient equation-based optimisation. Unit models described by more sophisticated expressions were simplified by creating corresponding surrogate models in linear or quadratic form. Based on the results and relationships reported in the literature, models of the new unit processes (EAF, electrolysers, etc.) were developed and included in the system. The DR shaft model developed in the work (cf. section 3.7) was applied to generate several thousand points in the feasible operation range, and these were used to develop a surrogate DR shaft model.

To find an optimal transition, an economic objective function was stated that took OPEX and CAPEX into account. As the transition period is expected to be long, a horizon of 25 years was set, allowing investments every five years; naturally, these values can easily be changed. The starting point is a traditional integrated steel plant with two blast furnaces and basic oxygen furnaces, a coke plant, a combined heat and power plant (operated on by-product gases), air separation units, hot stoves, etc. (Figure 80, left). The new process units include the EAF, DR pellet plant, DR shaft furnaces, and electrolysers of different sizes (dashed region in Figure 80).

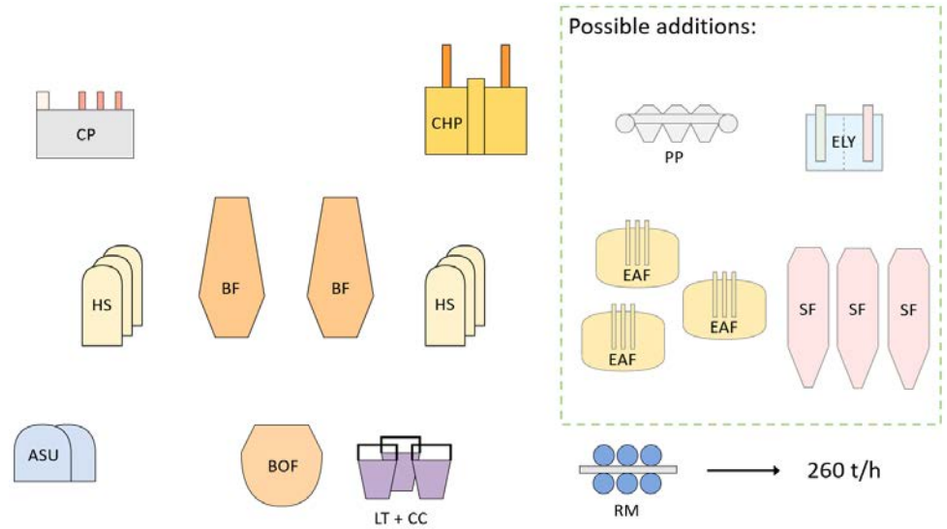

FIG 80 The main units in a traditional steel plant (left) and new units (right) to be optionally added at the beginning of the sub-periods.

After every subperiod, new units may be included and old ones phased out, with the requirement of providing a constant flow of rolled steel from the plant (Figure 80). To trigger the changes in the plant over the time horizon, the BFs must be relined (a considerable investment) or closed after a certain number of years. The external conditions, including the price of electricity, the penalty for CO_2 emissions, grid emission factors, and scrap price, drive the changes through the economic objective of the optimisation. The Gurobi solver was used in Pyomo to optimise the decisions (i.e. what to invest in), flows in the plant, and operation states over the considered horizon. The decisions also potentially consider buying external fuels and selling by-products.

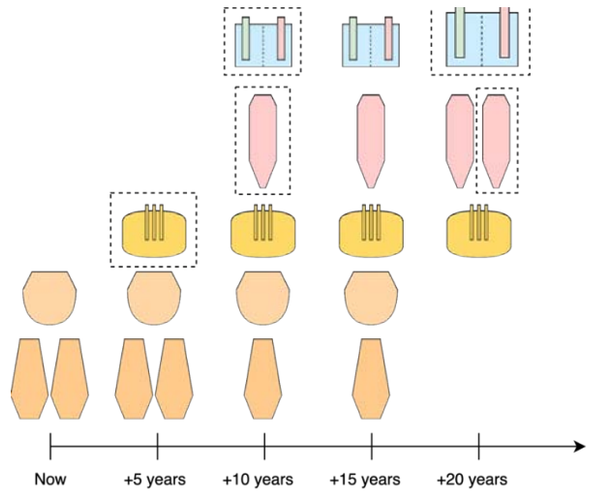

FIG 81 Schematic of the gradual transition from the initial to final state of an integrated steel plant, with potential investments every fifth year. Thesymbols within dashed regions indicate significant investments.

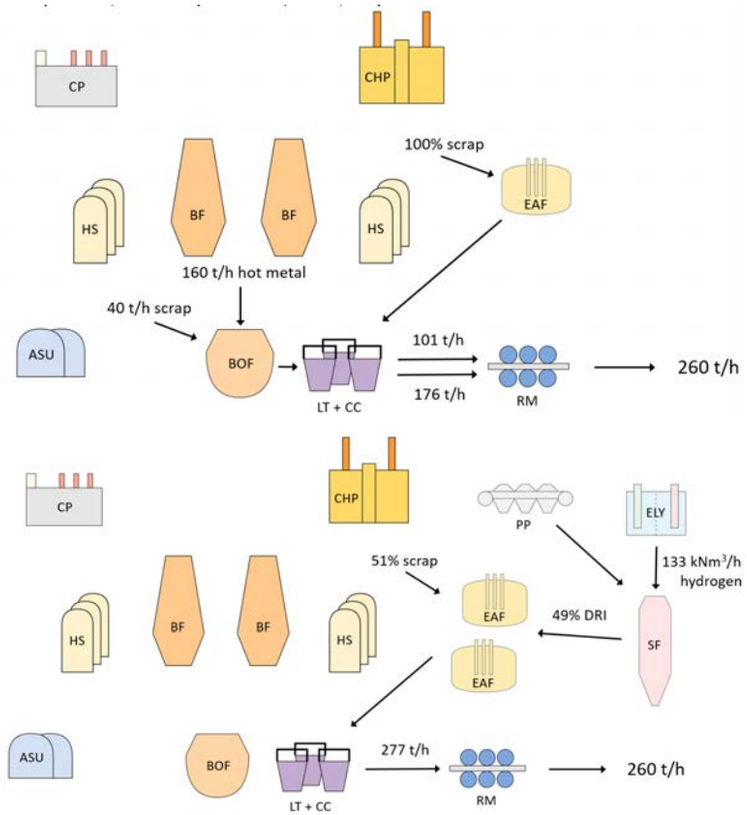

FIG 82 Optimal decisions at the beginning of the second (left) and third periods (right), showing gradual investments in the EAF, electrolysers, DR pellet plant, and shaft furnace, simultaneously phasing out BFs, hot stoves, and the coke plant.

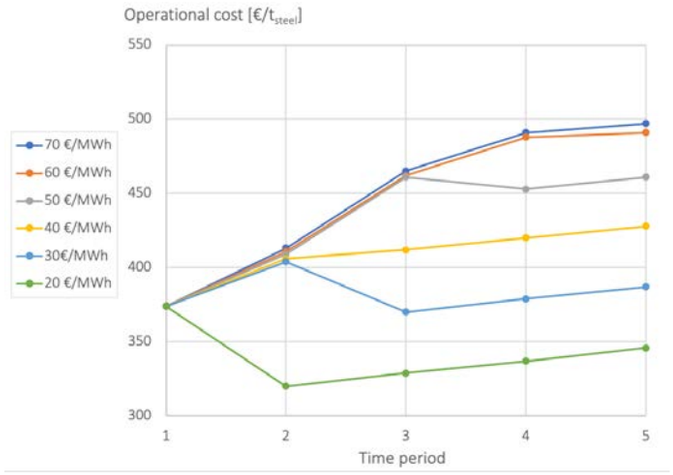

FIG 83 Evolution of specific operational costs from the starting point for the optimised routes using different prices of electricity for a scenario where the costs of CO_2 emissions and scrap increase with time.

RESULTS AND MAIN FINDINGS

A first version of the simulation environment of the evolving steel plant was developed within the FFS project, validating the overall performance of the models included and showing the general feasibility of the approach. The system has been evaluated under various external constraints (energy and raw material prices, emission penalties, etc.) that clearly indicate their role for the optimal transition.

As an illustration, results for a scenario will be presented where one BF must be relined or decommissioned after 10 years, the other after 20 years, and where the CO_2 emission and scrap acquisition costs gradually increase with time. The price of electricity was kept constant at a modest level (€40/MWh). Starting from the state depicted on the left of Figure 80, the optimal states of the plant at the start of the second (t = 5 a) and third (t = 10 a) periods are depicted in Figure 82, showing the partial replacement of ore by scrap (after five years) and then phasing out the BFs and investing in the DRI route (after ten years) with a considerable share of scrap as an input.

The sensitivity of the optimisation results with respect to the electricity price is illustrated in Figure 83, which shows the evolution of the specific operational costs during the different stages of the transition. The lowest electricity price (€20/MW, green curve) leads to an early adoption of the hydrogen-based production concept, with reduced costs that increase with time due to growing emissions costs. For electricity prices exceeding €40/MW, the operational costs unavoidably increase with time, but the optimal investments become insensitive to the electricity price at higher values (cf. €60 or €70/MWh). This demonstrates the important effect of the external conditions on the optimal transition path. Further external constraints may be imposed to better reflect the market conditions in the scenarios.

The system developed will be further extended with respect to modelling details and scenarios. It will also be extended to a consideration of the mini-mill concept that SSAB is adopting to explore how future investments should be directed. The research activities will also be continued within two European research projects.

REFERENCES

Haikarainen C, Pettersson F, Saxén H. (2023) Optimizing the transition pathway of a steel plant towards hydrogen-based steelmaking, 10th International Conference on Modelling and Simulation of Metallurgical Processes in Steelmaking (SteelSIM2023)

Haikarainen C., Shao L., Pettersson F., Saxén H. (2023) Mathematical optimization modeling for scenario analysis of integrated steelworks transitioning towards hydrogen-based reduction, submitted

RECYCLING

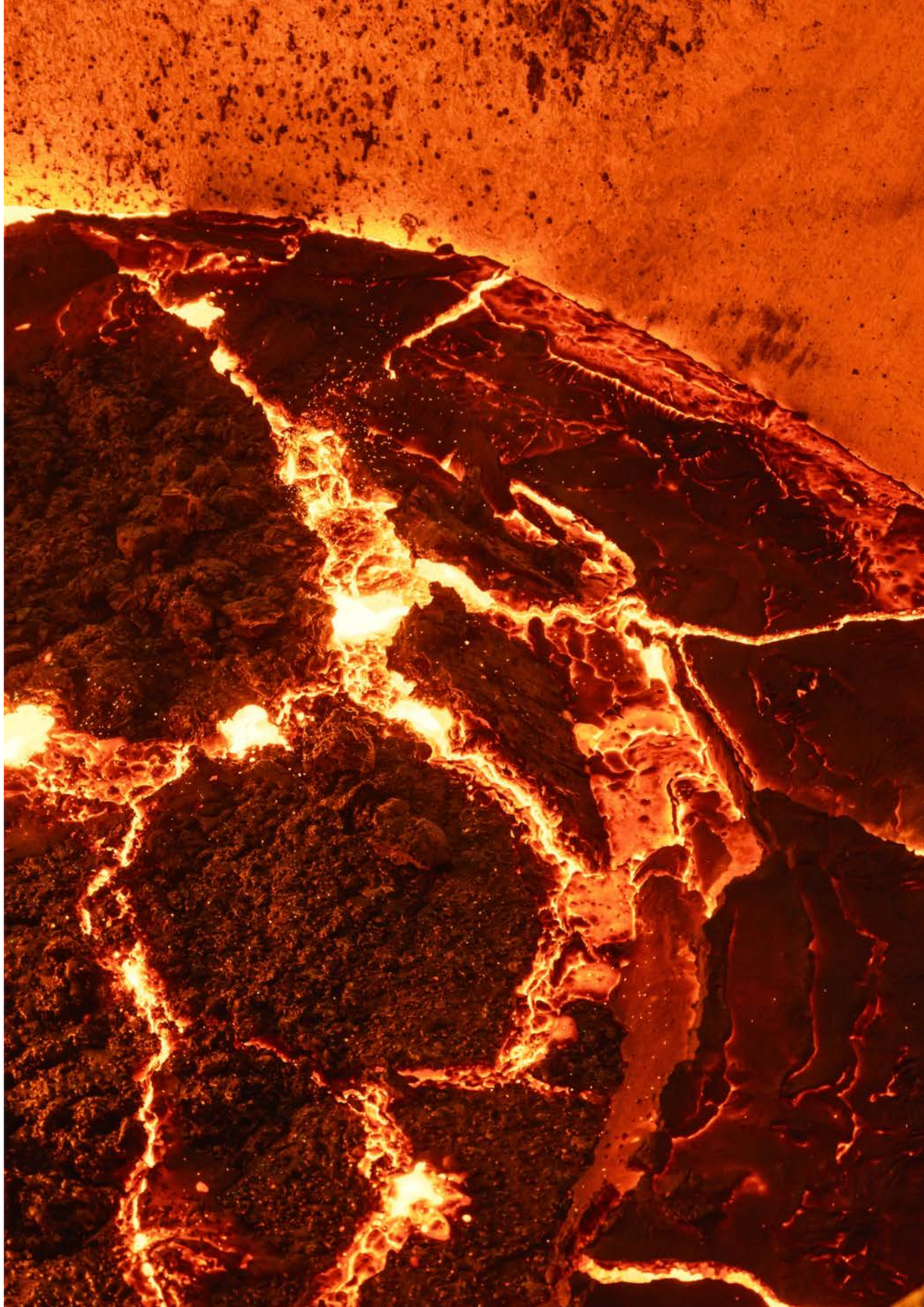

FFS TOWARDS FOSSIL-FREE STEEL

CONTRIBUTORS

Jaakko Louhisalmi I SSAB Europe
Rita Kallio I University of Oulu
Juha Koskineni I Tapojärvi
Teppo Riihimäkii I VTT

5.1 Recycling concept

Towards fossil-free steelmaking by-products

BACKGROUND

The electric arc furnace as a process and the by-products generated in the process are well known and studied. In terms of by-product material flows, the DRI-EAF route is much simpler than the fully integrated BF-BOF route. The generated by-product volumes are also lower. However, there are certain major challenges with the sustainability the processing and recycling of EAF by-products.

SSAB aims to revolutionise iron-ore-based steelmaking, and the target is to be the first in fossil-free steel production. Sustainable steel production can only mean improved overall material efficiency, which requires improvements in by-products' recycling and utilisation, which are at a very high level with the current BF-BOF steelmaking route. Hydrogen-reduced DRI as a new raw material for EAF creates unprecedented properties for by-products, changing the opportunities for processing and utilisation.

EAF slag is typically utilised in road construction or as asphalt ballast material. In northern Finland and Sweden a lot of good-quality natural aggregates are available, and the market for this type of products is limited. On the other hand, as a result of the closure of blast furnaces, the availability of blast furnace slag will decrease, which has been very important for the cement industry in supporting them to decrease CO_2 emissions. This has created increasing interest in developing future fossil-free slags to be used as supplementary cementitious material.

EAF dust is typically classified as hazardous waste, and when scrap is used as the main raw material, the dust has a relatively high Zn content, varying between 15 and 40%. This zinc-containing dust is treated in a high temperature process heated with fossil fuels, which recovers only the zinc and leaves a large quantity of waste to be landfilled.

SOLUTION, METHOD

General knowledge about EAF steelmaking by-product flows, properties, and volumes was collected from technology suppliers, EAF producers, and by-product processors, as well as from the recent research in the area.

SSAB has conducted trial melts at the Swerim pilot EAF in Luleå with hydrogen-reduced DRI. The EAF slag and EAF dust were collected from five campaigns and transported to Raahe for examination in this project. This provided a unique opportunity to study the properties of real fossil-free steelmaking by-products. In addition, the EAF slag samples were acquired from Ovako Imatra and the SSAB steel mill in Montpelier, USA.

EAF slag

All slag samples were characterised in close cooperation with the University of Oulu, partly at the university and partly at the SSAB Raahe steel mill laboratory.

Samples were processed and analysed similarly to regular quality monitoring procedures for current slag products at the Raahe Research Centre. Bulk chemical composition was determined with X-ray fluorescence (XRF), and the C and S content was determined with LECO, in addition to which qualitative and semi-quantitative mineralogy was determined with X-ray diffraction (XRD). An optical procedure was applied to determine the amorphous content of the slag. Metallic iron and ferrous iron were determined using wet chemical methods, and the environmental properties (leaching) from selected samples were determined according to SFS EN 12457-3. Furthermore, the radioactivity of NORM in process samples (activity concentrations) was determined by the Radiation and Nuclear Safety Authority (STUK). These characterisation methods were supplemented with mineralogical data based on work conducted at the University of Oulu.

To learn about the handling and processing of the future slag and to study the suitability for a road construction pilot, EAF slags were processed at an industrial scale with the SSAB Raahe steel mill slag crushing equipment. Samples were taken from the produced product, and particle distribution and leaching properties were determined.

The aim was to replace granulated blast furnace slag with future EAF slag ,as SCM preliminary simulations and calculations were undertaken to evaluate the required modification of EAF slag chemical composition and the costs of modification.

EAF dust

Chemical composition depends mainly on raw materials, and process conditions can have a minor effect. DRI-based EAF dust does not contain zinc. The minimum Zn content for the Waelz kiln process is about 15%. The aim was fossil-free steelmaking with a significant share of DRI requires low zinc-containing dust to be treated sustainably.

VTT has developed a holistic method to recover zinc and iron from EAF dust. The objective of the tests was to evaluate DRI dust as a feed material for the process concept.

Ladle slag

Ladle slag samples were collected from SSAB's steel mill in the USA, where scrap is the main raw material but the steel grades produced are comparable to the grades to be produced in Raahe. Ladle slag as analysed at the SSAB Raahe laboratory.

RESULTS, FINDINGS, OUTPUT, AND IMPACT

EAF slag

The amount of EAF slag per tonne of steel varies greatly. Using clean and good-quality scrap as a raw material, slag production can be around 90–110 kg per tonne of steel. With high gangue DRI, slag production can be up to 200 kg per tonne of steel. Based on the simulation, slag production with very high-quality DRI could be as low as 60 kg tonnes of steel. To plan the new fossil-free steel production slag handling, 100 kg per tonne of steel was used as an average.

Based on total chemical compositions, DRI-based slags have lower binary basicity, higher total iron, and especially higher ferrous iron content than the scrap-based slags included in this study.

Furthermore, the vanadium and titanium content in DRI-EAF slags is higher, whereas scrap-based slags have significantly higher chromium and manganese content. According to the optical method, all EAF slags are crystalline, with negligible amorphous content.

The results of a leaching test for industrial-scale crushed EAF slag were not ready, but a leaching test for a smaller sample from one campaign was finished, and when these results were compared to Finnish landfill regulations, none of the leaching values exceeded the limits.

During the laboratory work, it was soon observed that the slag was more difficult to crush than the Finnish Class I aggregate. The measurement results showed that slag was considerably more wear-resistant than Finnish granite. This should be considered a significant feature, e.g. in terms of wear parts and maintenance costs. Hardness can also be seen in the crushing results as a lack of fines and medium-size fractions: see Figure 84.

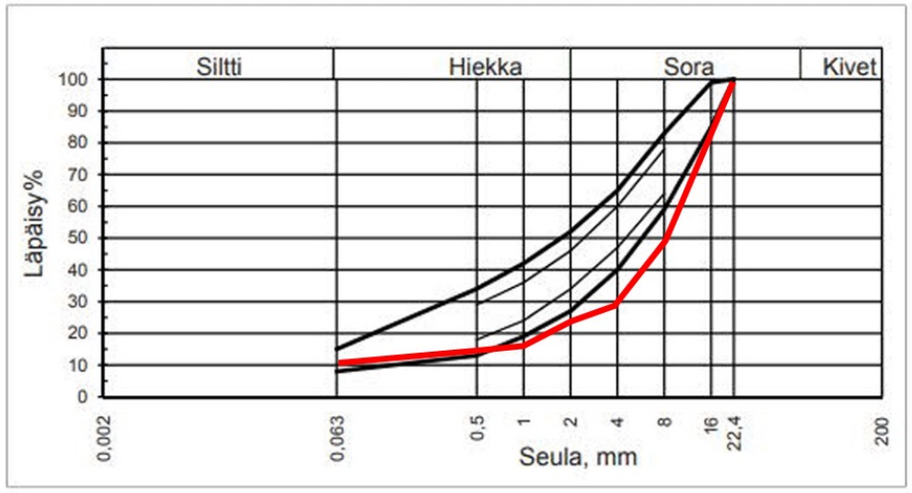

FIG 84 Particle size distribution for crushed slag aggregates vs the national PSD limits for asphalt aggregates 0/16 mm.

However, the Nordic ball mill test only gave a value to quality class 4. The result was weakened by rod-shaped and porous particles: see Figure 85. However, the reason for the difficult crushability and low hardness value remained unclear.

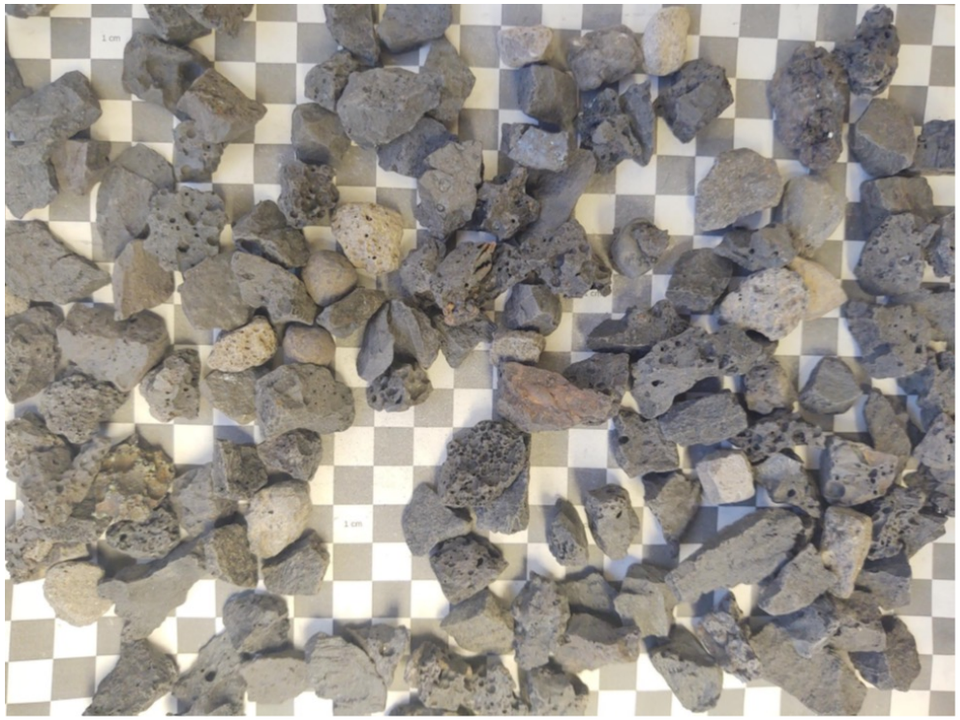

FIG 85 Tested EAF aggregates.

After this, the delays encountered were due to the increased radioactivity values of the slag measured by the subcontractor. The reason was the inherent properties of the raw materials of the steel. These have previously been known. It was estimated that there were no hazardous situations caused by radioactivity. The working methods were sufficient and did not need to be updated.

Both slag and metallics were determined as strongly magnetic. This was reflected in the difficulty of magnetically separating slag and metal. Even visually liberated slag particles stuck to the laboratory magnet.

The EAF slag was found to have no significant cementitious properties. In this respect, the properties differ from the earlier blast furnace slag.

EAF slag evacuation options were evaluated and compared during the project.

EAF dust

Typically, EAF dust is produced from about 17–20 kg per tonne of steel.

The VTT-developed process concept was suitable for DRI-based dust. However, some changes were needed for the process due to conventional and DRI dust composition differences. As the DRI dust zinc content was significantly lower, it correspondingly resulted in reduced zinc recovery units in the process. DRI dust alkali metals and calcium content was also significantly higher, which affected the process, as higher alkali metal concentration in the solution and high gypsum content in the leach residue limited its further use, such as in iron recovery. To overcome these issues a pre-treatment process to remove these substances prior to the VTT process concept was invented and tested. The pre-treatment consisted of diluted nitric acid leaching to produce a nitrate solution, and the leach residue was fed into the VTT-developed process. Furthermore, the nitrate solution was purified by removing aluminium and iron, for example, as well as heavy metals, etc., to obtain a pure nitrate solution for further use and optionally, the separation of different nitrate compounds. The process changes improved the VTT-developed process concept for DRI dust by reducing waste and improving holistic materials recovery to a sustainable low-waste process. The process concept requires further research to be validated. The compositions of conventional and DRI dust also need to be evaluated to test the different dust compositions corresponding to future feedstocks.

Ladle slag

Ladle slag production is expected to increase slightly from its current level. The role and function of ladle slag in the process remains the same and is therefore expected to have a similar chemical composition. It is planned to remove mini-mill ladle slag in two phases, and these slags may differ slightly. A preliminary comparison based on the analysis of the samples from USA EAF production ladle slag supported the understanding of similar properties. Ladle slag evacuation process was discussed, and it was decided to continue with existing ladle slag pots.

The overall challenge for the future research of by-products is the unknown varying share of scrap and DRI in the raw material mix of each melt. In addition, scrap quality variation and DRI quality variation and origin will result in variation in by-product properties, even though the produced steel grades will remain the same. This can have a significant effect on by-product recycling possibilities and utilisation potential.

FFS TOWARDS FOSSIL-FREE STEEL

CONTRIBUTORS

Mika Pahnila, Aki Koskela, Petri Sulasalmi, Timo Fabritius
University of Oulu

5.2 Biochar production and properties: requirements and use of bio-based materials in different processes in an integrated steel plant

BACKGROUND

In recent years, there has been increasing interest in using bio-based solutions in the steel industry. Many studies focusing on the potential to use the biochar (also referred to as a biocarbon) in the steel industry have been published. However, these studies have focused only the use of biomass in steelmaking without taking into account the processes and production methods behind producing biocarbon, and how different producing methods affect biocarbon properties and their suitability when using metallurgical applications. It is therefore essential to understand how different technologies and methods affect biocarbon yield and its properties during pyrolysis.

MATERIALS AND METHODS

This task was divided into sections: first, a literature review of different pyrolysis technologies was conducted; laboratory-scale pyrolysis experiments related to the most promising finding in the literature review were then conducted. The most promising finding in the literature review was that instead of using one heating ramp, it was possible to divide pyrolysis into multiple phases. This is called segmented pyrolysis, and according to the literature, it enhanced biocarbon properties, so it is more suitable for metallurgical use. However, in previous studies, the process time in segmented pyrolysis has always been higher than in conventional pyrolysis. The main idea here was to perform pyrolysis using the same process time in both cases and evaluating the differences in the produced biocarbon.

The pyrolysis experiments were undertaken using a laboratory-scale vertical furnace in both conventional and segmented methods. The used feedstock was spruce cutter flakes. The biocarbon yield was determined, and its properties such as its ash composition and volatile matter content were further studied.

RESULTS AND DISCUSSION

Based on the literature, it can be said that pyrolysis is a very complicated process, and that biocarbon yield during pyrolysis is affected in multiple ways, including the used heating rate and used feedstock. In view of the suitable technology to produce the biocarbon needed in metallurgical applications, the main results here can be summarised as follows. For traditionally used pyrolysis technologies, the use of slow pyrolysis (heating rate under 1 °C/s) combined with a low pyrolysis temperature, below 500 °C, led to the best biocarbon yield. For emerging new technologies, microwave- and solar-assisted pyrolysis led to the best biocarbon yield during pyrolysis. Segmented pyrolysis is a promising technology for producing biocarbon with enhanced properties, but because of the limited number of studies, more research is required to fully understand its potential.

Based on the limited numbers of studies of the production of biocarbon using segmented pyrolysis and its potential to produce biocarbon, it was decided to continue the related laboratory-scale experiments. Figure 86 shows a comparison of biocarbon and fixed carbon yield between segmented and conventional pyrolysis. As Figure 86 shows, segmented pyrolysis led to an increased biocarbon temperature range, from 300 to 900 °C. In fixed carbon yield, segmented pyrolysis led to an increased fixed carbon yield when the temperature was below 700 °C.

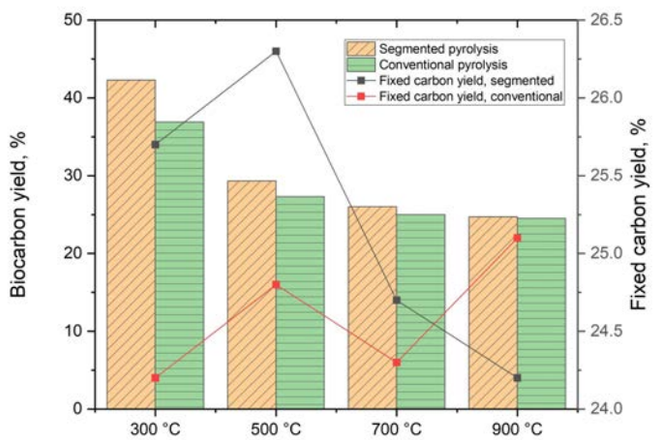

FIG 86 Comparison of biocarbon and fixed carbon between segmented and conventional pyrolysis.

Based on the determined hydrogen, carbon, and oxygen content, the hydrogen-to-carbon (H/C) and oxygen-to-carbon (O/C) ratios were calculated. These results show that using segmented pyrolysis led to increased H/C and O/C ratios. Moreover, biocarbons produced at 300 °C showed similar H/C and H/O ratios to lignite, which is the lowest grade of coal.

Based on the obtained results, it can be said that segmented pyrolysis is a promising way of producing the biocarbon needed for metallurgical applications. Moreover, the research showed it was possible to perform pyrolysis with the same process time as used in conventional pyrolysis. However, more research is still needed for a full understanding of how suitable the biocarbons produced in segmented pyrolysis are for metallurgical use. These studies may include kinetic studies of the produced biocarbons and even laboratory-scale experiments – for example, the foaming of slag.

PUBLICATIONS AND THESES

Pahnila, M., Koskela, A., Sulasalmi, P., Fabritius, T. (2023) A Review of Pyrolysis Technologies and the Effect of Process Parameters on Biocarbon Properties. Energies, 16, p. 6939.

FFS TOWARDS FOSSIL-FREE STEEL

CONTRIBUTORS

Rita Kallio, Sini Tyybäkinoja, Tuomas Alatarvas, Petri Sulasalmi
Eetu-Pekka Heikkinen I University of Oulu

5.3 Evaluation of suitable utilisation methods for residuals in selected future production scenarios

BACKGROUND

The by-products or residuals (slags, sludges, and dust) formed in electrical melting-based steelmaking differ from those in the traditional BF-BOF route. The handling and recycling of the by-products depends greatly on the properties – chemical and mineralogical characteristics – and volumes of their production. Slags are the major by-products in both current and future steel production. The slag's composition and mineralogy will have a major effect on how the slag can be further utilised. Furthermore, various cooling methods affect the crystalline or amorphous content, as well as the strength and particle size, of the produced slag.

In this task, a knowledge base for new DRI-EAF slags was gathered at the University of Oulu. This task focused on composition (chemical, mineralogical), structure (texture, crystallinity), and other key properties. The work started with a master's thesis study in which the effect of the cooling rate on the structure of EAF slags was studied. Additionally, modelling efforts were included (Factsage), as well as the possibility of modifying as-received slags to improve their cementitious character. A roadmap for possible routes to target various applications was created for this (Figure 87).

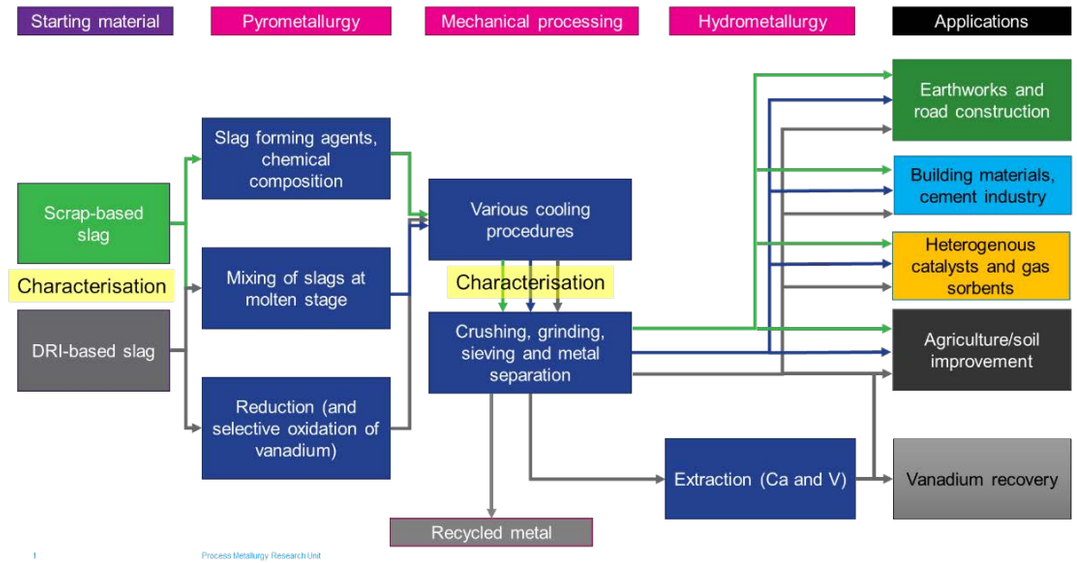

FIG 87 Roadmap for targeting various slag applications.

MATERIALS AND METHODS

At the outset, preliminary studies of the effect of the cooling rate on the structure of EAF slags were made in a master's thesis (Tyybäkinoja, 2022). The tests were performed for one DRI-based slag and synthetic slag samples. Further sets of both DRI-based and scrap-based slags were then received for detailed characterisation, in both original pieces and as crushed material. Detailed mineralogy was conducted on selected slag pieces applying electron probe microanalysis (EPMA) for accurate mineral chemical composition and field emission scanning electron microscopy (FESEM) for modal mineralogy, both applied on polished carbon-coated sections. These were complemented with wet chemical methods for iron oxidation states, total chemical composition with X-ray fluorescence (XRF), a qualitative indication of crystalline phases with X-ray diffraction (XRD), and amorphous content with optical microscopy. Furthermore, FESEM with electron backscatter diffraction (EBSD) was applied to granulated samples to detect microcrystalline/cryptocrystalline phases. The first sets of granulation experiments were conducted in cooperation with Luleå University. A study of quantitative XRD was also initiated in cooperation with Weimar University to test the applicability of an external standard method for EAF slags, providing challenges for quantitative XRD due to high FeOt content.

With regards to other EAF side stream, the mass and energy balance model done that was introduced in Chapter 3.2 was expanded to allow the possibility for dust recycling in the EAF process. For example, the feature enabled a study of the Zn enrichment within the EAF dust for possible Zn recovery when Zn-containing scrap was used as raw material.

RESULTS AND DISCUSSION

The mineralogy of DRI-EAF slags is dominated by dicalciumsilicate larnite (β-Ca_2SiO_4) and magnesiowustite (Fe,Mg)O, with gehlenite ($Ca_2Al_2SiO_7$), or mayenite ($Ca_{12}Al_{14}O_{33}$) and brownmillerite ($Ca_2(Al,Fe_)O_5$) occurring as alumina-containing phases. Due to high TiO_2 and V_2O_3 in DRI slags, accessory phases such as perovskite and Ca-vanadate are not uncommon. The DRI-EAF slags included in this study are more reduced in character (~70% of iron occurs as divalent) than scrap-based slags (~40 and ~60% as divalent from the total), which also reflects the abundant brownmillerite-srebrodolskite solid solution occurring as another iron-containing phase in scrap-based slags. In all slags, phosphorus occurs almost solely in the larnite, chromium is mainly incorporated into the monoxide phase except for scrap EAF slag1, whereas vanadium distribution is more varied. Examples of modal mineralogy and P_2O_5, V2O3, and Cr_2O_3 deportment are provided in Figure 88. All the polished blocks represent completely crystalline slags. To increase amorphous content and thus improve possible cementitious properties, a first set of granulation experiments with and without modification ± reduction was successfully carried out at Luleå University. With a suitable modifying agent and targeted reduction degree, promising results with respect to both the quality of completely amorphous slag and metal were produced. Further experiments will be conducted to confirm these preliminary results and test a variety of reductants.

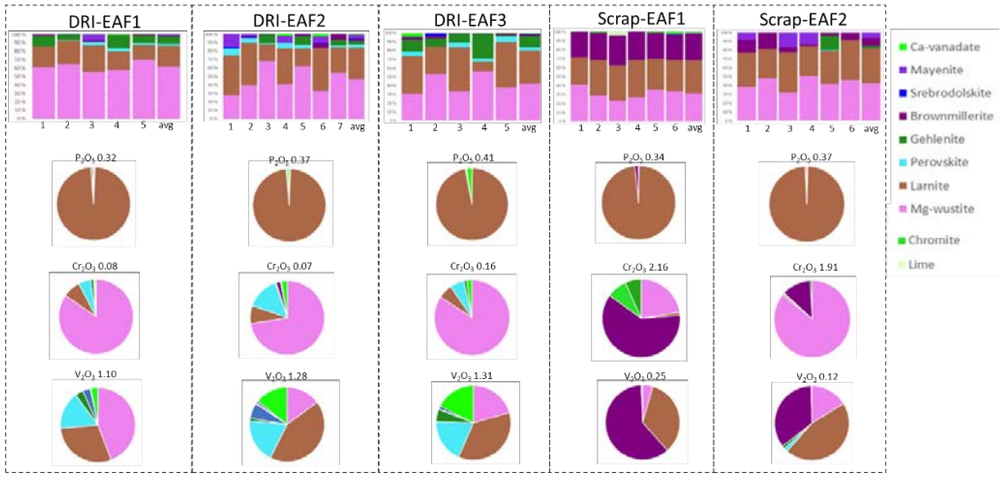

FIG 88 Results of modal mineralogy and P_2O_5, Cr_2O_3, and V_2O_3 deportment in slag samples.

Regarding the EAF dust, the dust is an environmentally dangerous material because of the presence and potential leaching of several toxic elements (i.e. Cd, Cr, Zn, and Pb). Regarding Zn, the use of DRI with Zn-containing scrap can considerably decrease the share of ZnO formed in the EAF process. Another possibility is to enrich the Zn content within the EAF dusts by recycling a sufficient proportion of dust back to the process to recover Zn from the dust once the content is sufficiently high. To study this, the mass and energy balance model developed for the EAF process (see Chapter 3.2) was equipped with a dust recycling feature which enables the study of different scenarios when the desired proportion of dust is directed back to the process. Figure 89 shows the results of a scenario study where the accumulation of Zn in the dust was modelled with different proportions.

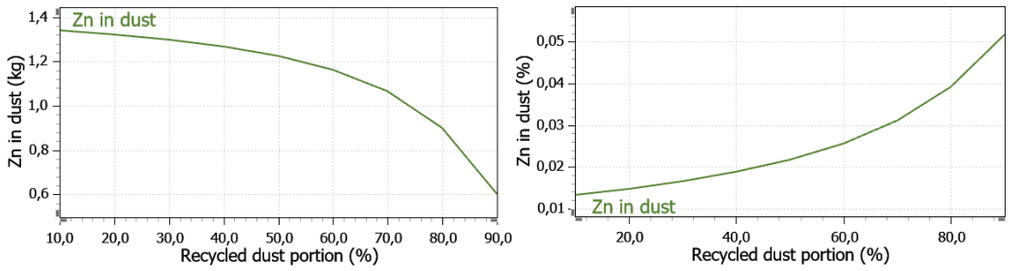

FIG 89 Results of a scenario study where the accumulation of Zn in EAF dust and the share of recycled dust back to the process varied.

PUBLICATIONS AND THESES

Kallio, R., Heikkinen, E.-P., Isteri, V., Koskela, A., Abdelrahim, A., Sulasalmi, P., Visuri, V.-V., and Fabritius, T. (2023) Overview of Recent Research Activities on Circular Economy in the Iron and Steel Industry at the Process Metallurgy Research Unit, University of Oulu. Presentation at the ESTEP Annual Event 2023 (3.10–5.10.2023). Proceedings will be published.

Tyybäkinoja, S., Heikkinen,E.-P, Alatarvas, T., Sulasalmi, P., Louhisalmi, J, Oey, T., Kekäläinen, P., Karhu, M., and Leivo M. (2023) Experimental study on the solidification structure of EAF slags, 8th International Slag Valorisation Symposium

Tyybäkinoja, S. (2022) The Effect of Cooling Rate on Structure of EAF Slags, Master's thesis, University of Oulu

FFS TOWARDS FOSSIL-FREE STEEL

CONTRIBUTORS

Maria Kokko, Ulla Lassi, Mikael Manninen
Sustainable Chemistry Research Unit, University of Oulu

5.4 Recovery of Vanadium from Future EAF Slags

BACKGROUND

The transition from carbon-based to more environmentally friendly steelmaking processes is currently becoming a reality in the steel industry. Current initiatives in the Nordic countries aim to shift steelmaking from the traditional BF-BOF route to the H_2-DRI-EAF route. This will increase the amount of H_2-DRI-EAF slag in the future. Such EAF slags may contain small amounts of vanadium, which has been classified as a critical metal by the European Union [1]. However, the high concentrations of readily leachable Ca and Si in the slag make the hydrometallurgical recovery of vanadium difficult. It is therefore important to study the dissolution behaviour of vanadium and other elements. From the perspective of process design, it is also important to be able to model and predict the behaviour of vanadium in aqueous solutions. In the present task, the recovery of Ca and V from the H_2-DRI-based EAF slag by a two-stage direct leaching process (Figure 90) was investigated [2]. In addition, the solubilities of some industrially relevant vanadium salts (NH_4VO_3 and $NaVO_3$) in water were accurately determined within a considerable temperature range [3].

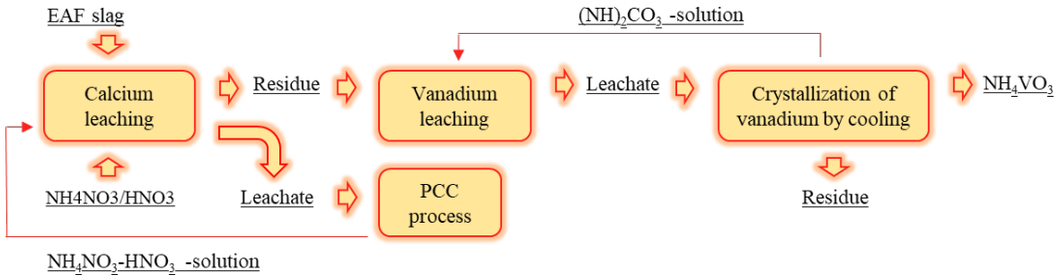

FIG 90 The two-stage vanadium recovery process investigated in the present work.

MATERIALS AND METHODS

Leaching experiments

Vanadium-containing EAF slag produced in a pilot H_2-DRI-EAF facility was obtained from SSAB. The laboratory-scale optimisation of the process shown in Fig. 90 was conducted using a statistical experiment design (DOE). In the first stage, Ca was selectively leached in a NH_4NO_3-HNO_3-H_2O solution, and the remaining V-containing residue was separated. The residue was directed to the second stage, where V was leached in an alkaline carbonate salt solution, preventing the remaining Ca and Mg dissolving. Two alternatives for the carbonate media were tested, the Na_2CO_3-NaOH-H_2O and (NH_4)-$2CO_3$-H_2O solutions. V can be recovered from the final leachate by precipitating it as NH_4VO_3. Five responses (Ca, V, Si, Mg recoveries, and Ca selectivity) were investigated in the Ca stage, and three (V, Si recoveries, and V selectivity) in the V stage. Factorial experiments were used to investigate the effects of operating conditions on the responses. The concentrations of the elements in the solutions were analysed by inductively coupled plasma–optical emission spectroscopy (ICP–OES), and the compositions of the solids were determined with the aid of microwave-assisted acid digestion coupled with ICP-OES.

Solubility determinations

Due to the lack of reliable and extensive solubility data in the previous literature, the solubilities of ammonium and sodium metavanadate in water were determined in the temperature range from 298.15 to 333.15 K at atmospheric pressure [3]. The isothermal saturation method was applied, and a special apparatus constructed for solubility measurements was used in the experiments. Empirical equations were fitted to the present data and to the available literature data, and analytical expressions for the solubilities of the studied salts were given. Finally, the capabilities of modelling the aqueous solubility of NH_4VO_3 with thermodynamic models currently available in the literature were investigated.

RESULTS AND DISCUSSION

The principle of the two-stage process in Fig. 90 was confirmed to be feasible, although the vanadium recovery remained somewhat low (~40%). The effects of the various parameters could be clearly resolved from the data. It was found that the proportion of nitric acid to ammonium nitrate, liquid-to-solid ratio (L/S), and temperature significantly affected the outcome of the Ca leaching step. In the V leaching step, the temperature and L/S ratio were significant variables, but only in the $(NH_4)2CO_3$-H_2O system, the concentration of the leaching reagent had an effect in the studied range. Although some educated speculations could be given, the mechanisms behind the observed effects remain unclear, and further research is needed to better understand the complex multiphase systems present in the studied process. Only by better understanding the phenomena behind the process can significant advances in the hydrometallurgical recovery of vanadium be achieved.

Accurate solubility data were obtained in the solubility determinations. Most notably, the data for the hydrated salt $NaVO_3 \cdot 2H_2O$ were apparently reported for the first time for a considerable range of temperatures. The obtained data are of practical value for the industry, as they can be directly used to estimate the solubility of these salts in simple aqueous systems. However, comprehensive thermodynamic models for aqueous vanadium systems remain a distant prospect, and the predictive capabilities of the current models are very limited [3].

PUBLICATIONS AND THESES

Manninen M., Vielma T., and Lassi U. (2023) A closer look into solubility in the binary $NaVO_3$-H_2O and NH_4VO_3-H_2O systems, Journal of Chemical and Engineering Data, 68, 9, pp. 2500–2511

REFERENCES

[1] D.-G. for I.M.I.E. and Sme. European Commission, Proposal for A Regulation of the European Parliament and of the Council of 16 March 2023 establishing a framework for ensuring a secure and sustainable supply of critical raw materials and amending Regulations (EU) 168/2013, (EU) 2018/858, 2018/1724 and (EU) 2019/1020, (COM/2023/160 final), (2023) https://eur-lex.europa.eu/legal-content/EN/TXT/?uri=CELEX:52023PC0160 (accessed 20 September 2023).

[2] Kokko M., Manninen M., Hu T., Lassi U., Vielma T., and Pesonen J. (2023) Hydrometallurgical Recovery of Vanadium and Calcium from Electric Arc Furnace Slags from Hydrogen Based Steel Production. Manuscript in preparation.

[3] Manninen M., Vielma T., Lassi U., (2023) A Closer Look into Solubility in the Binary $NaVO_3$–H_2O and NH_4VO_3–H_2O Systems from 298.15 to 333.15 K and 0.1 MPa, J. Chem. Eng. Data., 68, pp. 2500–2511. https://doi.org/10.1021/acs.jced.3c00367.

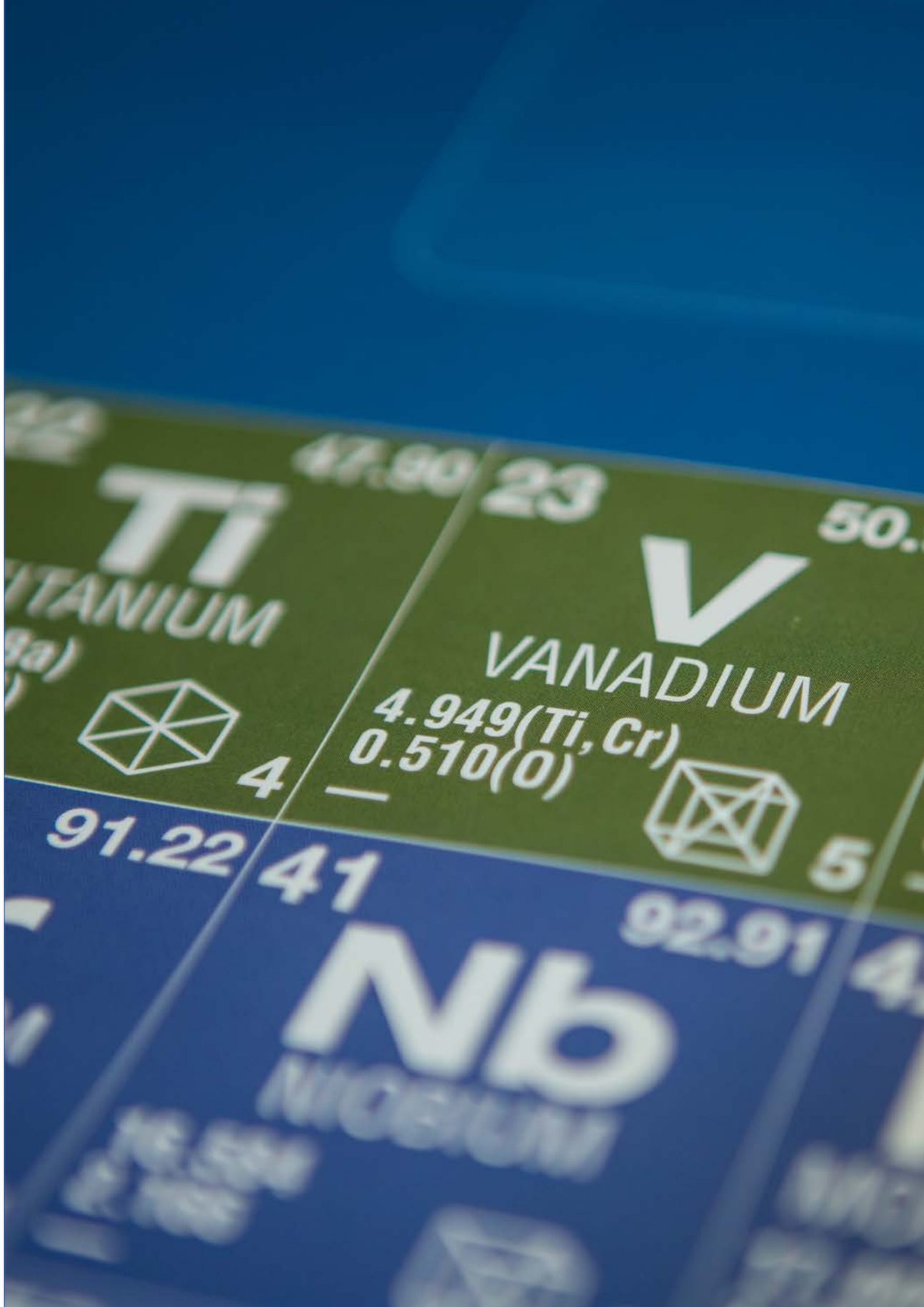

FFS TOWARDS FOSSIL-FREE STEEL

CONTRIBUTORS

Katja Ohenoja, Vitalii Ponomar
Fibre and Particle Engineering Research unit, University of Oulu

5.5 The use of EAF and ladle slags as cementitious binders

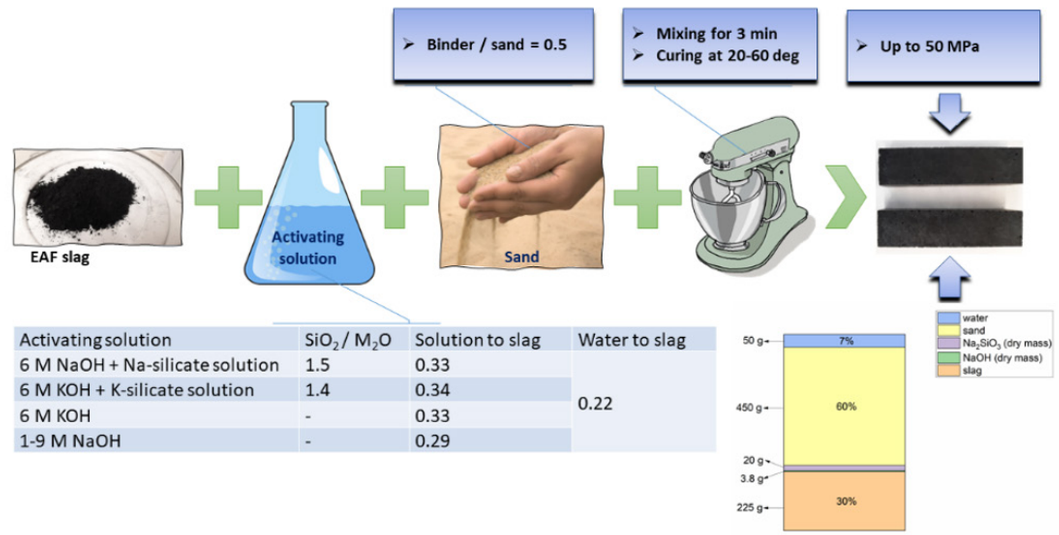

Activating solution	SiO_2 / M_2O	Solution to slag	Water to slag
6 M NaOH + Na-silicate solution	1.5	0.33	0.22
6 M KOH + K-silicate solution	1.4	0.34	
6 M KOH	-	0.33	
1-9 M NaOH	-	0.29	

FIG 91 The overall scheme of the experimental procedure used to obtain AAMs.

BACKGROUND

The steel industry is striving to transition to low CO_2 steelmaking processes by decarbonising operations. For example, initiatives like hydrogen-based iron production with direct reduction, which involves the use of hydrogen to reduce iron oxides to metallic iron without metallurgical coke, are underway in countries like Finland and Sweden. The subsequent refining of direct reduced iron (DRI) into steel occurs using electric arc furnaces (EAFs). This shift in the steelmaking process will affect the composition and quantity of by-products, resulting in a future shortage of blast furnace slag (BFS). Consequently, EAF slag from hydrogen-based iron production is emerging as a new raw material for use in cementitious materials. Previous efforts have explored the use of EAFs and other steel slags as cementitious supplementary materials in blended cements. Unlike BFS, EAF slag is neither hydraulic nor pozzolanic due to the absence of tri-calcium silicates and amorphous SiO_2 content. This WP therefore explores alternative ways to introduce EAFs from DRI process to the design of alternative low-CO_2 binders, including alkali-activated materials, carbonated precast concrete, and supplementary cementitious materials (SCM).

MATERIALS AND METHODS

The project's starting materials consist of several pilot-scale EAFs from DRI process, SSAB in Finland. A comprehensive characterisation of these slags includes chemical, physical, and mineralogical analyses, along with microstructural examination. Chemical composition analysis is performed using X-ray fluorescence analysis (XRF) or inductively coupled plasma mass spectrometry (ICP-MS), mineral composition determined through X-ray diffraction analysis (XRD), and energy- and wave-dispersion spectrometry (EDS-WDS). The hydraulic reactivity of the clinkers is assessed using isothermal calorimetric measurements. To gain deeper insights into reactivity, dissolution tests are conducted, comprising batch dissolution and batch titration experiments. Evaluating cementitious properties is conducted with mortars and pastes prepared by mixing slag powder with water, alkaline solutions, and OPC in addition to curing in a CO_2 atmosphere. The determination of the paste nanostructure involves a range of techniques, including XRD, thermogravimetric analysis (TGA), Fourier-transform infrared spectroscopy (FT-IR), scanning electron microscopy coupled with energy dispersive X-ray spectroscopy (SEM-EDX), and STEM-EDX. Hardened properties include the measurement of compressive and flexural strengths (in accordance with EN 196-1), porosity, and density.

RESULTS AND DISCUSSION

In this WP, four samples of electric arc furnace (EAF) slag from hydrogen-based iron production were analysed, revealing variations in their chemical and mineral composition. These slags were rich in iron (Fe) and calcium (Ca), with silicon (Si) the second, third, or fourth most abundant component. The slags exhibited low amorphous content and contained various crystalline phases, including larnite wüstite-periclase, åkermanite-gehlenite, and magnetite-magnesioferrite solid solution, among others.

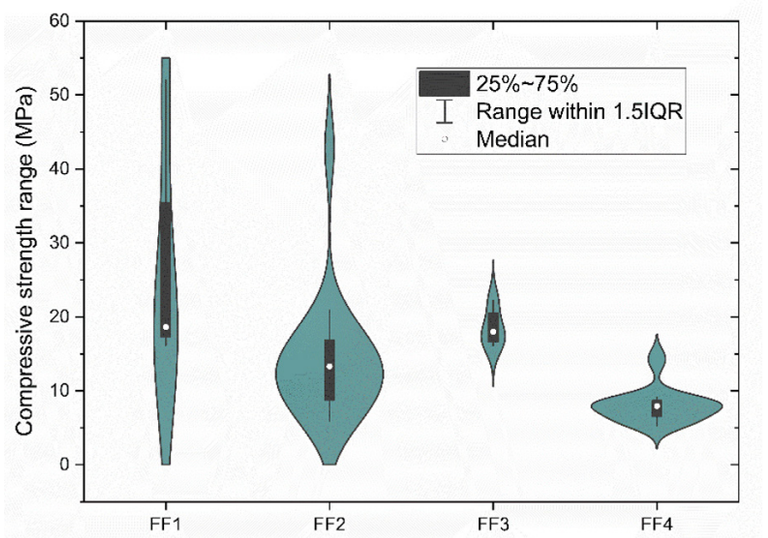

FIG 92 Compressive strength range for alkali-activated EAF slags.

When mixed with alkaline solutions, fresh pastes exhibited a short setting time that could be controlled by adjusting the waterglass modulus and the solution-to-slag ratio. The resulting alkali-activated pastes and mortars displayed varying compressive strengths (ranging from 10 to 50 MPa) depending on the sample and mix design, with a median value of approximately 20 MPa for less basic slags and about 10 MPa for more basic slags. Factors influencing mechanical properties included curing time, alkali content in the activating solution, and relative humidity during curing, while variables like curing temperature, waterglass modulus, and particle fineness had a minimal impact. In summary, in optimal conditions, the alkali activation of EAF slag can yield materials with mechanical properties comparable to ordinary Portland cement (OPC)-based concrete. However, further research is needed to assess their long-term durability.

Another subtask explored the feasibility of using EAF slag from hydrogen-based iron production as the sole binder for CO_2-activated cementitious materials in a simulated flue gas atmosphere. Two slags with varying chemical compositions were examined. Adjusting the water-to-slag ratio to appropriate values (0.14–0.16) and curing the moulded masses in the simulated flue gas atmosphere resulted in the development of compressive strength, reaching approximately 20 MPa after one day of curing. Extended CO_2 exposure led to progressive strength increases, with higher basicity slag showing faster initial strength development. This strength development was correlated with mineralogical changes, particularly the transformation of belite (larnite) into the C-S-H phase and $CaCO_3$. The degree of carbonation was linked to H_2O content and polymerised Si-O, indicating an increased hydrated phase content such as C-S-H or decalcified C-S-H phases.

PUBLICATIONS AND THESES

Ponomar, V., Ohenoja, K., Fabritus, T., and Illikainen, M. (2023) Recycling of electric arc furnace slag from hydrogen-based iron production in cementitious binders. 3rd ECI International Conference: Alkali Activated Materials and Geopolymers: Sustainable Construction Materials and Ceramics Made Under Ambient Conditions

Ponomar, V., Ramteke, D. D., Ohenoja, K., and Illikainen, M. (2023) CO_2-assisted hydration of EAF slags in a simulated flue gas atmosphere as a sustainable way to concrete production. Nature Sustainability (Submitted)

FFS TOWARDS FOSSIL-FREE STEEL

PUBLICATIONS

Journal

Ghosalya, M. K., Talebi, P., Singh, H., Klyushin, A., Kokkonen, E., Mansouri, M. A., Huttula, M., Cao, W., Urpelainen, S., Solar Light Driven Atomic and Electronic Transformations in Ni@NiCO3/NiO Hybrid Photocatalyst Revealed by Ambient Pressure X-ray Photoelectron Spectroscopy, submitted

Haapakangas J., Riikonen S., Airaksinen S., Heikkinen E.-P., Fabritius T. (2024) Oxide Scale Formation on Low-Carbon Steels in Future Reheating Conditions, Metals, 14(2), 189

Haikarainen C., Shao L., Pettersson F., Saxén H. (2023) Mathematical optimization modeling for scenario analysis of integrated steelworks transitioning towards hydrogen-based reduction, submitted

Heidari A., Niknadah N., Iljana M., Fabritius T. (2021) A Review on Kinetics of Iron Ore Reduction by Hydrogen, Materials, 14(24), 7540

Iljana M., Abdelrahim A., Bartusch H., Fabritius T. (2022) Reduction of Acid Iron Ore Pellets under Simulated Wall and Center Conditions in a Blast Furnace Shaft, Minerals 2022, 12(6), 741

Iljana M., Heikkinen E.-P., Fabritius T. (2021) Estimation of Iron Ore Pellet Softening in a Blast Furnace with Computational Thermodynamics, Metals 2021, 11(10), 1515

Iljana M., Paananen T., Mattila O., Kodrakov M., Fabritius T. (2022) Effect of Iron Ore Pellet Size on its Metallurgical Properties, Metals 2022, 12(2), 302

Ilmola J., Seppälä O., Pohjonen A., Larkiola J., (2022), Virtual rolling automation and setup calculations for six stands FEM finishing mill, IOP Conference Series: Materials Science and Engineering, 1270, 012060

Klyushin A., Ghosalya M., Kokkonen E., Eads C., Jones R., Nalajal N., Gopinath C. S., Urpelainen S. (2023), Photocatalytic setup for in situ and operando ambient-pressure X-ray photoelectron spectroscopy at MAX IV Laboratory, Journal of Synchrotron Radiation, Vol. 30, 3, 613-619

Kuutti K., Ghosalya M., Porri P., De Bellis J., Jokimies P., Singh H., Wang S., King G., Fernández-Catalá J., Schüth F., Kokkonen E., Huuhtanen M., Huttula M., Urpelainen S., Rautiainen S. (2024) Ball mill synthesized Pt nanoparticle/TiO2 catalyst for methylcyclohexane dehydrogenation, Applied Catalysis B, submitted

Manninen M., Vielma T., Lassi U. (2023) A closer look into solubility in the binary $NaVO_3$-H_2O and NH4VO3-H2O systems, Journal of Chemical and Engineering Data, 68, 9, pp. 2500–2511

Mitas B., Visuri V.-V., Schenk J., (2022) Mathematical Modeling of the Ejected Droplet Size Distribution in the Vicinity of a Gas-Liquid Impingement Zone, Metallurgical and Materials Transactions B, 53, pp. 3083–3094

Norrena, J., Louhenkilpi, S., Visuri, V.-V., Alatarvas, T., Bogdanoff, A. and Fabritius, T. (2023). Assessing the Effects of Steel Composition on Surface Cracks in Continuous Casting with Solidification Simulations and Phenomenological Quality Criteria for Quality Prediction Applications. Steel Research International, Vol. 94, No. 5. 2200746.

Norrena, J., Louhenkilpi, S., Visuri, V.-V., Alatarvas, T., Bogdanoff, A. and Fabritius, T. (2023). Development of Interpretable Machine Learning Models for Predicting Transverse Cracks in Continuous Casting of Steel with Phenomenological Quality Criteria from Solidification and Heat Transfer Simulations. Steel Research International (Submitted)

Pahnila, M., Koskela, A., Sulasalmi, P., Fabritius, T., (2023), A Review of Pyrolysis Technologies and the Effect of Process Parameters on Biocarbon Properties. Energies, 16, 6939

Pauna, H. et al., (2022), Hydrogen plasma smelting reduction process monitoring with optical emission spectroscopy – Establishing the basis for the method, Journal of Cleaner Production, Vol. 372, 133755.

Ponomar, V., Ramteke D.D., Ohenoja, K., Illikainen, M. (2023) CO2-assisted hydration of EAF slags in a simulated flue gas atmosphere as a sustainable way to concrete production. Nature Sustainability, submitted

Pylvänäinen M., Nissilä J., Visuri V.-V., Laurila J., Niemi A. H., Tuomikoski S., Paananen T, Liedes T. Effect of Gas Forming Compounds on the Vibration of a Submerged Lance in Hot Metal Desulfurization, Steel Research International, 94, 2300072

Quimbayo J. M., Sasikala Devi J., Ghosalya A. A., Huttula M. K., Alatalo M., Urpelainen S., Ojala S., Photocatalytic degradation of Diuron, submitted

Quimbayo J. M., Ojala S., Urpelainen S., Huuhtanen M., Cao W., Huttula M., Keiski R. L. (2022), Nanostructured Photocatalytic Materials for Water Purification, In M. P. Shah, S. P. Bera, B. Y. Tore (ed.) Advanced Oxidation Processes for Wastewater Treatment, Boca Raton: CRC Press.

Seppälä, O, Pohjonen A., Mendonça J., Javaheri V., Podor R., Singh H., Larkiola J., (2023), In-situ SEM characterization and numerical modelling of bainite formation and impingement of a medium- carbon, low-alloy steel, Materials & Design, 230, 111956

Shao L., Xu J., Saxén H., Zou Z.-S. A numerical study on process intensification of hydrogen reduction of iron oxide pellets in a shaft furnace. Fuel, Vol. 348 (2023) 128375.

Vuolio T., Visuri V.-V., Sorsa A., Paananen T., Tuomikoski S, Fabritius S. (2023) Machine Learning Assisted Identification of a Grey–Box Hot Metal Desulfurization Model, Materials and Manufacturing Processes, 38, 15, pp. 1983–1996

Vuolio T., Visuri V.-V., Tähtilä H., Pekuri P., Fabritius T. (2024) The Synergistic Effect of Na2O on Hot Metal Desulfurization Kinetics in CaO-Na_2O-SiO_2-Al_2O_3-MgO Slag System, Chemical Engineering Science, 284:119525

Weiss R., Ikäheimo J. (2024) Flexible Industrial Power-to-X Production enabling Large Scale Wind Power Integration: A Case Study of future Hydrogen Direct Reduction Iron Production in Finland, Applied Energy, submitted

Yu S., Shao L., Zou Z.-S., Saxén H. A Numerical Study on the Performance of the H2 Shaft Furnace with Dual-row Top Gas Recycling. Processes, Vol. 9 (2021) 2134.

Conference

Haikarainen C, Pettersson F, Saxén H. (2023) Optimizing the transition pathway of a steel plant towards hydrogen-based steelmaking, 10th International Conference on Modelling and Simulation of Metallurgical Processes in Steelmaking (SteelSIM2023)

Heidari A., Ghosalya M., Heikkilä A., Iljana M., Urpelainen S., Fabritius T. (2023) Surface reduction behavior of iron oxides, oFEMS EUROMAT 2023

Heidari A., Iljana M., Fabritius T. (2023) A comparison of reduction behavior of DRI and blast furnace pellets in CO-H_2 atmosphere, METEC & 6th ESTAD

Hoikkaniemi E., Sulasalmi P., Visuri V.-V., Fabritius T. (2023) Biochar as a slag foaming agent in EAF – A novel experimental setup, 5th European academic EAF Symposium, Oulu, Finland

Ilmola, J., Paananen, J., Larkiola, J. (2023) Effect of work roll surface warming on hot strip temperature development in industrial scale virtual rolling model, Numiform conference

Ilmola, J., Paananen, J., Seppälä, O., Pyykkönen J., Larkiola, J. (2023) Phenomenon Based Model for Virtual Hot Strip Rolling, Thermec conference

Kallio, R., Heikkinen, E.-P., Isteri, V., Koskela, A., Abdelrahim, A., Sulasalmi, P., Visuri, V.-V., Fabritius, T. (2023) Overview of Recent Research Activities on Circular Economy in the Iron and Steel Industry at the Process Metallurgy Research Unit, University of Oulu, ESTEP Annual Event 2023

Norrena, J., Louhenkilpi, S., Visuri, V.-V., Alatarvas, T., Tähtilä, H. and Fabritius, T. (2023) Development of Machine Learning Models for Predicting Defect Formation in Continuous Casting of Steel with Phenomenological Quality Criteria from Solidification and Heat Transfer Simulations, 10th International Conference on Modelling and Simulation of Metallurgical Processes in Steelmaking (SteelSIM2023)

Oey T., Kekäläine P., Karhu M., Leivo M., Louhisalmi J., Tyybäkinoja S., Heikkinen E.-P., Alatarvas T., Sulasalmi P. (2023) Influence of Composition and Cooling Rate on the Reactivity and Performance of Novel Steel Slags as Cement Replacements, 8th International Slag Valorisation Symposium

Pauna, H. et al., (2022), Optical emission spectroscopy as a tool for process control of steelmaking burners, 8th International Congress on the Science and Technology of Steelmaking.

Ponomar, V., Ohenoja, K., Fabritus, T., Illikainen, M. (2023) Recycling of electric arc furnace slag from hydrogen-based iron production in cementitious binders, 3rd ECI International Conference: Alkali Activated Materials and Geopolymers: Sustainable Construction Materials and Ceramics Made Under Ambient Conditions

Salucci E, D'Angelo A, Ghosh S, Russo V, Grénman H, and Saxén H. (2023) Modelling of iron oxide reduction with hydrogen – from intrinsic kinetics to dynamic bed operation. Paper presented at the 14th European Congress of Chemical Engineering (ECCE2023), Berlin, Germany

Salucci E, Ghosh S, Russo V, Grénman H, and Saxén H. (2023) Modelling of iron oxide reduction with hydrogen. Proceedings of the 33rd European Symposium on Computer Aided Process Engineering (ESCAPE33)

Salucci E, Ghosh S, Russo V, Grénman H, and Saxén H. (2023) Modelling of iron oxide reduction with hydrogen. Paper presented at the SteelSim 2023 conference, University of Warwick, UK

Tyybäkinoja S., Heikkinen E.-P, Alatarvas T., Sulasalmi P., Louhisalmi J, Oey T., Kekäläinen P., Karhu M., Leivo M. (2023) Experimental study on the solidification structure of EAF slags, 8th International Slag Valorisation Symposium

Weiss R., Ikäheimo J. (2023) Flexible Industrial Power-to-X Production as Virtual Hydrogen Storage enabling Large Scale Wind Power Integration: A Case Study of future Hydrogen Direct Reduction Iron Production in Finland, SDEWES2023 conference

Theses

Hagström A. (2023) Reduction of iron oxides in fluidized bed ovens, Bachelor's thesis, University of Oulu

Hoikkaniemi E. (2022) Use of biochar as a slag foaming agent in EAF steelmaking, Master's thesis, University of Oulu

Kanto, T. (2022) Renewable hydrogen storage and supply options for large-scale industrial users in Finland, University of Oulu

Mattila E. (2023), Menetelmät suorapelkistetyn raudan valmistamiseksi, Bachelor's thesis, University of Oulu

Mehtälä M. (2023) Management of metallic impurities in production of strip steels in EAF process, Master's thesis, University of Oulu

Pyhtilä. T. (2022) Review of selection rules for casting powders, Master's thesis, University of Oulu

Raitanen, M. (2023) DRI as the Raw Material of EAF, Bachelor's thesis, University of Oulu

Tirroniemi S. (2023) Kaasumaisten polttoaineiden poltinkäytön vertailu HSC-Sim-mallinnuksen avulla, Bachelor's thesis, University of Oulu

Tyybäkinoja, S. (2022) The Effect of Cooling Rate on Structure of EAF Slags, Master's thesis, University of Oulu

ISBN
978-952-62-4015-2

Publisher and contact information

Process Metallurgy Research Unit
Faculty of Technology
University of Oulu
PO Box 4300 I 90014 University of Oulu
FINLAND